Oil to Source Rock Correlation in Western Newfoundland

by

Martin Schwangler

A thesis submitted in partial fulfillment of the requirements for the degree of

Master of Science

Department of Earth and Atmospheric Sciences

University of Alberta

Abstract

The presence of natural oil seeps, abandoned well sites (generally containing light oil), and high quality source rocks along the coast of western Newfoundland has refocused interest on the region as an area for potential petroleum exploration and development. Most of the oil seeps and old well sites are located in the Cow Head and Port au Port Peninsula areas. These areas lie in the Humber Zone, located on the eastern margin of the Anticosti Basin - the structural front of the northeastern Canadian Appalachians. The current study aims to characterize source rocks and oils in this active petroleum system.

The geologic history of the area is complex, and has important implications for the petroleum system. Neoproterozoic continental breakup was followed by the development of a passive continental margin containing coeval shelf carbonates and continental slope and rise deposits of the Humber Arm Allochthon. During the Taconian (Ordovician) and Acadian (Devonian) orogenies, westward thrusting imbricated continental slope and rise deposits, creating thrust sheets that repeat Lower Paleozoic strata. This underlying geology created an active petroleum system with potential reservoirs in the overridden platform carbonates, which are time-equivalent to slope deposits of the Cow Head Group, containing source rocks. Other potential reservoirs can be found in shelf proximal carbonate conglomerates associated with debris flows. The connection between the identified source rocks and produced hydrocarbons is not well understood.

In the present analysis, I show that high-quality source rocks were deposited during two distinct periods: the Cambrian Series 3 to Furongian Series, and the Ordovician Floian stage. These late Cambrian to early Ordovician deep marine gravity flow deposits contain viable type I/II and type II/III source rocks. Total organic carbon (TOC) concentrations of up to 9.45 wt% and hydrogen index values as high as 841 [mg HC/g TOC] demarcate the Middle Arm Point Formation of the Cow Head Group.

Detailed biomarker and isotope analysis of source rock extracts show a statistically significant change in source dependent biomarker composition from the Cambrian to the Ordovician, identifying both bacterially (Cambrian) and algal (Ordovician) derived organic matter. The same

change in biomarker composition can be identified in bitumen and oil samples, linking the source intervals to two endmember petroleum groups. Analysis of thermal maturity-sensitive biomarkers reflect the complex tectonic history of western Newfoundland. In the Cow Head area both source rocks generate oil with a wide ranging of maturities (0.7 to 1.11 $\%R_o$ equivalent), related to the dipping character of the imbricated thrust stacks containing source rocks. The Port au Port No.1 well was charged by the Cambrian source rock and then underwent secondary cracking, indicated by concentrations of 3 + 4-methyldiamantane. Low maturity natural seeps from Port au Port Bay can be related to the Middle Ordovician Middle Arm Point Formation.

Biomarker and carbon isotope data were successfully used to correlate oil to source rocks in western Newfoundland and are a valuable tool to resolve thermal and generation history of oils in tectonically complex petroleum basins.

PREFACE

The study presented in this thesis was undertaken to examine the geochemistry of the under-explored petroleum system in western Newfoundland. The need for a greater understanding of the petroleum geology in this basin has been recognized by the Government of Newfoundland and Labrador, who founded in cooperation with Nalcor Energy, the Petroleum Exploration Enhancement Program to investigate the area for its exploration potential. This study will contribute to a better understanding of the extant petroleum basin and help to advance in potential exploration pursuits.

This thesis includes examination of the source potential and distribution of deep marine deposits of the Cow Head Group to identify viable source intervals, integrated with a detailed biomarker and isotope analysis of oil and source extracts, and a successful oil to source rock correlation.

Chapter 2 will be submitted to AAPG Bulletin, or Marine and Petroleum Geology under the authorship Schwangler, M., Harris, N.B., Waldron, J.W.F., Oil to source rock correlation in western Newfoundland. Schwangler, M. was responsible for data collection and manuscript composition, Harris, N.B and Waldron, J.W.F assisted in data collection and contributed to manuscript edits.

Acknowledgments

I would like to thank my principle supervisor Dr. Nicholas Harris and committee member Dr. John Waldron for their constant support and guidance through this research. I would also like to thank my lab colleagues and friends Ryan Lacombe and Morgan Snyder for their assistance in the field, as well as Shawna White for great discussions that enriched my understanding of the local and regional geology of western Newfoundland. I greatly appreciate the help from Larry Hicks, and Earl Keough - a fisherman from Parson's Pond, in locating most of the oil seeps. Thank you to Tony Garza, John Zumberge, Alex Zumberge and Brian Jarvie at GeoMark Research for their support and analyzing of samples. I would like to thank Ron Hill, Chief Geochemist at EOG Resources for his editorial support. A special thanks to Jordanne Taylor for her patience and support in improving my English writing skills. Most importantly, I want to thank my family for their infinite support and encouragement. Funding for this project was provided by the Government of Newfoundland and Labrador, as part of the Petroleum Exploration Enhancement Program (PEEP).

Table of Contents

List of Tables

List of Figures

ABBREVIATIONS

A

α ..... "Down" position of hydrogen atom relative to a plane
%Aro ..... Percent aromatic hydrocarbons
%Asph. ..... Percent Asphaltenes
ALS ..... Alternating least square analysis
API° ..... American Petroleum Institute gravity

B

β ..... "Up" position of hydrogen atom relative to a plane
b/cy ..... branched/cyclic
BNH (C28H) ..... Bisnorhopane (17α,18α,21β-28,30-bisnorhopane)
BTEX ..... Benzene, toluene, ethylbenzene, and xylene isomers

C

°C ..... Degree Celcius
C15+ ..... Carbon skeleton larger than 15 carbon atoms
C27% ..... C27-sterane relative percentage
C28% ..... C28-sterane relative percentage
C29% ..... C29-sterane relative percentage
C30M ..... Moretane
CF ..... Correction factor
Conc ..... Concentration
CPI ..... Carbon preference index
CSIA ..... Compound specific isotope analysis

D

DBT ..... Dibenzothiophene
DBT/P ..... Dibenzothiophene/phenanthrene
DIA ..... Rearranged C27 sterane (diasterane)
DNA ..... Desoxyribonucleic acid

E

EOM ..... Extract organic matter

F

°F ..... Degree Fahrenheit

f ..... conversion factor

FID ..... Flame ionization detector

G

g ..... Gram

GC ..... Gas chromatography

GC/MS ..... Gas chromatography/mass spectrometry

GSMSMS ..... Gas chromatography/mass spectrometry mass spectrometry

H

H ..... Hopane

HC ..... Hydrocarbon

HCA ..... Hierachichal cluster analysis

HI ..... Hydrogen index; (S2x100)/TOC

I

IRMS ..... Isotope ratio mass spectrometer

K

km ..... Kilometer

M

m/z ..... Mass/charge

Ma ..... Million years

MDR ..... Methyldibenzothiophene ratio

mg ..... Milligram

min ..... Minute

MP ..... Methylphenanthrene

MPI-1 ..... Methylphenanthrene index

N

n-C ..... saturated normal-alkanes (*n*-alkanes)

ng ..... nanogram

Ni ..... Nickl

NSO ..... Nitrogen, Sulfur, Oxygen compounds

%NSO ..... Percent Nitrogen, Sulfur, Oxygen compounds

O

OEP ..... Odd-to-even preference

OI ..... Oxygen index; (S3x100)/TOC

P

P ..... Phenanthrene

PAH ..... Polycyclic aromatic hydrocarbons

PCA ..... Principle component analysis

Ph ..... Phytane

PI ..... Production Index

ppm ..... Parts per million

Pr ..... Pristane

Q

QQQ ..... Triple quadrupole mass spectrometer

R

R ..... Rectus (*lat.)* = right

%Rc ..... Calculated vitrinite reflectance

%Ro ..... Vitrinite reflectance

Reg ..... Regular sterane

RF ..... Response factor

S

S ..... Sinister (*lat.)* = left

%Sat ..... Percent saturated hydrocarbons

S1 ..... Free hydrocarbons present in the sample before the analysis

S2 ..... Volume of hydrocarbons that formed during thermal pyrolysis of the sample

S3 ..... The CO2 yield during thermal breakdown of kerogen

SIM ..... Single ion mode

T

TET ..... Tetracyclic

Tm 17α, 21β-22,29,30-trisnorhopane

T_{max} ..... maximum temperature from rock-eval analysis
TNH (27Ts)..... Trisnorhopane (17α,18α,21β-25,28,30-trisnorhopane)
TOC ..... Total organic carbon
Ts..... 18α, 21β-22,29,30-trisnorhopane
type I ..... Oil prone kerogen
type II..... Oil/gas prone kerogen
type III..... gas prone kerogen

U

UCM ..... Unresolved complex mass
UTM..... Universal transverse mercator

V

V..... Vanadium
VPDB..... Vienna Pee Dee Belemnite
VREQ-5 ..... Vitrinite reflectance equivalent

W

wt% ..... Weight percent

Chapter 1: Introduction

1.1. Western Newfoundland - a Frontier Basin

Newfoundland is situated on the eastern margin of Canada, and the west coast of the island comprises a portion of the Anticosti Basin referred to as the Humber Zone (Figure 1.1). This area contains an active but poorly studied onshore petroleum system. Despite past exploration and limited exploitation, the basin remains unsuccessful in terms of economic oil production.

The presence of hydrocarbons and potential source rocks in the area, however, has refocused interest on the Humber Zone. Earlier studies have identified the Ordovician Green Point Formation, part of the deep marine succession of the Humber Arm Allochthon (comprising the Humber Zone), as a viable source rock (Macauley, 1987; 1990; Weaver, 1988; Weaver and Macko 1988; Sinclair, 1990; Fowler et al., 1995). Although a number of petroleum system elements have been identified, and an intact petroleum system is demonstrated by Port au Port No.1 well on the Port au Port Peninsula, a detailed investigation including systematic source rock sampling, and oil to oil, and oil to source correlation has not yet been performed.

In 2007 the government of Newfoundland and Labrador initiated, in cooperation with Nalcor Energy, the Petroleum Exploration Enhancement Program (PEEP). PEEP aims to improve understanding of western Newfoundland's regional geology, and petroleum geology specifically, on an academic level. This will further onshore exploration efforts, with the hope of continued development of the area's oil and gas industry.

1.2. Research Question

This research aims to advance our knowledge of the petroleum basin present in western Newfoundland, specifically addressing these questions:

- What is the distribution of potentially active source rock intervals in the study area, focusing on organic matter quantity and quality, as well as the thermal maturity distribution of the identified source intervals?
- What are the biomarker and isotope characteristics of the source rock extracts produced from collected samples?
- What are the biomarker and isotope characteristics of collected oil and can this be used to establish oil families? Can these be linked to the identified source rock interval(s)?
- What are the implications for maturity, migration, and mixing of the oil based on biomarker parameters.

1.3. Overview of Methods

To investigate the above research questions, 17 samples of oil and bitumen, and 197 source rock samples were collected in western Newfoundland during the 2015 field season. Additional data included in this study are source rock samples from the Port au Port Peninsula collected by R. Lacombe in 2014 (Lacombe, 2017). The main sample locations for potential source rocks are the Port au Port Peninsula, the Bay of Islands, and the Cow Head area (Figure 1.1). Source rock samples were taken along measured sections with good biostratigraphic definition from coastal outcrops and available core cuttings. Theses samples were later analyzed for total organic carbon (TOC) and Rock-eval at GeoMark Research (Houston). Sample locations for oil and bitumen are located in the Port au Port Peninsula and Cow Head area (Figure 1.2). Light oils, from old well sites, and bitumen from natural seeps in quarries and coastal outcrop, were analyzed for biomarker and stable carbon isotopes at GeoMark Research. Additionally, extracts from viable source intervals were analyzed for biomarker and carbon isotopes to facilitate oil to source rock correla-

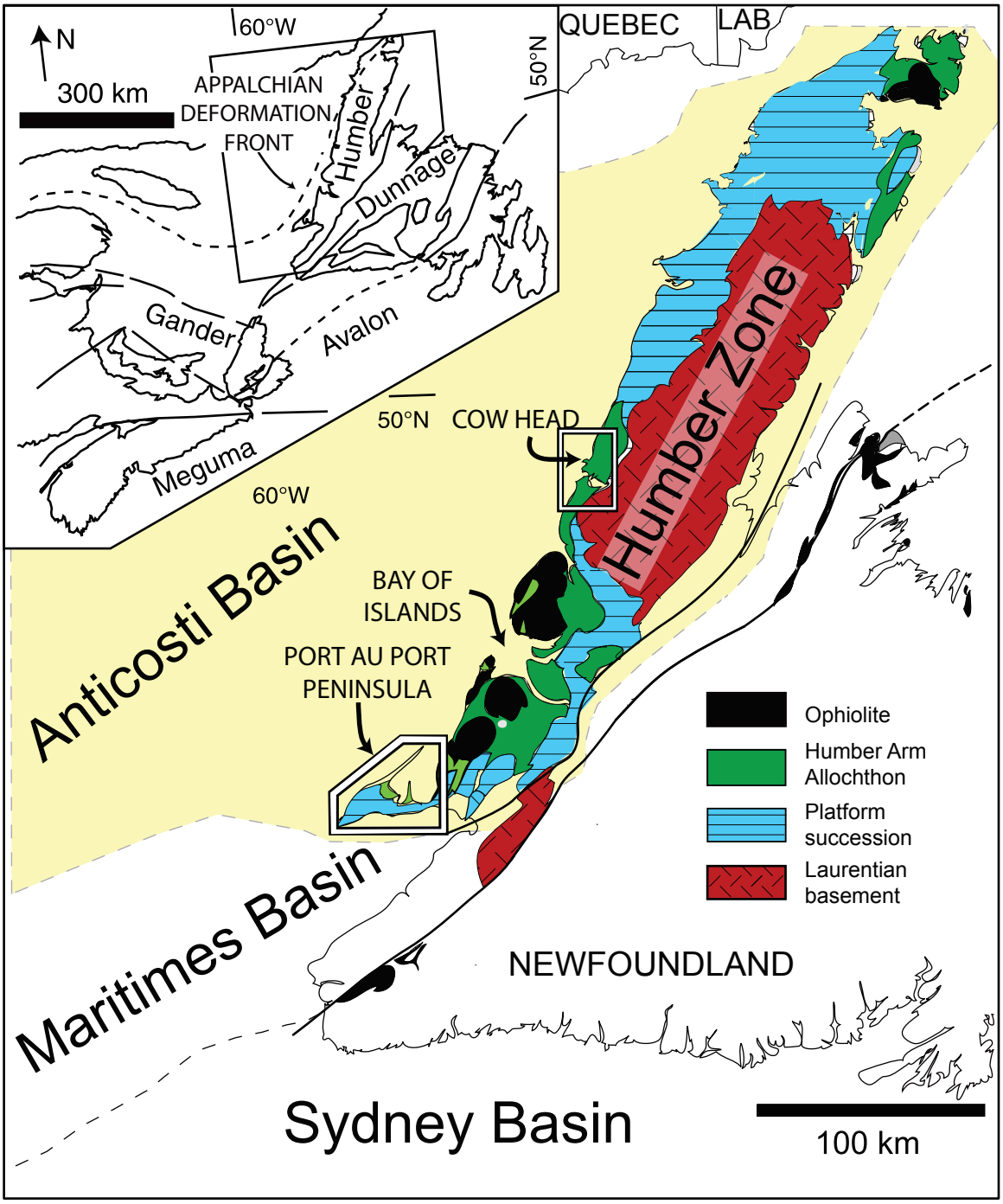

Figure 1.1: Simplified geologic map of western Newfoundland.
Geologic map illustrating lithotectonic subdivision and petroleum basins of western Newfoundland and location of study areas (modified after Waldron et al., 2003; Enachescu, 2011).

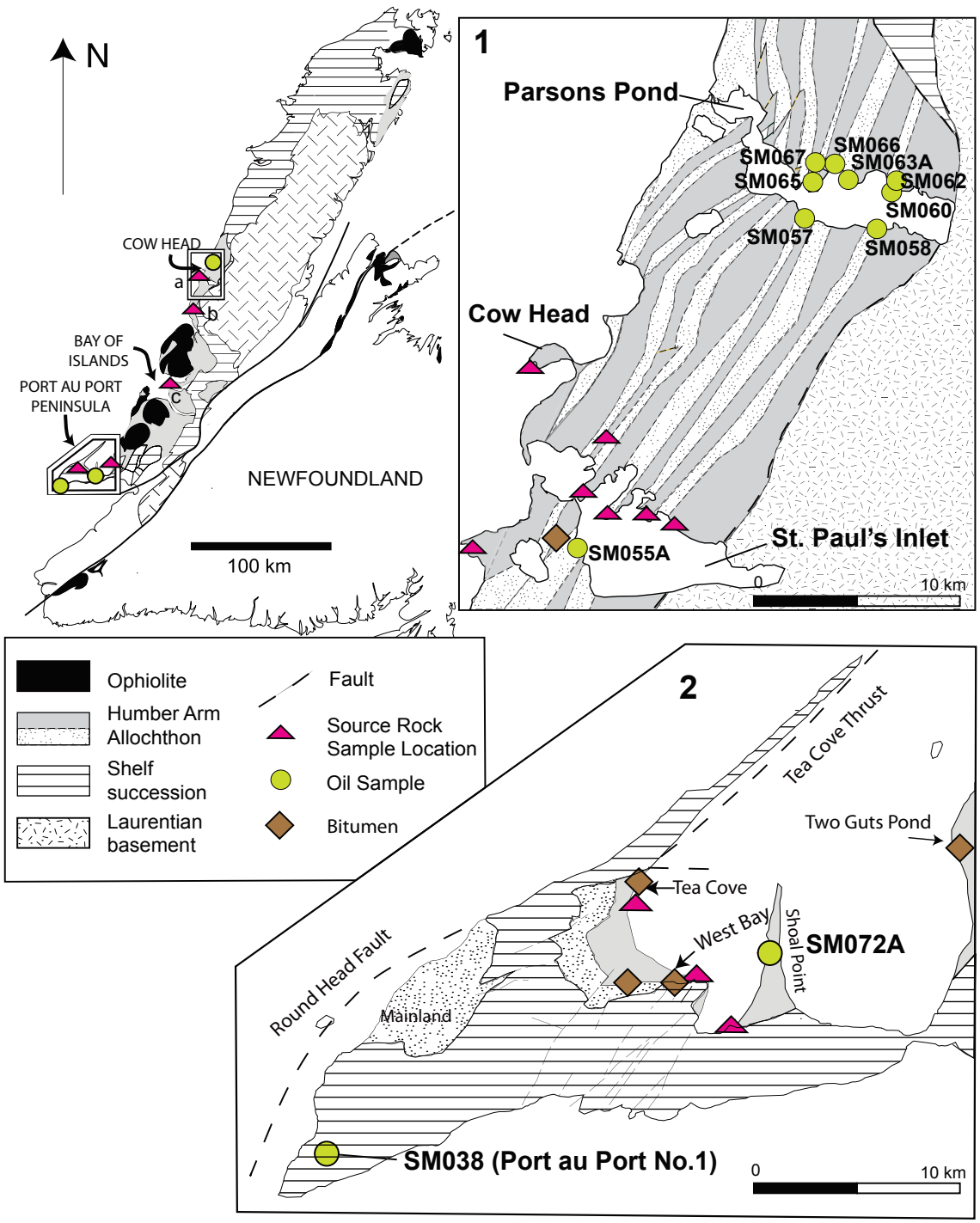

Figure 1.2: Overview map with main sample location for oil and source rocks.
Map 1, 2 show main sample location in more detail. Map 1 is based on unpublished work by Shawna White (2017); map 2 is modified after Cooper et al. (2001), the base map is modified after Waldron et al. (2003). 1: Parson's Pond sample location, including eight individual oil samples (green circles). St. Paul's Inlet sample location, including one oil sample (green circle) and 115 source rock samples from seven different measured sections (James and Stevens, 1986). b: Measured section from Green Point is shown w on the overview map (pink triangle). c: Northern Head sample location including 34 individual source rock sample (pink triangle) from measured sections from Botsford (1987). 2: Port au Port Peninsula sample location, including two individual oil samples and 35 source rock samples (pink triangles) from measured sections from Lacombe (2017).

tion. Triple quadrupole (QQQ) and compound-specific carbon isotope analysis aided interpretations on the thermal history of identified oil families.

1.4. Overview of Biomarkers

Biomarkers are organic molecules present in oil and source rocks, which have carbon skeletons that can be correlated to functionalized compounds occurring in the original source material. In crude oil and source rocks, biomarkers are derived from two main groups: prokaryotic and eukaryotic precursor organisms.

Prokaryota are single celled organisms without internal lipid membranes to segregate organelles. In contrast, eukaryota are single or multi-celled organisms with internal membranes to segregate the nucleus, containing deoxyribonucleic acid (DNA), and other cell organelles, e.g., mitochondria and chloroplasts (Figure 1.3). The primary role of lipid membranes is to regulate the intake and excretion of molecules during metabolism and reproduction.

Biomarker molecules are primarily derived from the cell membranes and attached functional groups found in these organisms. Throughout evolution the constitution of cell membranes changed, becoming more complex in structure and functionality. In early evolutionary history primitive organisms (Archea) had a monolayer lipid membrane encapsulating their DNA. Over time, this monolayer lipid membrane evolved into the bilayer lipid membrane seen in eubacteria. Later in their evolutionary history, eubacteria membranes incorporated terpenoids to allow for additional functions. With the evolution of eukaryotes, other molecules such as sterols, proteins, and carbohydrates were introduced into bilayer lipid membranes, allowing for transportation of larger, more complex molecules between cells and for energy storage.

1.4.1 Bulk composition of Petroleum

Oils consist of a complex mixture of hydrocarbon and non-hydrocarbon molecules. The bulk composition primarily consists of saturates, olefins (alkenes), aromatics, NSO's (nitrogen, oxygen, sulfur compounds), polar compounds, and asphalthenes. Saturates are a class of hydrocarbons that are characterized by single carbon-carbon and carbon-hydrogen bonds. Saturates include compounds with linear carbon skeletons (*n*-alkanes or paraffins) and branched or cyclic

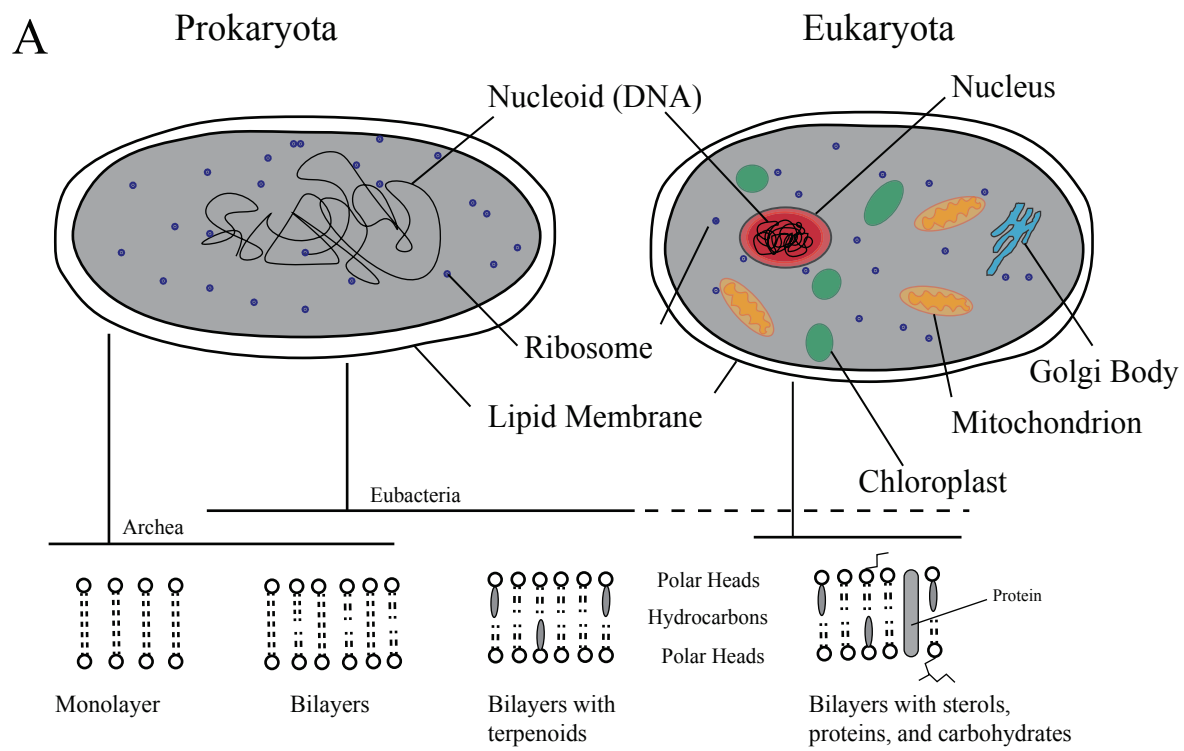
A
Prokaryota
Eukaryota
Nucleoid (DNA)
Nucleus
Ribosome
Lipid Membrane
Golgi Body
Mitochondrion
Chloroplast
Eubacteria
Archea
Polar Heads
Hydrocarbons
Polar Heads
Protein
Monolayer
Bilayers
Bilayers with terpenoids
Bilayers with sterols, proteins, and carbohydrates

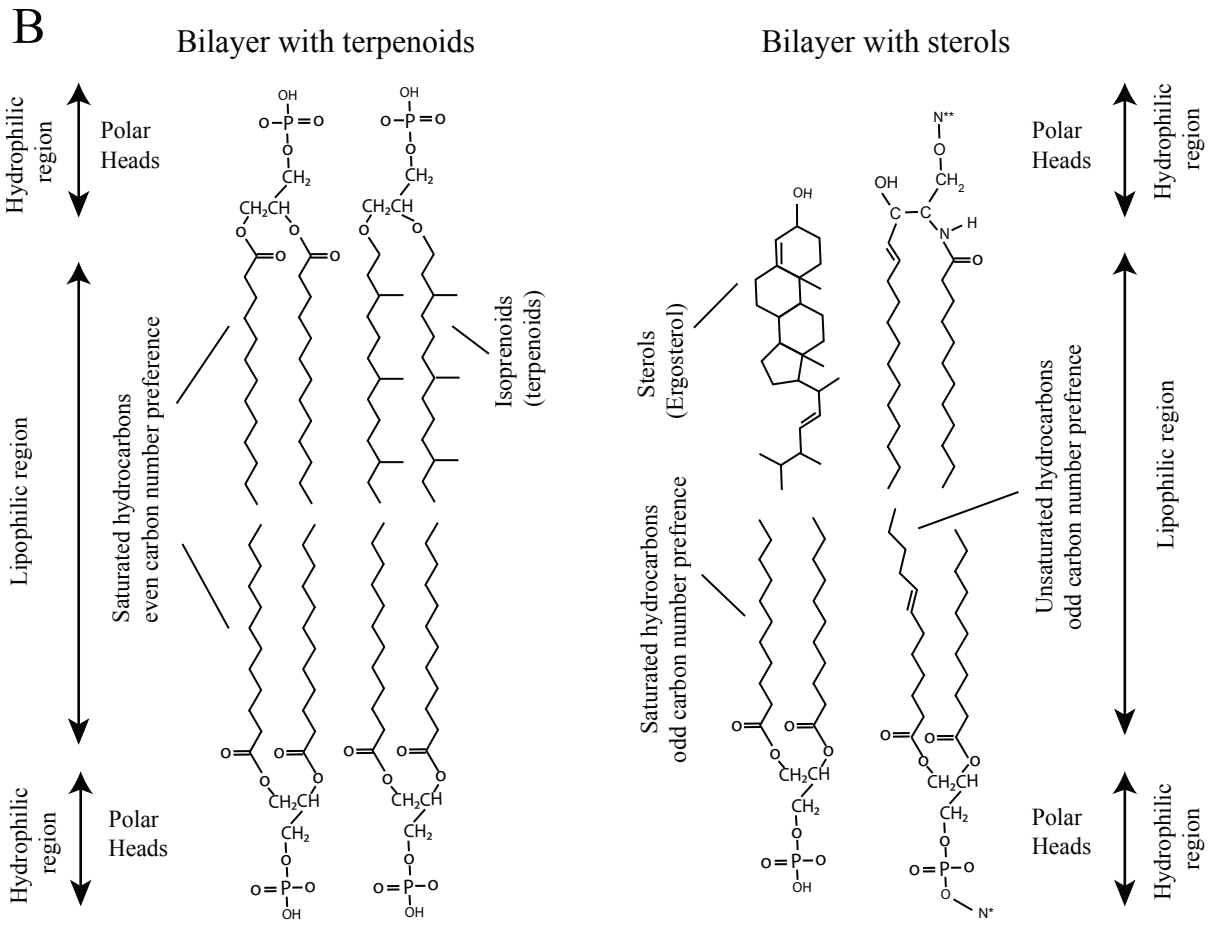
B
Bilayer with terpenoids
Bilayer with sterols
Hydrophilic region
Polar Heads
Lipophilic region
Saturated hydrocarbons even carbon number preference
Isoprenoids (terpenoids)
Sterols (Ergosterol)
Saturated hydrocarbons odd carbon number prefrence
Unsaturated hydrocarbons odd carbon number prefrence

Figure 1.3: Prokaryotic and eukaryotic cells in comparison (A) (after Peters et al., 2005). Schematic evolution of lipid membranes and comparison of a schematic eubacterial and eukaryotic cell membrane at a molecular level (B).
A: Prokaryota are defined by a lipid membrane enclosing the nucleoid (DNA) and ribosomes. Eukaryota are cells with lipid membranes, including cell organelles separated by membranes and DNA enclosed in a nucleus. Originally primitive lipid membranes evolved to highly functional membranes including terpenoids, sterols, proteins, and carbohydrates.
B: Bilayer with terpenoids schematizes an eubacterial lipid membrane built with phospholipids. The polar head (containing phosphor) is attached through ether or ester bonds to fatty acids (predominantly even numbered saturated hydrocarbons or acyclic isoprenoids).
Bilayer membranes including sterols are associated with eukarioyta. The high functionality and specificity of the membrane is accommodated by attaching a number of different moieties as polar heads to the fatty acids. Included are phospholipids (polar head containing phosphor), glycolipids (carbohydrate chains attached to the hydrophilic head) and complex alcohols (sterols). The fatty acids attached to the polar heads can be unsaturated hydrocarbons showing predominantly odd carbon number preferences. To increase functionality a variety of nitrogen based proteins (N*) and sugar chains (N) can be attached to the hydrophilic heads.**

arrangements (iso-alkanes and cycloalkanes, respectively). Cycloalkanes (naphthalenes) exist as monocyclic and polycyclic alkanes. With increasing carbon numbers, a homologous series of compounds results, ranging from C1 to C65 and above, in oil and source rocks (Huang et al., 2003). Biomarkers are part of the saturated fractions, and include *n*-alkanes, terpenoids, and steranes (Figure 1.4, Figure 1.5). Olefins (alkenes) are unsaturated hydrocarbons, containing one or more double carbon-carbon bonds. Alkenes are uncommon in crude oil, but may be generated during refining processes. Aromatic hydrocarbons have one or more benzene rings in their molecular structure. In petroleum, aromatic molecules include benzene, toluene, ethylbenzene, and xylene isomers (BTEX). Also included are polycyclic aromatic hydrocarbons (PAH), such as naphthalene, phenanthrene, and dibenzothiophene (Figure 1.4). Polar compounds are molecules with an electric dipole as a result of bonding with atoms with high electronegativity, including nitrogen, sulfur, and oxygen (NSO). Heavy oils generally contain a higher amount of NSO-compounds and metal-containing compounds (heteroatom-containing molecules). Smaller polar molecules are commonly referred to as resins. Asphaltenes are a class of organic compounds that do not dissolve in organic solvents and contain a larger amount of heteroatom-containing molecules (Berkowitz, 1997).

1.4.2 Relevant Biomarkers

Key biomarker molecules in petroleum include *n*-alkanes, isoprenoids, steranes, and aromatics. The following will outline commonly used biomarker classes, their origin, and information they provide.

n-Alkanes are a group of molecules that are either indigenous or derived from membrane lipids. Membrane lipids in eubacteria and eukaryotes are mainly composed of fatty acids connected to a polar head (Figure 1.3). Bacteria, algae, and diatoms most commonly have even carbon number fatty acid chains, between 12-24 carbon atoms long. These chains are connected through ether or ester bonds to a polar head (often containing phosphate), which has various functional groups attached. Waxes, which form a subgroup of lipid membranes, are predominantly related to higher plants and animals. Waxes are organic molecules composed of complex

alcohols (e.g. sterols), fatty acids, or alkanes (Figure 1.3). The alkanes of waxes usually show an odd carbon number preference. n-Alkane distribution can be used to distinguish between different source compositions and to evaluate maturation (Bray and Evans, 1961). The carbon preference index (CPI) and odd-to-even preference (OEP) are two early identified maturity parameters, which are still used (Huang et al., 2003). Isoprenoids (terpenoids) are a diverse group of straight chained or cyclic lipid compounds, which provide the main biomarkers used for oil-to-source rock correlation (Figure 1.5). Information on age, source composition, redox conditions, level of biodegradation, facies, and thermal maturity can be obtained from these markers. All isoprenoids follow the "isoprene rule" discovered by German chemist Otto Wallach in 1887: isoprenoids are composed of isoprene subunits that are linked head-to-head, head-to-tail, or tail-to-tail. This creates a wide variety of cyclic and acyclic molecules (Nes and McKean, 1977); examples are given in Figure 1.4 and Figure 1.5. The number of isoprene units that form each molecule classifies them into different groups (Peters et al., 2005):

- Monoterpane (C10): two isoprene units
- Sesquiterpane (C15): three isoprene units
- Diterpanes (C20): four isoprene units
- Sesterterpanes (C25): five isoprene units
- Triterpanes (C30): six isoprene units
- Tetraterpanes (C35): eight isoprene units
- Polyterpanes ($C5_{n(n > 8)}$): nine or more isoprene units

Other terpenoids used for correlation and assessment of depositional environment and source composition are aryl-isoprenoids and carotenoids. Also important for correlation and source determination are aromatic biomarker molecules, some of which are listed in Figure 1.4.

Isoprene (C5)

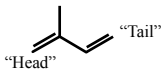

Monoterpanes (C10)

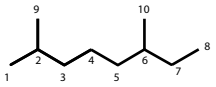

2, 6-Dimethyloctane

Sesquiterpanes (C15)

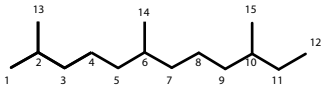

Franesane (C15)
2, 6, 10-Trimethyldodecane

Diterpanes (C20)

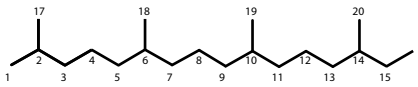

Phytane (C20)
2, 6, 10, 14- Tetramethylhexadecane

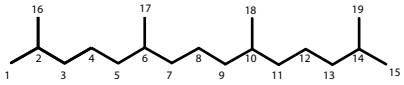

Pristane (C19)
2, 6, 10, 14- Tetramethylpentadecane

Sesterterpanes (C25)

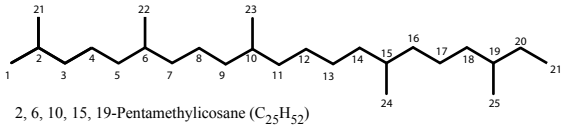

2, 6, 10, 15, 19-Pentamethylicosane ($C_{25}H_{52}$)

Tetraterpanes (C30)

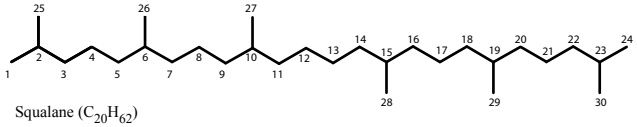

Squalane ($C_{20}H_{62}$)

Aromatics

Monoaromatics

Benzene (C6H6)

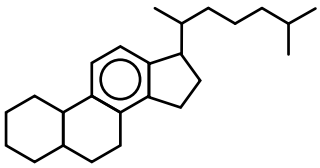

Monoaromatic Steroid (C27H42)

Diaromatic

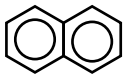

Naphtalene (C10H8)

Triaromatics

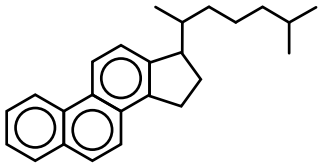

Triaromatic Steroid (C26H32)

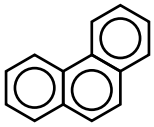

Phenanthrene (C14H10)

Thiophenes

Thiophene

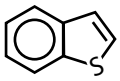

Benzothiophene

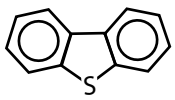

Dibenzothiophene

Figure 1.4: Molecular structures of representative acyclic terpenoids and aromatic compounds in oil.

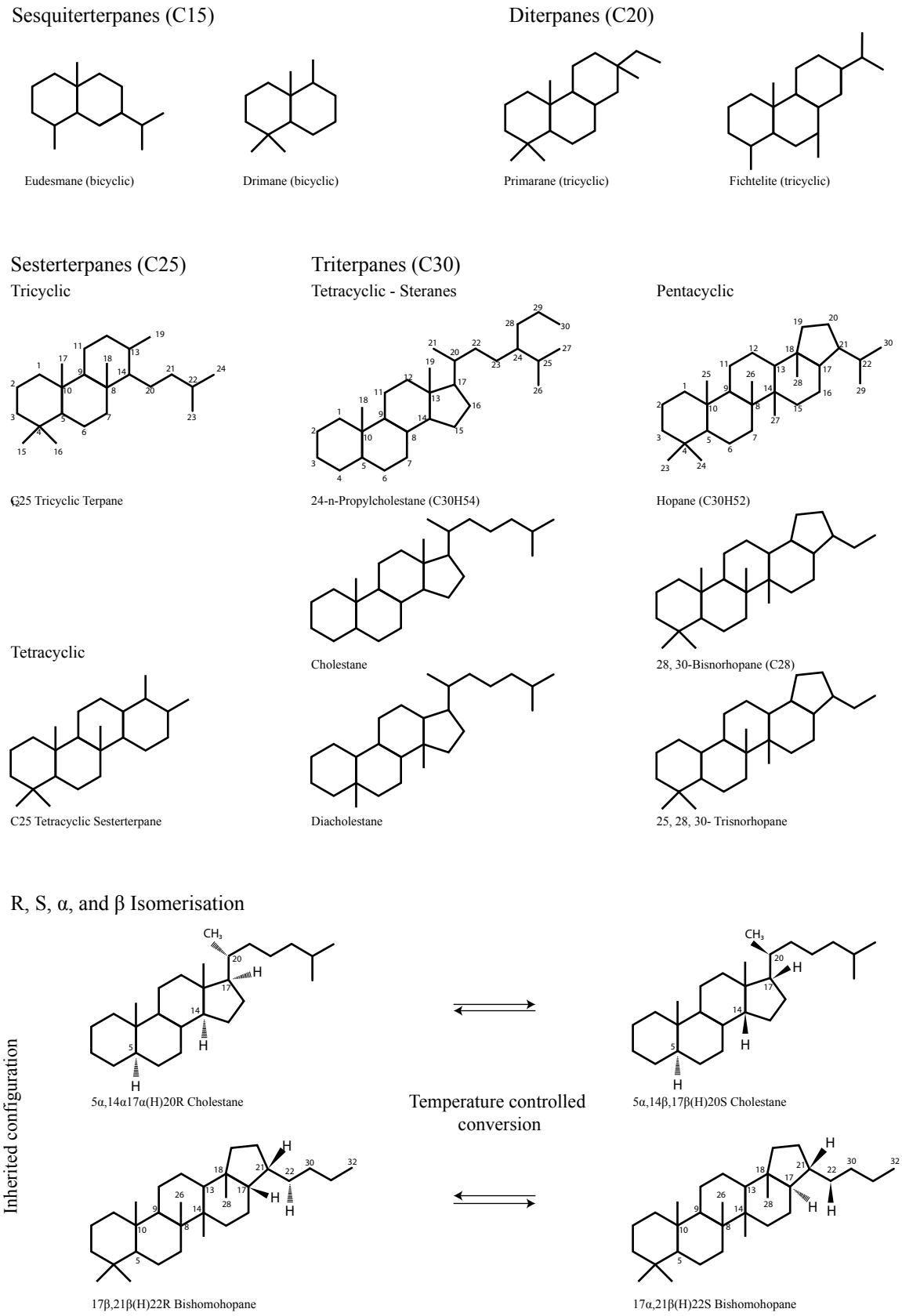

Figure 1.5: Molecular structures of representative cyclic terpenoids compounds in oil.

1.4.3 R, S, α, AND β STEREOISOMERS

Stereoisomers are molecules with the same number and kind of atoms bonded together but differ in their atom orientation in three dimensional space. The change in orientation of atoms in space at asymmetric centers generates chiral compounds. This information is included in naming biomarkers molecules. Commonly, the α (alpha = down) and β (beta = up) nomenclature is used for asymmetric centers in the carbon rings, the R (*lat.* rectus = right) and S (*lat.* sinister= left) nomenclature is used for asymmetric centers outside of the ring structures (Cahn et al., 1966). "Up", "down", "rectus", and "sinister" are defined relative to the plane formed by the ring system of the molecule. In nature, enzymes impose a certain configuration at asymmetric centers of molecules, which become unstable at higher temperature and change position. Depending on the stability of the molecules and the kinetic pathways involved, isomerization can occur in any proportion of the possible configurations (α, β and R, S). Pentacyclic triterpanes (hopanes) show asymmetric centers at C-21 and all ring junctures (C-5, C-8, C-9, C-10, C-13, C-14, C17, and C-18). Homohopanes (hopanes with methyl groups attached at C30) have an additional optically active carbon atom at C-22 (i.e. 22R and 22S). The original, biological stereochemical orientation for hopanes is 17β,21β(H)-hopane, which becomes successively converted into αβ-hopanes and βα-moretanes. For homohopanes, the original, biological orientation is the 17β,21β(H) 22R-configurations; with increasing temperature there is an increase in molecules showing αβ22S- and βα22S-configurations (Figure 1.5). Tetracyclic triterpanes (steranes) show asymmetric centres at a number of carbon atoms, but only C-14, C-17, and C-20 are important during catagenesis of steranes. The inherited configuration of steranes is 5α,14α,17α,(H)20R. With increasing temperatures the hydrogen atoms and methyl side-chains reorient into ααα20S, αββ20R, and αββ20S. Two examples of chiral molecules are shown in Figure 1.5. A complete discussion of organic geochemical nomenclature and associated mechanisms to form isomers is beyond the scope of this work. Interested readers can find more information in most organic geochemistry textbooks.

1.5. CONCLUSION

This geochemical study enables us to improve our knowledge of the composition and distribution of viable source rocks and oil in the petroleum system in western Newfoundland. Delineating the source kitchen for oils, their composition, and thermal history is an important step in evaluating the prosperity of the petroleum system. The results and interpretations made in this study will help to de-risk potential hydrocarbon plays in the area and develop a regional petroleum basin analysis to further constrain timing of oil generation and migration pathways.

1.6. References

Berkowitz, N., 1997, Fossil hydrocarbons: chemistry and technology: San Diego, Academic Press, 351 p.

Bray, E. E., and E. D. Evans, 1961, Distribution of n-paraffins as a clue to recognition of source beds: Geochimica et Cosmochimica Acta, v. 22, no. 1, p. 2–15.

Botsford, J. W., 1987, Depositional history of Middle Cambrian to Lower Ordovician deep water sediments, Bay of Islands, western Newfoundland, PhD: Memorial University of Newfoundland, 508 p.

Cahn, R. S., C. Ingold, and V. Prelog, 1966, Specification of Molecular Chirality: Angewandte Chemie International Edition in English, v. 5, no. 4, p. 385–415, doi:10.1002/anie.196603851.

Cooper, M., J. Weissenberger, I. Knight, D. Hostad, D. Gillespie, H. Williams, E. Burden, J. Porter-Chaudhry, D. Rae, and E. Clark, 2001, Basin evolution in western Newfoundland: new insights from hydrocarbon exploration: AAPG bulletin, v. 85, no. 3, p. 393–418.

Enachescu, M., E., 2011, Petroleum Exploration Opportunities in Exploration Opportunities in Anticosti Basin, Offshore Western Newfoundland and Labrador Call for Birds NL11-01.

Fleming, J. M., 1970, Petroleum exploration in Newfoundland and Labrador, geologic map: Department of Mines, Agriculture and Resources, Mineral Resources Division : St. John's, NL, Canada, Mineral Resources Report. Newfoundland and Labrador, Mineral Resources Division, 1970.

Fowler, M. G., A. P. Hamblin, D. Hawkins, L. D. Stasiuk, and I. Knight, 1995, Petroleum geochemistry and hydrocarbon potential of Cambrian and Ordovician rocks of western

Newfoundland: Bulletin of Canadian Petroleum Geology, v. 43, no. 2, p. 187–213.

Huang, H., S. R. Larter, and G. D. Love, 2003, Analysis of wax hydrocarbons in petroleum source rocks from the Damintun depression, eastern China, using high temperature gas chromatography. Organic Geochemistry, v. 34, no. 12, p. 1673–1687, doi:10.1016/S0146-6380(03)00172-4.

James, N. P., and R. K. Stevens, 1986, Stratigraphy and correlation of the Cambro-Ordovician Cow Head Group, western Newfoundland: Geological Survey of Canada Bulletin, 143 p.

Lacombe, R., 2017, Stratigraphic and Structural Relationships in the Foreland Basin and Humber Arm Allochthon on Port au Port Peninsula, western Newfoundland: University of Alberta, 162 p.

Macauley, G. (ed.), 1990, Ordovician oil shale-source rock sediments in the central and eastern Canada mainland and eastern Arctic areas, and their significance for frontier exploration: Ottawa, Canada, Energy, Mines, and Resources Canada, Paper / Geological Survey of Canada 90–14, 51 p.

Macauley, G., 1987, Organic Geochemistry of some Cambro-Ordovician Outcrop Samples Western Newfoundland: Geologic Survey of Canada 1503.

Nes, W. R., and M. L. McKean, 1977, Biochemistry of steroids and other isopentenoids: Baltimore, University Park Press, 690 p.

Peters, K. E., C. C. Walters, and J. M. Moldowan, 2005, The biomarker guide: Cambridge, UK ; New York, Cambridge University Press, 2nd edition.

Sinclair, I. K., 1990, A Review of the Upper Precambrian and Lower Paleozoic Geology of western Newfoundland and the Hydrocarbon Potential of the Adjacent Offshore Area

in the Gulf of St. Lawrence: Canada-Newfoundland Offshore Petroleum Board, v. GL-CNOPB, no. 90–1, p. 79.

Weaver, F. J., 1988, Source Rock Studies of Natural Seep Oils near Parson's Pond on the West Coast of Newfoundland, Master Thesis: Memorial University of Newfoundland, 178 p.

Weaver, F. J., and S. A. Macko, 1988, Source rocks of western Newfoundland: Organic geochemistry, v. 13, no. 1–3, p. 411–421.

Waldron, J. W. F., G. S. Stockmal, R. C. Courtney, and J. DeWolfe, 2003, The Appalachian foreland basin beneath the Gulf of St. Lawrence: Abstracts, Geological Society of America, Northeastern section, Annual Meeting, Halifax, NS.

Chapter 2: Oil to Source Rock Correlation in Western Newfoundland

2.1. Introduction

The west coast of Newfoundland is known for natural oil seeps in two areas: Port au Port Peninsula and Cow Head (Figure 2.1). Both areas experienced an early exploration history, with drilling occurring in the early 20th century (Howley, 1875; Weatherhead, 1922; Baker, 1928; Brown, 1938). Drilling was pursued again in the 1960's and early 2000's (Fleming, 1970; Fowler et al., 1995). Yet, to date, the origin of the oil seeps is not well studied or understood, nor has drilling led to economic oil discoveries. Understanding of the characteristics of potential Cambrian and Ordovician source rocks in western Newfoundland is also fragmentary. The complex tectonic history and thermal development of this petroleum basin may have generated oil of different maturities, adding to the complexity and problematic nature of linking source rock and oil seeps. Biomarker and isotope data are particularly useful in challenging tectonic settings to resolve the impact of the subsurface geometry on the thermal and generation history of oils, and to resolve mixing of different oil families.

I have carried out systematic sampling of measured outcrop sections containing potential source rocks. Pyrolysis and extract data from the outcrop samples, combined with biomarker and isotope data from natural seeps and oil recovered from shallow wells, allow us to establish oil families, relate source intervals to generated oil, and gain insight into the origin of the organic matter, maturity and potential migration and mixing.

2.2. Regional Geology and Stratigraphy

2.2.1. Structural evolution

The west coast of Newfoundland is part of the Anticosti Basin, one of the large Appalachian Basins in North America (Figure 2.1). Understanding the geologic evolution of this western part of the Anticosti Basin is crucial for interpretation of the geochemical data obtained in this study. Initial evolution of the basin began with the breakup of Rodinia and opening of the Iapetus Ocean between 615 ±2 Ma and 555 +3/-5 Ma in the Neoproterozoic (Stukas and Reynolds, 1974; Kamo et al., 1989; Cawood et al., 1996; Cawood et al., 2001; van Staal et al., 2012). Multiple phases of rifting during the Cambrian created horst and graben structures infilled with terrestrial clastic sediments of the basal Labrador Group (Figure 2.2). Cambrian rifting ended before the end of Cambrian Series 2 (508 Ma) (Williams and Hiscott, 1987; Hibbard et al., 2007; Leslie et al., 2008; Peng et al., 2012), and the rift evolved into the passive margin of Laurentia. This Cambrian to Ordovician passive margin is preserved in the Humber Zone, which is bounded to the west by the deformational front of the Appalachian orogen in western Newfoundland (Figure 2.1).

Deposition and subsequent destruction of the passive margin, including platform and continental slope and rise deposits, took place during the Taconian and Acadian orogenies (ca. 488 to 460 Ma and ca. 420 to 404 Ma, respectively; Figure 2.2) (Williams, 1975; Williams and Hiscott, 1987; James et al., 1987). The Taconian orogeny resulted from the collision between Laurentia and a number of microcontinents (e.g. the Dashwood Microcontinent) during the closure of the newly formed Iapetus Ocean (Figure 2.2) (Waldron and van Staal, 2001). The earliest evidence for the onset of the Taconian orogeny is intrusions into metasediments dated at 488 Ma (Dubé et al., 1996). During the main stage of the Taconian orogeny, the young oceanic crust of the Iapetus Ocean was subducted to the east, causing imbrication of the continental slope and rise deposits and their emplacement onto the platform (Figure 2.2) (Stevens, 1970; Williams 1975; Waldron and van Staal 2001). In western Newfoundland, this imbricated stack is referred to as the Humber Arm Allochthon. This loading event created a peripheral bulge, resulting in subtle

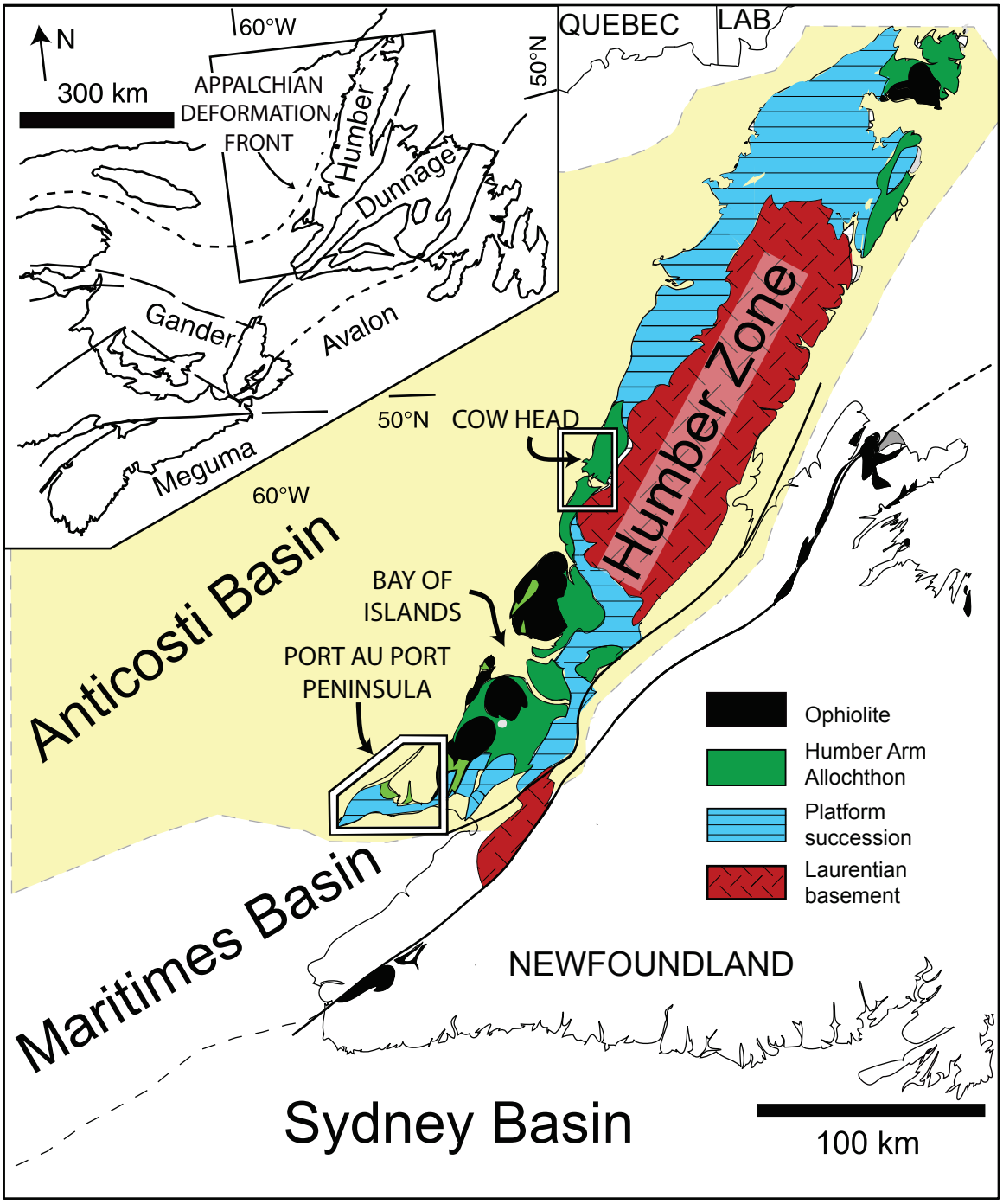

Figure 2.1: Simplified geologic map of western Newfoundland.
Geologic map illustrating lithotectonic subdivision and petroleum basins of western Newfoundland and location of study areas (modified after Waldron et al., 2003; Enachescu, 2011).

uplift, of the shelf. Erosion, and karstification of carbonates, manifested by the St. George Unconformity. It marks the peak Taconian deformation, and the transition into a drowned passive margin (Jacobi, 1981; Knight et al., 1991; Hibbard et al 2007). The time interval missing at the unconformity lasted from late Floian (ca. 470 Ma) to Darriwillian time (ca. 466 Ma) (Dallmeyer and Williams, 1975; Stenzel et al., 1990). Although the Taconian orogeny was a shortening event overall, the drag created by the subducting oceanic crust and the additional loading of the Humber Arm Allochthon reactivated older syn-rift normal faults within the foreland basin. After the passage of the peripheral bulge, carbonate sedimentation resumed in the shallow marine environment. Coeval flysch sedimentation took place in the deeper basin, sourced from the approaching Allochthon as well as from the platform (Knight et al., 1991; Quinn 1992a, Quinn et al., 1999). During the middle Ordovician (460 +/- 5 Ma), an ophiolite complex was formed in a supra-subduction zone fore-arc setting and obducted onto the platfrom, forming the current structurally highest slice (Dallmeyer and Williams, 1975; Waldron and van Staal, 2001; Dewey and Casey, 2013) (Figure 2.1, Figure 2.2).

Later significant subsidence was signaled by post-Taconian foreland basin sedimentation of marine sediments during the Late Ordovician (Quinn et al., 1999). This was followed by Acadian (Devonian) shortening, which overprinted earlier Taconian extensional structures, and inverted originally normal faults in the Port au Port and Cow Head area into major reverse faults (Figure 2.2) (Waldron and Stockmal, 1991; Stockmal and Waldron, 1993; Waldron et al., 1993; Waldron et al., 1998). Thick-skinned westward thrusting and thin-skinned eastward thrusting created a triangle zone just offshore of western Newfoundland (Stockmal and Waldron, 1990). These multiple deformational events gave rise to the present-day tectonic framework in western Newfoundland, where continental slope and rise deposits of the Humber Arm Allochthon are thrusted and structurally overlie platform carbonates. The obducted ophiolite complex represents the structurally highest slice (Figure 2.1).

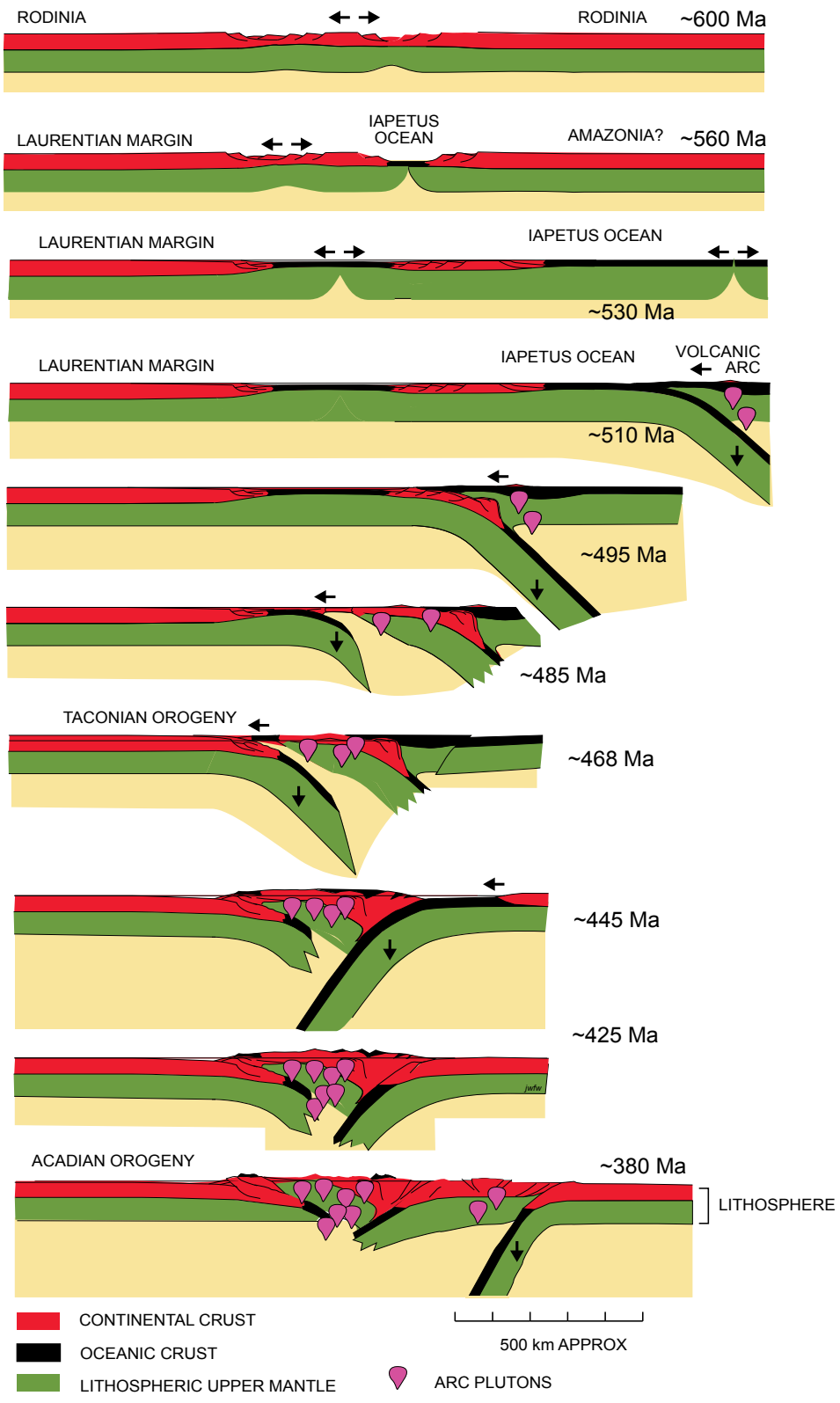

Figure 2.2: Schematic tectonic evolution of the Humber Zone.
Time steps include the breakup of Rodinia, the opening and closure of the Iapetus ocean, and the Taconinan and Acadian orogenies (modified after Waldron and van Staal, 2001; van Staal et al., 2014).

2.2.2. Stratigraphic Evolution

Sedimentary rocks representing the passive margin of Laurentia in western Newfoundland are subdivided into shelf clastics, platform carbonates, and contemporaneous continental slope and rise sediments deposited in the Cambrian to Ordovician Period (Figure 2.3). The deep marine sedimentary rocks were tectonically emplaced and deformed during the Taconian and Acadian orogenies and now overlie the platform deposits as an allochthonous package. Post-Taconian foreland basin deposits overlay turbidity current deposits.

2.2.2.1. Platform Stratigraphy

The base of the shelf stratigraphy consists of terrestrial, clastic sediments of the Labrador Group (Figure 2.3) varying in thickness, deposited during Cambrian Series 2 to 3 rift and drift phase (James et al., 1987; Cawood et al., 2001). Sandstones of the basal Bradore Formation are overlain by the younger Forteau Formation composed of predominantly limestone deposited in a deepening upward succession topped by marine shales, which in turn are overlain by sandstones of the Hawke Bay Formation (Williams and Hisott, 1987; Cawood et al., 2001).

The overlying Port au Port Group (Figure 2.3) was deposited during the passive margin phase and consists of shallow marine carbonates and dolomites of the Berry Head, Petit Jardin and March Point Formation (Chow and James 1987, Westrop, 1992).

This is overlain by the St. George Group (Figure 2.3) representing Early Ordovician carbonate facies deposited in subtidal to peritidal environments (Knight and James, 1987). Subtidal to peritidal limestones and dolostones of the Watts Bight, and Boat Harbour Formation are overlain by fossiliferous subtidal limestone and dolostone of the Catoche Formation, and peritidal limestone and dolostone of the Aguathuna Formation (Knight et al., 1991).

The top of the St. George Group (uppermost Floian) is placed at the St. George Unconformity (Klappa et al., 1980; Knight and James, 1987) separating it from the overlying Table Head Group (Figure 2.3) (Jacobi, 1981; Knight et al., 1991; Dallmeyer and Williams, 1975; Stenzel et al., 1990).

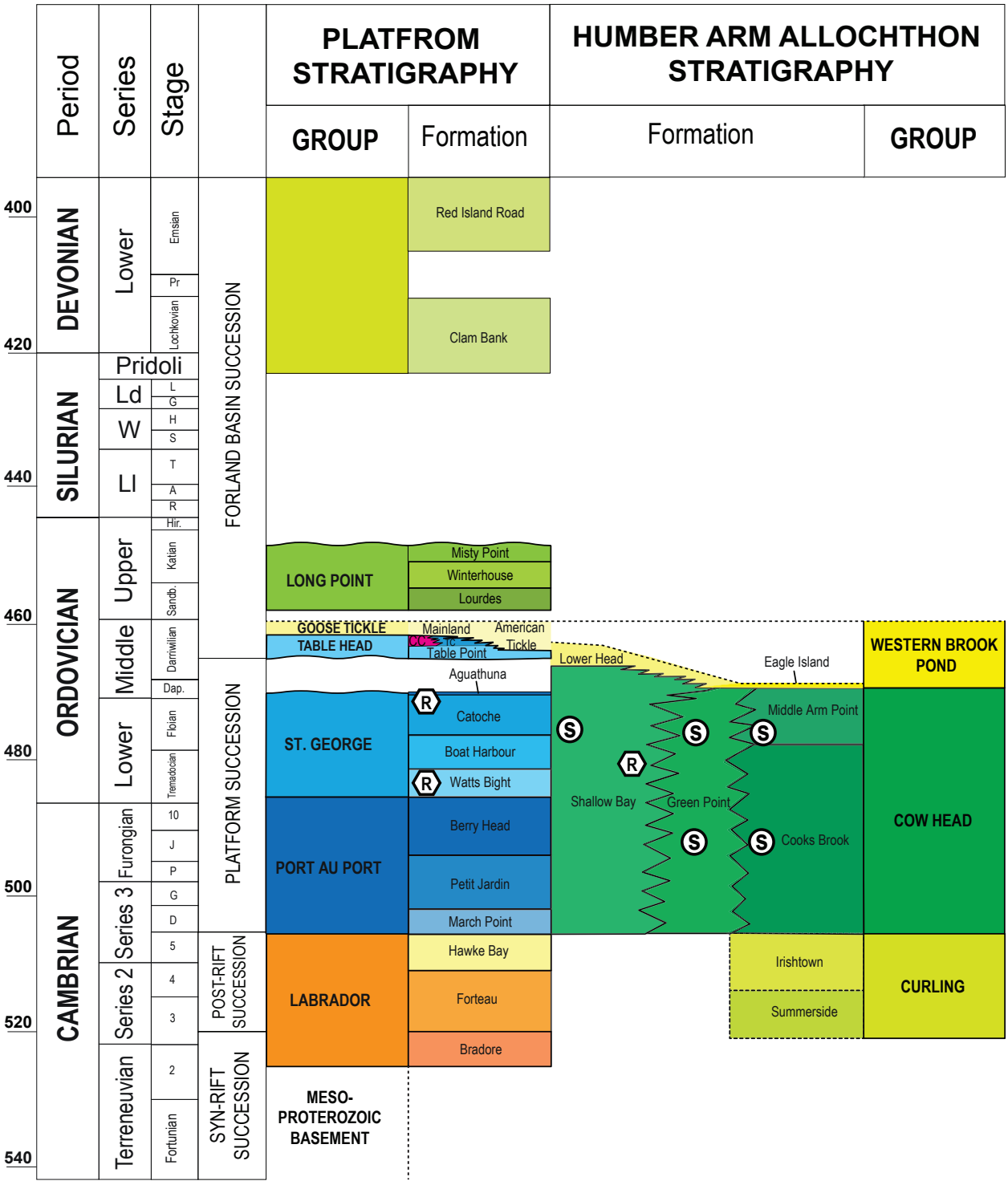

Figure 2.3: Stratigraphic table of western Newfoundland.
Abbreviations: CC=Cape Cormorant Conglomerate; TC= Table Cove; R=Reservoir; S= Source Rock. Dating of the strata is based on biostratigraphic ages from trilobites, conodonts and graptolites from Bergström et al. (1974), James and Stevens (1986), Botsford (1987), Knight and Boyce (1987), Knight and Boyce (1991), Lindholm and Casey (1989), Boyce et al. (1992), Quinn et al. (1999), Burden et al. (2001), Cawood and Nemchin (2001), Cawood et al. (2001), Burden et al. (2002), Zhang and Barnes, (2004), Quinn et al. (2004), Batten Hender and Dix (2008), and Maletz et al. (2011), Peng et al. (2012), White et al. (2012), Lacombe (2017).

Because rocks in the Port au Port, St. George Group, and the basal unit of the Table Head Group have similar geophysical properties, they are combined in seismic interpretation and termed 'platform succession' (Figure 2.1) (Waldron et al., 1998).

2.2.2.2. Stratigraphy of the Allochthon

The continental slope and rise deposits were formerly subdivided into Cow Head Group (James and Stevens, 1986) and the more distal Northern Head Group (Botsford, 1987). The Cow Head Group consists of the proximal Shallow Bay Formation and more distal Green Point Formation; the Northern Head Group is divided into Cooks Brook Formation and overlying Middle Arm Point Formation (James and Stevens 1986; Botsford, 1987). Field observations demonstrate that the proximal part of the Northern Head Group is lithologically similar to the distal part of the Cow Head Group, suggesting that the Cooks Brook Formation and Middle Arm Point Formation can be incorporated into the Cow Head Group as a more distal part of the continental slope and rise sediments (Lacombe, 2017). I propose to include the Northern Head Group in the Cow Head Group, while maintaining the formation level distinction, as the formations represent mappable units, and are well defined in their type locations. This simplified stratigraphic classification is shown in Figure 2.3.

The continental slope and rise sediments represent sediment gravity flow deposits associated with pervasive passive margin instabilities and repeated margin collapse (James and Stevens, 1986; Botsford, 1987; Weaver, 1988; James et al., 1987).

2.2.2.3. Flysch Sediments

Allochthonous Lower Head sandstone stratigraphically overlies the Cow Head Group (James and Stevens, 1986). Field observations demonstrate that the time-equivalent Eagle Island sandstone, found in the Bay of Islands and defined by Botsford (1987), contains the same allochthonous source material (Lacombe, 2017). I propose to combine the Lower Head and Eagle Island sandstones within the Western Brook Pond Group, a term abandoned by James and Stevens (1986), and revived by Lacombe (2017), retaining the formation level distinction (Figure 2.3).

The autochthonous Goose Tickle Group stratigraphically overlies the Table Head Group,

and consists of three formations (Quinn et al., 1992a). The Black Cove Formation, composed of grey and green shales with minor siltstone (Stenzel et al., 1990). The gradational boundary to the overlaying American Tickle Formation is defined by a lithology where more than one third of the strata consists of green siltstone (Stenzel et al., 1990). The American Tickle Formation comprises siltstones with lesser sandstone and carbonate conglomerate beds, and represents the main part of the Goose Tickle Group (Quinn, 1992b).The American Tickle Formation contains graptolites from Darriwilian 3 with no upper contact found. The overlaying Mainland Formation consists of sandstone with siltstone and mudstone interbeds. According to Quinn et al. (1992a, 1995) the Mainland Formation is locally restricted to the Port au Port Peninsula and contains graptolites from Darriwilian 3 with no upper contact found.

2.2.2.4. Post-Taconian Foreland Deposition

Post-Taconian foreland basin deposits occur in the Long Point Group, which is subdivided into Lourdes, Winterhouse, and Misty Point Formations. The Lourdes Formation represents peritidal, fossil rich marine limestone mixed with siliciclastics deposited in an overall deepening upward trend in the Sandbian (Quinn et al., 1999; Batten Hender and Dix, 2008). A transitional contact with the overlaying Winterhouse Formation, which consists of storm dominated siltstones, sandstones, and minor limestone and limestone conglomerate, is interpreted to result from the gradual deepening of the basin (Quinn et al., 1999). This is overlain by medium- to coarse-grained red sandstone of the Misty Point Formation (Quinn et al., 1999).

2.2.3. Hydrocarbon Source Rocks

Prior to this study, a small number of potential source rocks samples from western Newfoundland were analyzed by Macauley (1987, 1990), Weaver (1988), Weaver and Macko (1988), Sinclair (1990) and Fowler et al. (1995). These studies included samples collected from the most promising shale intervals in the Port au Port and Cow Head area. These samples show a wide range of hydrocarbon potential from marginal to excellent (Table 2.1). Weaver and Macko (1988) interpreted the dataset collected by Weaver (1988) and concluded that the Ordovician Green Point Formation was the most likely source for the oils collected from Parson's Pond and

St. Paul's Inlet, located just South of Parson's Pond. Average total organic carbon (TOC) values were reported at 4.21 wt% and average hydrogen indices (HI) at 471 with low oxygen indices (OI). Macauley (1987, 1990) and Fowler et al. (1995) reported similar values for the Green Point Formation in the Cow Head area (Table 2.1). Source rock characteristics for the shelf-proximal Shallow Bay Formation reported in Sinclair (1990), cited in Fowler et al. (1995), show TOC values between 0.76 wt% and 2.18 wt%, and HI values ranging from 188 to 382 with generally low OI values (Figure 2.4A). The richest source rocks from the Port au Port Peninsula are reported from the most distal portion of the Cow Head Group, formerly assigned to the Green Point Formation but now interpreted as Middle Arm Point Formation (Lacombe, 2017). Macauley (1987, 1990) and Fowler et al. (1995) reported high TOC intervals (max. 10.35 wt%), high HI (max. 759) and low OI values for those units. Fowler et al. (1995) concluded that the Paleozoic algae *Gleocapsomorpha prisca* (*G. prisca*), found in their Cambrian to Ordovician samples, were responsible for type I/II organic matter. This is supported by an odd-to-even carbon number preference found in their oil samples (Fowler et al., 1995).

Table 2.1: Compiled source rock characteristics.
Analysis results from previous studies reporting average (av.) values for TOC, HI and OI. CH = Cow Head area; PaP = Port au Port area; HAA = Humber Arm Allochthon.

Formation	Number of samples	TOC av.	HI av.	OI av.	Authors
Green Point CH	15	4.21	471	17	Weaver 1988, Weaver and Macko, 1988
Green Point CH	3	4.61	605	17	Macauley, 1987, 1990
Green Point CH	5	3.65	356	9	Fowler et al., 1995
Green Point PaP	3	8.13	712	8	Macauley, 1987, 1990
Green Point PaP	4	6.41	576	5	Fowler et al., 1995
Shallow Bay	4	0.90	300	4	Weaver 1988, Weaver and Macko, 1988
Shallow Bay	2	1.75	303	50	Sinclair, 1990
Shallow Bay	1	1.21	379	8	Fowler et al., 1995
Table Head	6	0.55	270	28	Weaver 1988, Weaver and Macko, 1988
Table Head	1	0.61	215	13	Fowler et al., 1995
Black Cove	2	0.99	218	19	Sinclair, 1990
Black Cove	1	0.84	312	36	Fowler et al., 1995
HAA undivided	2	1.06	363	36	Macauley, 1987, 1990
Table Cove	1	0.82	290	58	Sinclair, 1990
Mainland	4	5.95	552	13	Fowler et al., 1995
Curling	1	1.20	354	7	Fowler et al., 1995

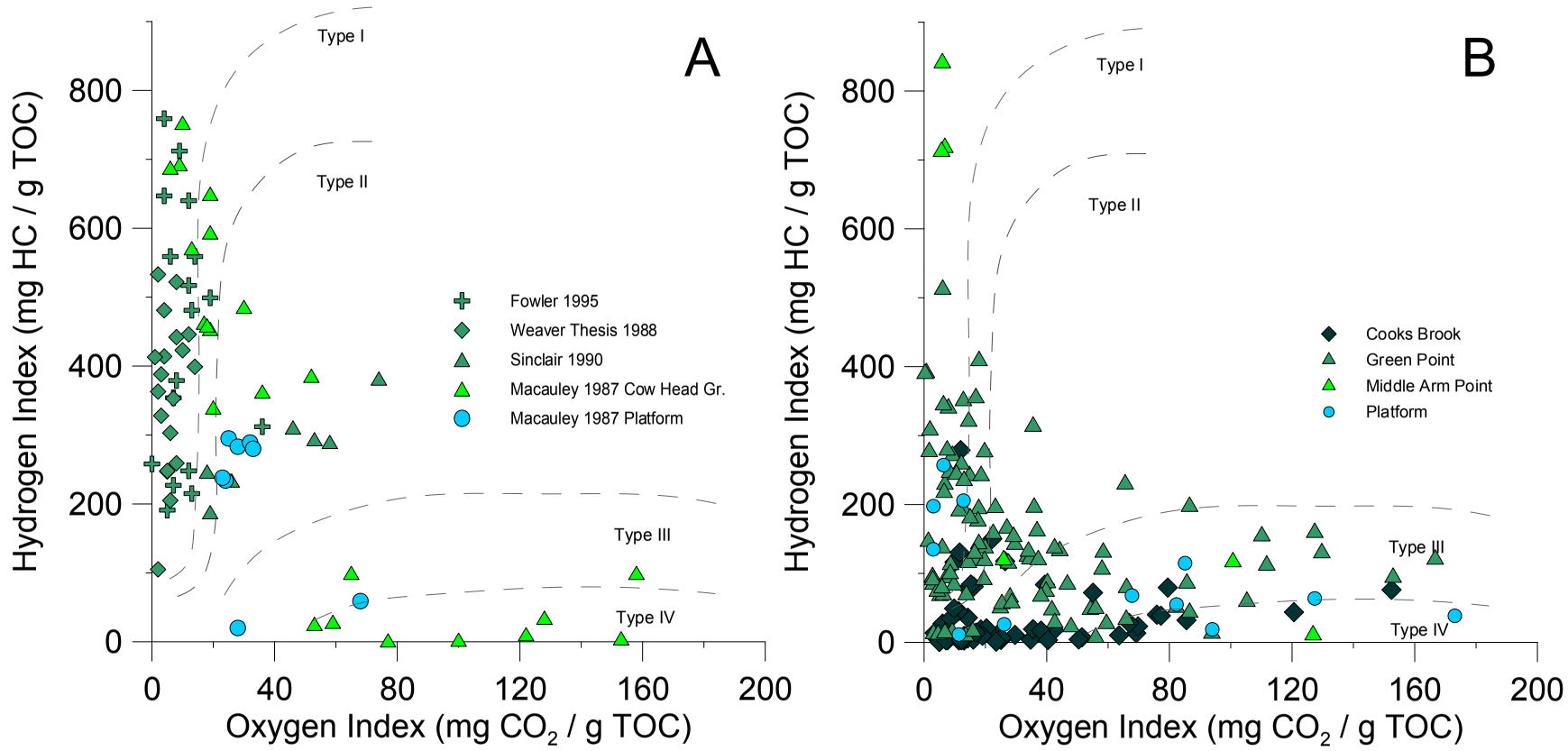

Figure 2.4: Pseudo-van-Krevelen diagrams from previous work (A) and this study (B).
A: Pseudo van Krevelen diagram showing Hydrogen Index (HI) versus Oxygen Index(OI) from previous studies; symbols with green color illustrate source rocks from the Cow Head Group, samples in blue represent platform rocks. B: Pseudo van Krevelen diagram from source rocks collected along the western coast of Newfoundland including 170 km of coastal outcrop from the Port au Port Peninsula area, Bay of Island to the Cow Head area. Samples were collected from the Cow Head Group and Table Head Group (platform). Different shades of green represent different formations within the Cow Head Group. Platform samples are represented in blue.

2.3. Geochemical Sampling

2.3.1. Source rocks

Our dataset includes analyses of 197 source rock samples collected systematically from measured sections in outcrop and from available core. Measured sections from James and Stevens (1986), Botsford (1987) and Lacombe (2017) were used to provide a representation of the proximal to distal variation along the continental slope and rise deposits. These measured sections are reasonably well constrained by biostratigraphic work (James and Stevens, 1986; Botsford, 1987; Lacombe, 2017). They are located along the coast, from Green Point to Cow Head (Green Point and Shallow Bay Formation), the Bay of Islands (Cooks Brook and Middle Arm Point Formation), and the Port au Port Peninsula (Middle Arm Point Formation) (Figure 2.5).

2.3.2. Oils

Seventeen oil and bitumen samples were collected (Table 2.2). The dataset includes 11 oil samples from natural oil-seeps and old, accessible well sites along the coast, and six bitumen samples from quarries. Sample location are shown in Figure 2.5. An additional five tar samples were collected along the coast. Upon analysis, the tar samples were found to be discharge from ships and are therefore excluded from further discussion.

2.3.3. Sampling Methods

2.3.3.1. Source Rocks

Samples were taken every 3-5 m along measured sections, with finer spacing (1 m) in black shale lithologies. To minimize the impact of weathering, I collected samples as far from any adjacent water as possible and obtained freshly broken samples whenever possible. Additionally, all samples were cleaned to prevent contamination by recent organic matter.

In the 2015 field season minor modifications were made to Botsford's original (1987) measured sections in the Bay of Islands to account for parts of the sections that had eroded, and to add additional detail on sedimentary structures. The most extensively sampled area between Green Point and Cow Head includes measured sections from James and Stevens (1986) on Mar-

Table 2.2: Location of oil, bitumen and tar samples.

	Area	Sample ID	Well Name/Location	UTM Easting	UTM Northing
Bitumen	Port au Port	SM034A	West Bay	355086	5386933
		SM036A	Aguathuna	366159	5380192
		SM033A	Tea Cove	356194	5390914
		SM039B	Two Guts Pond	376861	5388097
	Green Point	SM053B	Green Point	442198	5521295
	St. Pauls Inlet	SM050B	St. Paul Quarry	430352	5503851
Oil	Port au Port	SM038	Port au Port #1	335490	5372856
		SM072A	Shoal Point	363778	5386982
	St. Pauls Inlet	SM055A	Fox Well	442619	5520723
	Parsons Pond	SM057A	Sandy Point	453704	5536605
		SM058	Well #7	456884	5535944
		SM060	Oil Point #2	457844	5537994
		SM062	Highland Brook 1	454753	5539277
		SM063A	Highland Brook 2	454448	5539167
		SM065	Highland Brook W3	454408	5538817
		SM066	Highland Brook W1	454270	5538364
		SM067	Highland Brook W2	454282	5538382

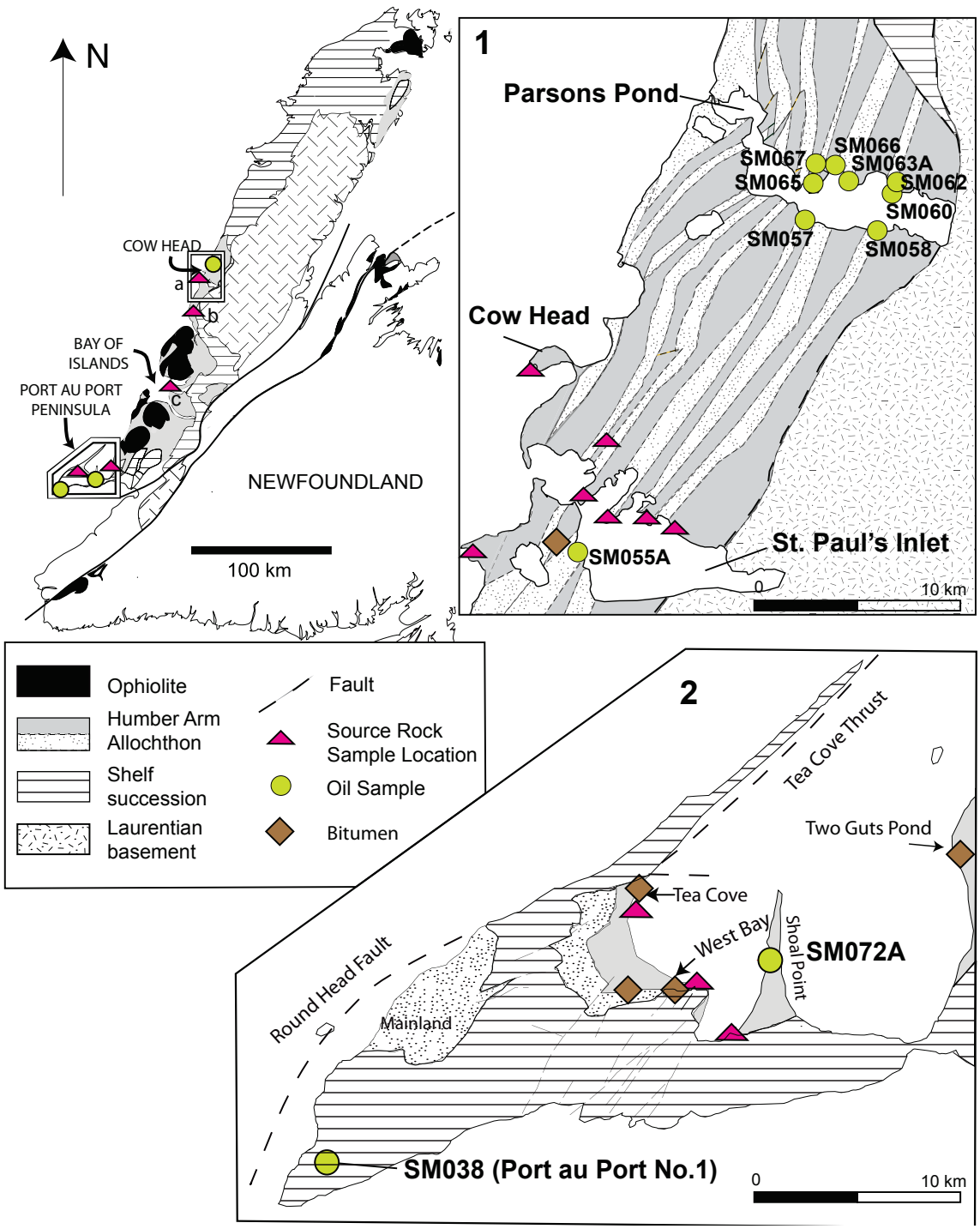

Figure 2.5: Overview map with main sample location for oil and source rocks.
Map 1, 2 show main sample location in more detail. Map 1 is based on unpublished work by Shawna White (2017); map 2 is modified after Cooper et al. (2001), the base map is modified after Waldron et al. (2003). 1: Parson's Pond sample location, including eight individual oil samples (green circles). St. Paul's Inlet sample location, including one oil sample (green circle) and 115 source rock samples from seven different measured sections (James and Stevens, 1986). b: Measured section from Green Point is shown w on the overview map (pink triangle). c: Northern Head sample location including 34 individual source rock sample (pink triangle) from measured sections from Botsford (1987). 2: Port au Port Peninsula sample location, including two individual oil samples and 35 source rock samples (pink triangles) from measured sections from Lacombe (2017).

tin Point, Green Point, Broom Point, St. Paul's North, Long Point, Black Brook, The Scrape, and The Point of the Head on Cow Head Peninsula. The Scrape measured section was modified from the original by James and Stevens (1986), due to the erosion of 30 m of outcrop subsequent to the original work. Detailed measured sections with sample locations are listed in Appendix B.

2.3.3.2. Oil and Bitumen

Nine oil samples were collected from abandoned drill sites where oil was found above water in the well bore. To avoid contamination by other petroleum based materials, I collected samples in individual glass bottles tied to yarn. Bitumen samples found on beach outcrops (four) and in quarries (two) were collected with a clean knife (washed with water and acetone) and stored in glass vials to prevent contamination. Two samples were collected from natural seeps using individual glass vials. One was highly viscous and was collected with a clean knife; the other was collected mixed with water and afterwards decanted to separate the oil from water.

2.3.4. Analytical Methods

Source rock samples were analyzed for TOC by LECO analysis at GeoMark Research LLC (Houston). Samples were decarbonated, dried, and weighed to obtain a percent carbonate value based on weight loss. The LECO C230 instrument was calibrated by combustion of standards at 1200°C in the presence of oxygen. The generated and catalytically converted carbon dioxide was measured using an infrared cell. Combustion of samples was completed and compared to the calibration standard to determine TOC. The acceptable standard deviation for TOC is 3% variation from established value. Additionally, approximately 100 mg of washed, ground (60 mesh) whole-rock sample was analyzed in the Rock-Eval II instrument. Organic-rich samples (S2>40.0 mg/g or TOC>7-8%) were analyzed at reduced weight. Operating conditions for Rock-Eval II are: 300°C for 3 minutes (S1), 300°C to 550°C at 25°C/min then hold at 550°C for 1 minute (S2), and S3 is trapped between 300 and 390°C. Instrument calibration was achieved by using an in-house rock standard made from Skull Creek Shale (S1 = 0.21, S2 = 9.02, S3 = 0.40, T_{max} = 418) (Brian Jarvie - GeoMark, personal communication). The standard deviation was considered acceptable under the following guidelines: T_{max} ± 2°C, and S1 ± 10%, S2 ± 10%, and S3 ± 20% variation from established value. Selected and random checks were completed on approximately 10% of the samples for both TOC and Rock-Eval analysis to ensure the standard deviation fell within the proposed margin.

Molecular compositions and stable isotopes for oil, bitumen, and extract samples were analyzed by GeoMark Research Ltd. Whole crude oils were injected in split mode and separated in a J&W DB-5 column (temperature programed from -60°C to 350°C at 12°C/min using an Agilent 7890A gas chromatograph with a flame ionization detector - FID). Helium was used as the carrier gas. Crude oils were injected into an Anton Par DMA 500 density meter, and API gravity was calculated using the "API Gravity @60°F" method. This process was triplicated for each sample to assess accuracy and reproducibility. Whole oils were measured on a vario ISOTOPE select elemental analyzer for wt% sulfur via the process of Dumas combustion.

After the <C15 fraction was separated by evaporation in a stream of nitrogen, and deas-

phalted using excess n-hexane, the C15+ deasphalted fractions were separated using temperature-activated (400°C) gravity-flow column chromatography with a 100-200 mesh silica gel support. Hexane was used to elute the saturated hydrocarbons, methylene chloride to elute the aromatic hydrocarbons, and methylene chloride/methanol (50:50) to elute the nitrogen-sulfur-oxygen (NSO) fraction. Following solvent evaporation, the recovered fractions were quantified gravimetrically. The C15+ saturated hydrocarbon fraction was subjected to molecular sieve filtration (Union Carbide S-115 powder), after the technique described by West et al. (1990), in order to concentrate the branched/cyclic biomarker fraction. GC/MS analysis of C15+ branched/cyclic and aromatic hydrocarbon fractions was performed using an Agilent 7890A GC interfaced to a 5975C mass spectrometer at a constant flow rate. The J&W HP-5 column was temperature-programmed from 150°C to 325°C at 2°C/min for the branched/cyclic fraction, and 100°C to 325°C at 3°C/min for the aromatic fraction. The mass spectrometer ran in the selected ion mode (SIM). In order to determine absolute concentrations of individual biomarkers a deuterated internal standard (d4-C29 20R Ethylcholestane; Chiron Laboratories, Norway) was added to the C15+ branched/cyclic hydrocarbon fraction, and a deuterated anthracene standard (d10) was added to the aromatic hydrocarbon fraction. Response factors (RF) were determined by comparing the mass spectral response at m/z 221 for the deuterated standard to hopane (m/z 191) and sterane (m/z 217) authentic standards. These RF were found to be approximately 1.4 for terpanes and 1.0 for steranes. Concentrations of individual biomarkers in the branched/cyclic fraction were determined using the equation shown below:

Conc.(ppm) = [(ht. biomarker)(ng standard)]/[(ht. standard)(RF)(mg b/cy fraction)]

Bulk stable carbon isotopic compositions ($^{13}C/^{12}C$) of whole oils and C15+ saturate and aromatic hydrocarbon fractions were measured on an Isoprime vario ISOTOPE select elemental analyzer and VisION isotope ratio mass spectrometer (IRMS). Results are reported relative to Vienna Pee Dee Belemnite (VPDB).

GC/MSMS was performed on an Agilent triple quadrapole mass spectrometer (QQQ) interfaced with an Agilent 7890. GC/MSMS provides quantitative analyses of whole oils and

extracts for terpane and sterane biomarkers as well as diamondoids, carotenoids, and alkyl aromatics. The alkyl aromatics allow for a prediction of the level of thermal maturity (in units of vitrinite reflectance equivalent (VREQ), even for light oils and condensates that have lost the usual biomarkers.

2.3.5. Statistical Analysis

Hierarchical cluster analysis (HCA) and principle component analysis (PCA) were employed to evaluate the multivariate dataset and identify groupings among the sample sets. Results were compared to the associated gas chromatograms to cross reference their accuracy. To deconvolve mixing between oil samples, alternating least square (ALS) analysis using sterane and terpane concentrations was used.

Sterane and terpane ratios and concentrations were used in HCA, PCA, and ALS analysis. PCA is an automated eigenvector analysis that includes an auto-scaling process to ensure the same significance for each parameter. HCA includes an auto-scaling process followed by an iterative calculation of Euclidian distances and agglomerative linkage calculation to establish clusters. The distances represent a measure of the similarity between individual samples. Six different linkage methods were employed (single link, complete link, centroid link, median link, flexible link, and incremental link) to evaluate the quality of the generated clusters. ALS was employed to deconvolve mixed oil samples; this also includes an autoscaling process. Algorithm settings for ALS were set to: ‘non-negativity for amounts and profiles’, ‘closure of amounts’, and ‘initial estimates from rows’. The same statistical methods were used for source rock extracts. However, the ASL analysis was unsuccessful due to limited data points.

2.4. Geochemical Results

2.4.1. Source Rock Samples

2.4.1.1. Port au Port Area

Thirty-five samples were collected and analyzed from the Port au Port area. Four samples from the Middle Arm Point Formation (Middle Ordovician) show TOC concentrations from 7.37 wt% to 9.45 wt% and HI values from 712 to 841 (Figure 2.6). Similar and even higher TOC values (7.19 to 10.35 wt%) were measured by Fowler et al. (1995) in samples collected from a boulder at Tea Cove, Port au Port Peninsula. Samples from the Table Cove Formation yield lower TOC average 0.63 %, yet smell strongly of hydrocarbons on broken surfaces. Using T_{max} to calculate vitrinite reflectance (%R_c), values lie between 0.65 to 0.89 %R_c (Table 2.3).

2.4.1.2. Bay of Islands

Thirty-four samples were collected and analyzed from Cooks Brook and Middle Arm Point Formation, Cow Head Group in the Bay of Islands (Cambrian Series 3 to Middle Ordovician). Three additional samples were collected from the underlying Summerside Formation, Curling Group (Cambrian Series 3). TOC values for the organically richer intervals range between 0.5 to 2.21 wt% (Table 2.3 and Figure 2.6). All samples show low S1 and S2 peaks, and depleted HI and OI values. This, in combination with extremely high T_{max} data and high Production Indexes (PI), suggests an overmature source rock.

For the remainder of the paper I use “middle to upper Cambrian” informally to refer to the approximately equivalent Cambrian Series 3 to Furongian on the timescale of Peng et al. (2012).

2.4.1.3. Cow Head Area

One-hundred-fifteen samples from seven measured sections were collected from the Cow Head area. The formations sampled include the Green Point Formation and Shallow Bay Formation, representing depositional settings ranging from proximal to distal continental slope and rise. There are two potential source rock intervals in the Green Point Formation (Figure 2.6). The middle to upper Cambrian Green Point Formation shows TOC values from 0.06 wt% in the

organically lean rocks, up to 1.71 wt% in the richer intervals. This is comparable to data reported by Weaver (1988) and Sinclair (1990), but substantially lower than reported TOC measurements from Macauley (1987), Macauley et al. (1990), and Fowler et al. (1995). The second potential source rock interval is the Middle Ordovician Green Point Formation, with TOC values ranging from 0.06 wt% in lean rocks, to 2.95 wt% in richer source rock intervals. The average TOC of the 115 samples is 0.63 wt%. Key parameters are shown in Figure 2.6 and Table 2.3.

Table 2.3: Rock-eval and TOC results for selected samples.

Extract Sample	Formation	Age	TOC (wt%)	S1 (mg HC/g)	S2 (mg HC/g)	S3 (mg CO2/g)	Tmax (°C)	%Ro (RE TMAX)	HI (S2x100/TOC)	OI (S3x100/TOC)	Potential (S1+S2)	PI (S1/(S1+S2)
PA009A	Table Head	Middle Ordovician	0.33	0.17	0.65	0.01	444	0.83	198	3	0.82	0.21
PA049A	Shallow Bay		1.82	1.39	6.57	0.29	441	0.78	361	16	7.96	0.17
SC003A	Middle Arm Point		9.07	3.05	76.25	0.54	435	0.67	841	6	79.30	0.04
SC004A	Middle Arm Point		9.45	3.45	67.83	0.64	434	0.65	718	7	71.28	0.05
SC005A	Middle Arm Point		7.37	3.07	52.49	0.42	434	0.65	712	6	55.56	0.06
SM056D	Green Point		1.17	0.41	3.75	0.17	441	0.78	321	15	4.16	0.10
SM064A	Green Point		1.47	0.41	4.06	0.29	439	0.74	276	20	4.47	0.09
SM068B	Shallow Bay		2.25	2.26	7.98	0.38	447	0.89	355	17	10.24	0.22
SM068D	Shallow Bay		2.12	1.12	8.66	0.38	440	0.76	408	18	9.78	0.11
SM078D	Green Point		0.67	0.28	1.62	0.07	444	0.83	244	11	1.90	0.15
SM078H	Green Point		2.95	0.71	11.50	0.01	441	0.78	390	0	12.21	0.06
SM077M	Green Point	Early Ord.	1.74	0.59	5.99	0.11	443	0.81	344	6	6.58	0.09
SM078L	Green Point		2.47	0.66	12.65	0.15	443	0.81	512	6	13.31	0.05
SM079D	Green Point		0.53	0.23	1.48	0.04	439	0.74	279	8	1.71	0.13
PA032A	Green Point	Middle – Late Cambrian	0.95	0.21	2.48	0.02	439	0.74	260	2	2.69	0.08
PA050A	Shallow Bay		0.67	0.44	1.52	0.16	442	0.80	228	24	1.96	0.22
SM052C	Green Point		1.09	0.34	3.04	0.13	439	0.74	279	12	3.38	0.10
SM054A	Green Point		1.44	0.42	5.63	0.12	439	0.74	391	8	6.05	0.07
SM054D	Green Point		1.51	0.45	5.13	0.12	442	0.80	340	8	5.58	0.08
SM054P	Green Point		1.17	0.28	4.10	0.15	436	0.69	350	13	4.38	0.06
SM054S	Green Point		0.86	0.20	2.34	0.08	437	0.71	271	9	2.54	0.08
SM077B	Green Point		1.19	0.35	3.29	0.02	446	0.87	276	2	3.64	0.10
SM077E	Green Point		0.91	0.22	2.34	0.11	446	0.87	259	12	2.56	0.09

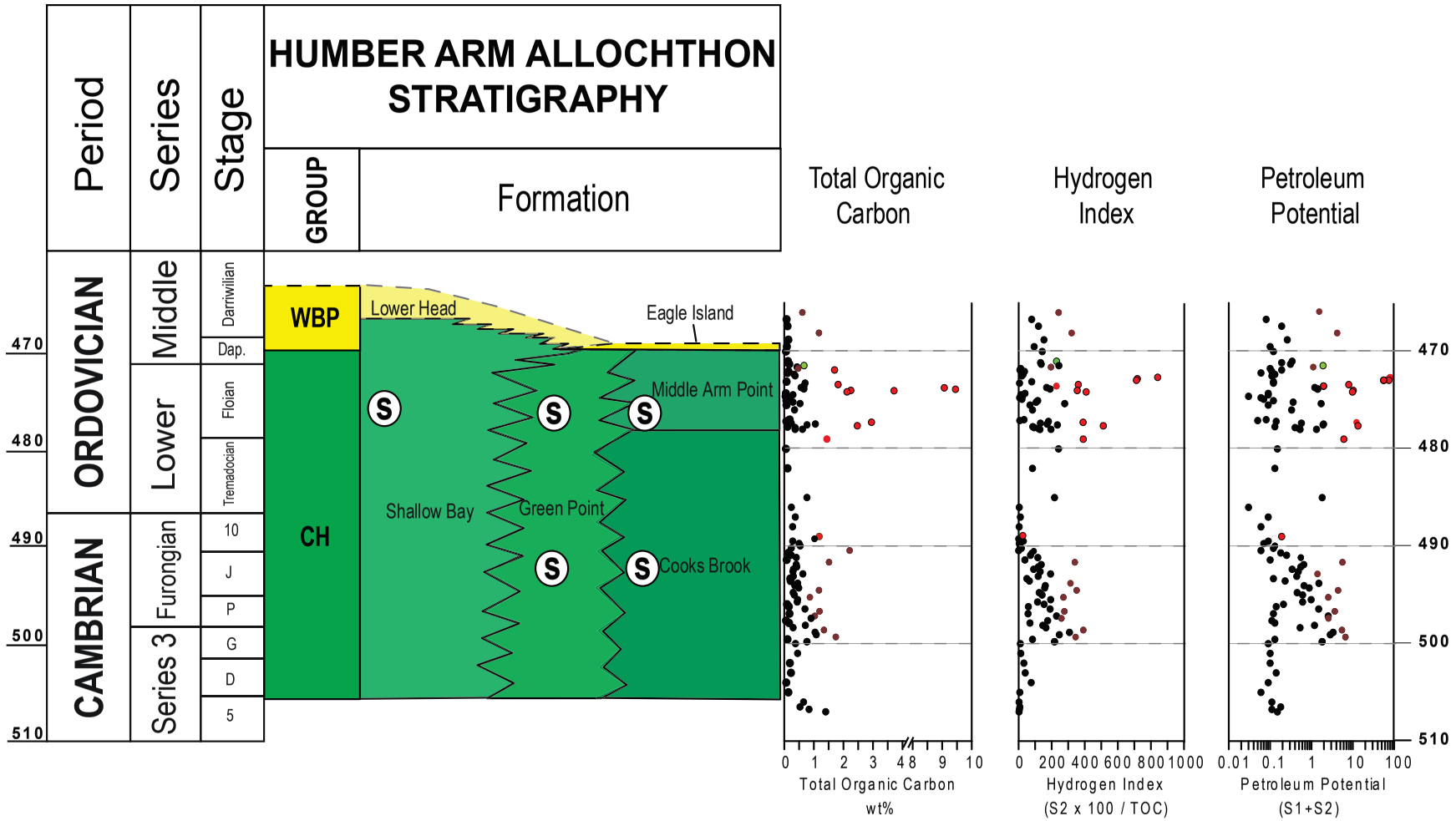

Figure 2.6: Pyrolysis analysis identifying two potential source intervals.
A middle to upper Cambrian and a Middle Ordovician interval characterized by high TOC wt%, Hydrogen Index and Petroleum Potential (S1+S2). S= Source rock; R = Reservoir; WBP = Western Brook Pond Group; CH = Cow Head Group. Samples selected for extract analysis are highlighted in red and green (Ordovician cluster) and brown (Cambrian cluster) (Figure 2.18).

2.4.2. Source Rock Extract Samples

Extracts from 23 source rocks and hydrocarbon-stained rocks were analyzed for biomarker and stable isotopes. The largest set of samples originates from the Cow Head Group (middle Cambrian to Middle Ordovician), while other samples came from the Table Head Group (Middle to Upper Ordovician), and one sample of oil-stained sandstone was taken from the Western Brook Pond Group (Middle Ordovician). Table 2.4 shows bulk composition of the extracted hydrocarbons, including important isoprenoid ratios, sulfur content carbon isotope values, carbon preference index (CPI), odd to even preference (OEP), and extracted organic matter (EOM).

The samples are relatively low in saturated hydrocarbons (4.35 to 44.44 wt%) and higher in aromatic (11.43 to 46.88 wt%) and NSO compounds (24.65 to 69.57 wt%) (Figure 2.8). Higher sulfur content is linked to higher NSO concentrations in the extracts. The source-dependent CPI is uncharacteristically low for Ordovician sample extracts; usually Ordovician samples show a clear enrichment in the uneven hydrocarbon chain lengths (e.g. Martin et al., 1963; Fowler and Douglas, 1984; Reed et al., 1986; Longman and Palmer 1987; Hoffmann et al., 1987; Jacobson et al., 1988; Douglas et al., 1991; Blokker et al., 2001). The carbon isotope values for whole extracts range from -28.46 to -32.36‰ (VPDB), and fall into the established isotope range for Paleozoic hydrocarbons (Sofer, 1984; Hatch et al., 1987; Andrusevich et al., 2000) (Figure 2.9). There was insufficient sample material for compound-specific isotope analysis. Extracted organic matter ranges from 352 to 5146 ppm. A clear positive correlation between S1 and the amount of EOM exists. Additionally, the Middle Ordovician samples (Middle Arm Point Formation and Green Point Formation) show higher amounts of EOM (average = 2104 ppm) when compared to the Cambrian samples (average = 623 ppm).

Key biomarker parameters in source rock extracts from Newfoundland that change significantly from the Cambrian to the Ordovician are summarized in Table 2.5 and Table 2.6. On average, all source rock extracts are relatively high in C27 steranes (25.06 to 35.52%) and low in C28 steranes (20.19 to 25.79%). Sterane concentrations have been shown to be facies dependent, but show some overlap in different depositional environments (Moldowan et al., 1985).

Cambrian source rocks (lower Green Point Formation) yield extracts that are dominated by tricyclic terpanes and have high 18α,21β-22,29,30-trisnorhopane (Ts) concentrations, but low sterane concentrations. These molecules have also been shown to be facies dependent (Peters and Moldowan, 1993).

Other facies-dependent parameters have been identified by many researchers (Hughes, 1984; Palacas et al., 1984; Tissot and Welte, 1984; Moldowan et al., 1985; Connan et al., 1986, Riolo et al., 1986), and while these can be found in extracts analyzed from the Ordovician (Upper Green Point Formation, Shallow Bay Formation, Middle Arm Point Formation) and Cambrian intervals (Green Point Formation, Cooks Brook Formation), they tend to be higher in the Ordovician sample extracts. Specifically, Ordovician extracts are characterized by high sterane/hopane ratios, odd to even preference indices (OEP), TET/C23, C29%, C26(R+S)/Ts, dibenzothiophene (DBT), and aryl isoprenoids (Figure 2.7). The Ordovician sample extracts are also higher in terpane and aromatic biomarkers, which are both source and maturity-related parameters (Radke et al., 1982, 1984; McKirdy et al., 1983), including high Ts/Tm ratios, phenanthrene (P), and methylphenanthrenes and associated isomers (3-MP, 2-MP, 1-MP, 9-MP). Because the analyzed sample extracts show similar maturities, the variation in biomarker concentrations known to be maturity and source dependent can be largely ascribed to changes in source composition. Sterane and terpane concentrations used in statistical evaluation of the extract samples are summarized in Table 2.7, Table 2.8, and Table 2.9.

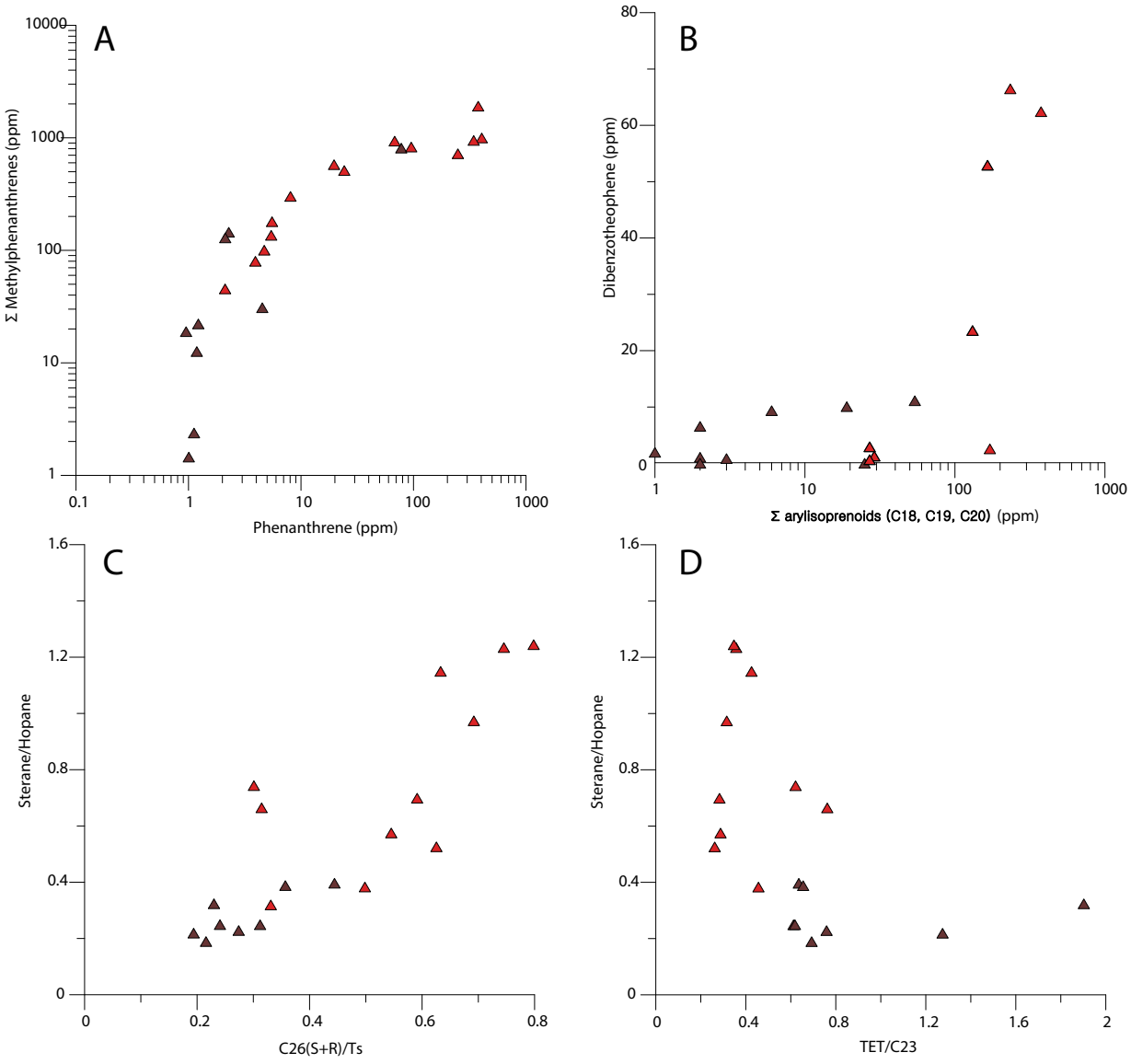

Figure 2.7: Selected graphs for source parameter for Cambrian (brown triangles) and Ordovician (red triangles) sample extracts.
A: The sum of methylphenanthrenes (3-MP, 2-MP, 1-MP, 9-MP) versus phenanthrene concentrations showing substantially higher concentrations in Ordovician samples than in Cambrian samples.
B: Dibenzothiophene (DBT) concentrations versus the sum of C18, C19, C20 arylisoprenoids shows substentially lower concnetrations in Cambrian samples compared to Ordovician samples.
C: Source dependent sterane/hopane to C26(R+S)/Ts shows lower ratios for Cambrian samples compared to Ordovician samples.
D: Source dependent ratios show higher sterane/hopane ratios and lower TET/C23 ratios for Ordovician samples and lower sterane/hopane ratios and higher TET/C23 ratios for Cambrian samples.

Table 2.4: Bulk composition for 23 selected extracts.

Extract	Age	% S	% Sat	% Aro	% NSO	% Asph	Sat / Aro	$13C_s$	$13C_a$	$13C_{wc}$	EOM (ppm)	CPI	OEP
PA009B	Middle Ordovician	0.66	42.5	22.5	35	0	1.89	-32	-30.89	-31.24	818	1.05	1.00
PA049A		0.36	36.78	24.14	37.93	1.15	1.52	-29.81	-30.12	-30.81	1307	1.03	0.97
SC003A		0.66	20.96	40.61	37.99	0.44	0.52	-29.1	-28.01	-28.46	3763	1.22	0.96
SC004A		1.84	14.61	44.13	40.4	0.86	0.33	-29.11	-28.08	-28.46	5146	1.32	0.94
SC005A		1.06	15.5	39.15	39.15	6.2	0.4	-29.35	-28.08	-28.52	5052	1.36	1.00
SM056D		0.72	21.62	32.43	45.95	0	0.67	-31	-30.48	-30.71	819	1.15	1.02
SM064A		1.63	14.89	31.91	51.06	2.13	0.47	-31.27	-29.55	-30.59	756	1.08	1.02
SM068B		0.55	41.55	33.1	24.65	0.7	1.26	-31.46	-29.85	-30.96	1907	1.02	1.03
SM068D		0.26	44.44	20.71	34.85	0	2.15	-30.53	-29.21	-30.28	2848	1.08	1.03
SM078D		0.43	39.68	30.16	30.16	0	1.32	-30.82	-31.29	-32.06	876	1.09	1.01
SM078H		8.43	15.52	36.21	36.21	12.07	0.43	-30.81	-30.4	-30.68	1264	1.33	1.02
SM079D	Early Ord..	1.27	43.64	20	34.55	1.82	2.18	-31	-31.85	-32.32	689	1.12	1.02
SM077M		0.74	24.59	39.34	32.79	3.28	0.62	-30.2	-28.93	-29.59	1072	1.20	0.99
SM078L		0.69	22.12	39.42	38.46	0	0.56	-29.57	-28.69	-29.18	1577	1.21	0.98
PA032A	Late Cambrian	0.49	10.53	26.32	55.26	7.89	0.4	-29.85	-28.66	-29.22	911	1.42	0.99
PA050A		0.27	32.69	23.08	44.23	0	1.42	-31.26	-31.22	-31.51	938	1.08	1.02
SM052C		1.06	34.29	11.43	54.29	0	3	-30.81	-30.23	-29.82	571	1.28	1.02
SM054A		0.81	17.24	41.38	34.48	6.9	0.42	-30.22	-29.49	-29.91	619	1.34	1.00
SM054D		1.61	9.38	40.62	50	0	0.23	-29.48	-28.93	-29.09	352	1.91	1.02
SM054P		0.74	20.93	34.88	44.19	0	0.6	-30.75	-30.63	-30.46	692	1.29	1.02
SM054S		1.51	4.35	26.09	69.57	0	0.17	-29.65	-29.73	-29.66	388	1.56	0.99
SM077B		0.96	18.6	41.86	34.88	4.65	0.44	-30.18	-29.5	-29.87	628	1.27	1.00
SM077E		2.31	12.5	46.88	40.62	0	0.27	-30.69	-30.55	-30.58	510	1.29	1.01

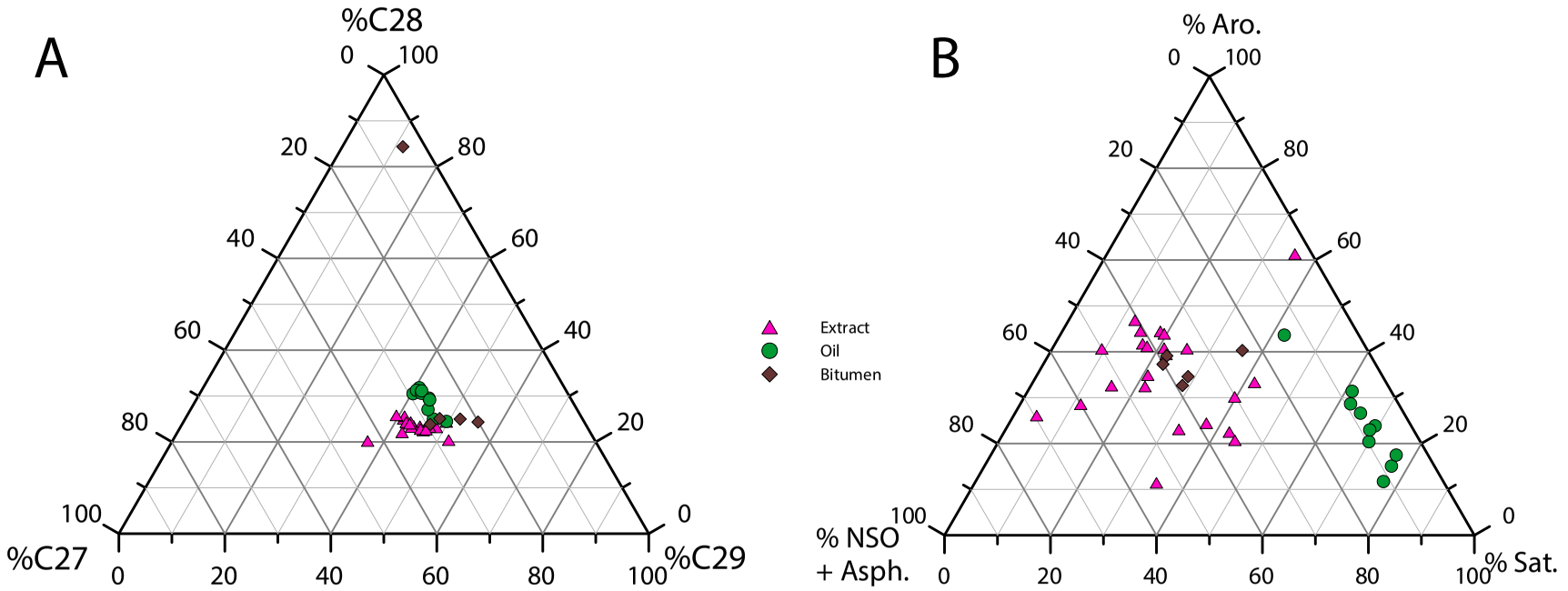

Figure 2.8: Ternary diagrams showing distribution of steranes and saturated, aromatic, and NSO plus asphaltenes.
A: Ternary diagram showing the sterane distribution of oil, extract and bitumen. B: Ternary diagram depicting distribution of saturated (%Sat.), aromatic (%Aro.) and nitrogen-sulfur-oxygen-compounds and asphaltenes (%NSO+Asph,) in oil, extract and bitumen samples.

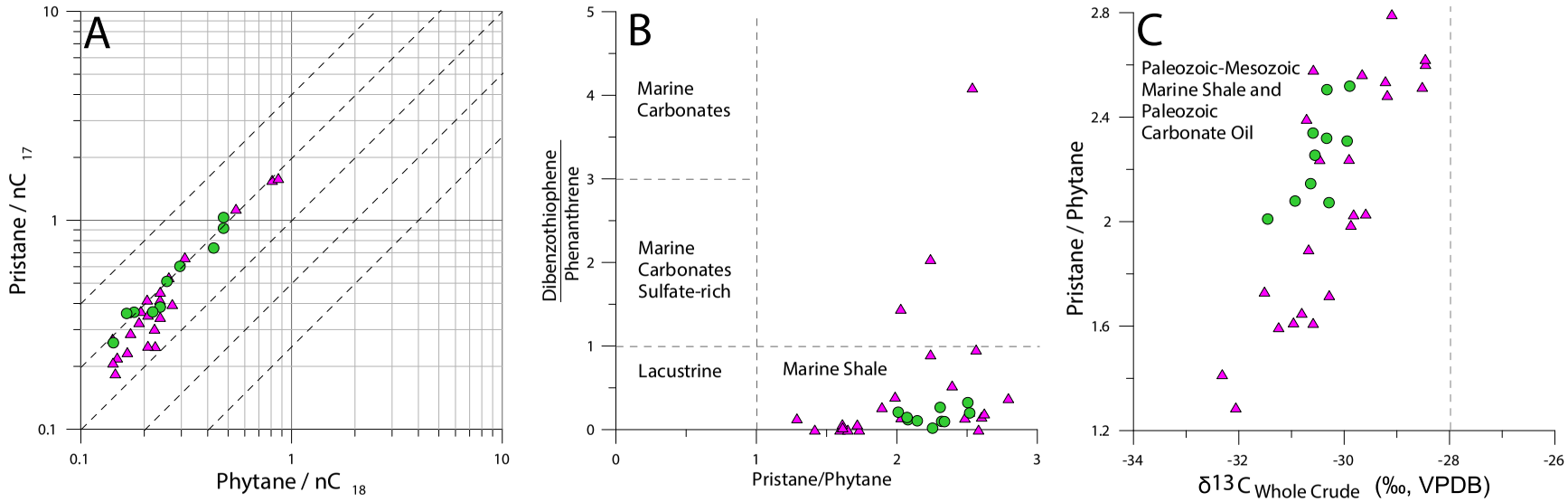

Figure 2.9: Pristane/phytane ratios plotted against different parameters to gain insight in depositional environment and age of the source. A: Pristane/nC17 versus Phytane/nC18 indicating slightly oxidizing depositional environment. B: Pristane/phytane versus Dibenzothiophene/Phenanthrene (DBT/P) indicating a marine shale as source rock (Hughes, 1984). C: Pristane/phytane versus δ13C indicating a Paleozoic age of the source rock (Chung et al., 1992).

Table 2.5: Selected sterane and terpane ratios for extract samples.
Parameters are explained in Appendix B.

Extract	Age	C19/C23	C22/C21	C24/C23	C26/C25	Tet/C23	C27T/C27	C28/H	C29/H	X/H	OL/H	C31R/H	GA/C31R	C35S/C34S	S/H
PA009B	Middle Ordovician	0.01	0.46	0.75	1.12	0.32	0.01	0.04	0.36	0.27	0.00	0.22	0.21	0.52	0.97
PA049A		0.04	0.27	0.74	0.92	0.36	0.00	0.06	0.42	0.41	0.01	0.23	0.35	0.52	1.23
SC003A		0.05	0.12	0.42	1.30	0.28	0.01	0.04	0.71	0.07	0.01	0.21	0.18	0.42	0.70
SC004A		0.04	0.11	0.42	1.21	0.26	0.01	0.06	0.70	0.08	0.01	0.18	0.14	0.42	0.53
SC005A		0.03	0.12	0.40	1.19	0.29	0.00	0.05	0.67	0.08	0.01	0.18	0.14	0.44	0.58
SM056D		0.02	0.34	0.62	1.24	0.76	0.01	0.02	0.43	0.18	0.00	0.19	0.24	0.55	0.66
SM064A		0.02	0.30	0.67	0.92	0.43	0.01	0.05	0.46	0.32	0.01	0.20	0.35	0.68	1.15
SM068B		0.10	0.22	0.73	0.94	0.35	0.01	0.05	0.39	0.30	0.01	0.23	0.29	0.48	1.24
SM068D		0.09	0.22	0.57	0.97	0.46	0.02	0.04	0.49	0.08	0.01	0.20	0.34	0.39	0.38
SM078D		-	-	-	-	-	-	-	-	-	-	-	-	-	-
SM078H		-	-	-	-	-	-	-	-	-	-	-	-	-	-
SM079D	E. Ord.	-	-	-	-	-	-	-	-	-	-	-	-	-	-
SM077M		0.04	0.22	0.60	1.14	0.59	0.02	0.01	0.56	0.07	0.01	0.15	0.16	0.56	0.32
SM078L		-	-	-	-	-	-	-	-	-	-	-	-	-	-
PA032A	Middle – Late Ordovician	0.00	0.31	0.53	1.20	0.61	0.01	0.01	0.58	0.06	0.00	0.18	0.19	0.41	0.25
PA050A		0.06	0.35	0.71	1.19	0.62	0.01	0.19	0.38	1.17	0.01	0.25	0.30	0.64	0.74
SM052C		0.00	0.55	0.64	1.19	0.65	0.01	0.02	0.51	0.06	0.01	0.17	0.22	0.58	0.39
SM054A		0.01	0.67	0.54	1.32	0.64	0.01	0.02	0.59	0.08	0.01	0.18	0.20	0.48	0.40
SM054D		0.00	-	0.88	1.59	1.90	0.01	0.01	0.69	0.05	0.01	0.19	0.17	0.00	0.32
SM054P		0.00	0.57	0.49	1.22	0.76	0.01	0.02	0.58	0.14	0.00	0.20	0.16	0.50	0.23
SM054S		0	-	0.63	1.28	1.27	0.01	0.01	0.61	0.09	0.00	0.16	0.20	0.70	0.22
SM077B		0.01	0.28	0.62	1.25	0.69	0.01	0.01	0.43	0.08	0.00	0.18	0.13	0.42	0.19
SM077E		0.01	0.43	0.69	1.38	0.62	0.01	0.01	0.46	0.15	0.00	0.18	0.18	0.91	0.25

Table 2.6: Selected sterane ratios for extract samples.
Parameters are explained in Appendix B.

Extract	Age	% C27	% C28	% C29	S1/S6	C29 20S/R	C29 bbS/aaR	C27 Ts/Tm	C29 Ts/Tm	DM/H	C26(S+R)/ Ts	C28/ C29	C27 20S/(20S+20R)	C28 20S/(20S+20R)	C29 20S/(20S+20R)	C27 bb/(bb+aa)	C29 bb/(bb+aa)
PA009B	Middle Ordovician	27.56	20.39	52.05	3.39	0.98	1.77	4.14	1.19	0.01	0.69	0.39	0.42	0.1	0.78	0.35	0.29
PA049A		30.15	23.44	46.41	2.71	0.90	1.53	2.39	1.13	0.01	0.75	0.51	0.42	0.09	0.76	0.39	0.48
SC003A		33.76	25.02	41.21	0.65	0.65	0.36	0.67	0.41	0.01	0.59	0.61	0.46	0.39	0.72	0.43	0.04
SC004A		32.63	23.49	43.88	0.69	0.67	0.36	0.65	0.41	0.01	0.63	0.54	0.44	0.44	0.76	0.35	0.02
SC005A		32.76	24.32	42.92	0.70	0.65	0.34	0.69	0.44	0.01	0.55	0.57	0.45	0.26	0.72	0.39	0.02
SM056D		42.95	20.19	36.85	3.61	0.85	1.05	2.02	0.74	0.01	0.31	0.55	0.44	0.03	0.85	0.37	0.13
SM064A		31.67	22.81	45.53	2.04	0.85	1.46	2.13	1.07	0.02	0.63	0.5	0.43	0.05	0.94	0.42	0.19
SM068B		29.74	23.25	47.02	2.26	0.92	1.60	2.27	1.06	0.01	0.80	0.49	0.42	0.15	0.83	0.41	0.13
SM068D		26.04	24.35	49.61	1.02	0.89	1.26	1.62	0.49	0.01	0.50	0.49	0.43	0.36	0.82	0.45	0.18
SM078D		-	-	-	-	-	-	-	-	-	-	-	-	-	-	-	-
SM078H		-	-	-	-	-	-	-	-	-	-	-	-	-	-	-	-
SM079D	E. Ord	-	-	-	-	-	-	-	-	-	-	-	-	-	-	-	-
SM077M		33.13	23.96	42.91	1.19	0.79	0.86	0.98	0.33	0.01	0.33	0.56	0.43	0.02	0.77	0.41	0.28
SM078L		-	-	-	-	-	-	-	-	-	-	-	-	-	-	-	-
PA032A	Middle – Late Cambrian	31.31	22.49	46.21	0.64	0.80	0.49	0.74	0.34	0.00	0.31	0.49	0.43	0.11	0.87	0.41	0.04
PA050A		31.47	23.42	45.11	5.21	0.74	1.49	3.41	1.78	0.03	0.30	0.52	0.42	0.02	0.74	0.33	0.49
SM052C		28.48	23.17	48.35	1.42	0.78	1.02	1.51	0.37	0.01	0.36	0.48	0.44	0.03	0.55	0.42	0.31
SM054A		33.19	23.23	43.58	1.21	0.67	0.60	0.83	0.40	0.01	0.44	0.53	0.43	0.03	0.85	0.4	0.07
SM054D		35.52	22.07	42.41	0.95	0.56	0.42	1.12	0.33	0.00	0.23	0.52	0.44	0.01	0.56	0.44	0.13
SM054P		33.28	25.60	41.11	0.95	0.69	0.44	1.05	0.59	0.01	0.27	0.62	0.45	0.02	0.8	0.43	0.16
SM054S		34.74	25.79	39.47	1.06	0.63	0.42	1.25	0.48	0.01	0.19	0.65	0.47	0.01	0.69	0.44	0.18
SM077B		30.71	22.68	46.61	1.04	0.92	0.91	1.32	0.47	0.01	0.22	0.49	0.43	0.04	0.85	0.43	0.11
SM077E		33.62	24.28	42.09	1.85	0.87	0.93	2.02	0.62	0.01	0.24	0.58	0.44	0.01	0.52	0.41	0.53

Table 2.7: Terpane concentrations (ppm) for extract samples.
Parameters are explained in Appendix B.

Extract	Age	C19T	C20T	C21T	C22T	C23T	C24T	C25S	C25R	TET	C26S	C26R	Ts	C27T	Tm	C28DM	C28H	C29DM	C29H	C29D	C30X	OL
PA009B	Middel Ordovician	0	0	2	1	12	9	6	6	4	6	6	18	0	4	0	2	1	14	16	10	0
PA049A		1	1	5	1	12	9	4	5	4	4	4	11	0	5	0	1	0	8	9	8	0
SC003A		1	7	21	3	25	11	5	4	7	7	6	21	1	31	1	3	1	56	23	5	1
SC004A		2	15	46	5	60	25	12	12	16	15	14	47	1	72	1	11	1	126	52	15	2
SC005A		1	9	29	4	41	17	8	8	12	10	9	34	0	50	0	7	1	91	40	11	1
SM056D		1	2	8	3	36	22	10	9	28	12	12	74	1	37	1	3	1	82	60	35	1
SM64A		1	4	20	6	61	41	22	20	26	19	19	61	1	28	0	4	1	41	44	29	1
SM68B		3	5	15	3	27	20	10	9	9	9	9	22	0	10	1	2	0	18	19	14	0
SM68D		3	8	14	3	30	17	9	9	14	8	8	33	1	21	0	5	1	56	27	9	1
SM078D		2	5	18	6	47	29	17	16	52	17	17	264	4	133	1	14	4	458	296	111	1
SM078H		0	11	13	4	52	35	12	12	38	20	20	203	2	166	4	4	5	315	169	80	4
SM077M	E. Ord.	1	3	11	2	23	14	6	6	13	6	6	38	1	39	1	2	1	68	23	9	1
SM078L		2	6	17	4	39	20	9	9	19	10	10	49	1	57	1	3	1	124	43	14	1
SM079D		0	1	3	1	11	7	4	4	9	4	4	38	1	21	0	5	1	51	51	38	0
PA032A	Middle – Late Cambrian	0	2	10	3	41	22	10	10	25	12	12	76	1	102	2	3	2	211	72	22	1
PA050A		1	2	5	2	10	7	3	3	7	4	4	27	0	8	1	6	1	12	22	37	0
SM052C		0	0	1	0	5	3	2	2	3	2	2	11	0	7	0	1	0	20	7	3	0
SM054A		0	0	2	1	20	11	6	7	13	9	8	38	1	46	1	3	1	98	39	13	1
SM054D		0	0	0	0	2	1	1	1	3	2	2	15	0	13	0	1	0	39	13	3	1
SM054P		0	0	2	1	18	9	6	5	14	7	7	50	1	48	0	2	1	85	50	21	1
SM054S		0	0	0	0	5	3	3	3	7	3	3	34	0	28	1	1	1	68	33	10	0
SM077B		0	2	11	3	32	20	8	8	22	10	10	92	1	70	1	3	2	157	74	30	1
SM077E		0	0	2	1	7	5	2	2	4	3	3	21	0	10	0	1	0	23	14	8	0

Table 2.8: Terpane concentrations (ppm) for extract samples.
Parameters are explained in Appendix B.

Extract	Age	C30H	C30M	C31S	C31R	GA	C32S	C32R	C33S	C33R	C34S	C34R	C35S	C35R
PA009B	Middle Ordovician	38	4	14	8	2	10	7	7	4	4	3	2	2
PA049A		19	2	7	4	2	5	4	3	2	2	1	1	1
SC003A		79	13	23	16	3	18	13	9	6	5	4	2	2
SC004A		181	31	46	33	5	38	27	18	12	11	7	4	3
SC005A		136	22	35	25	3	30	21	12	9	8	5	4	3
SM056D		190	21	53	36	9	28	19	15	10	8	6	5	2
SM64A		89	8	28	18	6	19	13	10	6	6	4	4	3
SM68B		45	4	17	11	3	12	8	7	4	4	3	2	2
SM68D		115	11	35	23	8	21	15	12	8	8	5	3	3
SM078D		1196	110	396	267	45	232	159	133	87	75	50	26	19
SM078H		603	90	102	74	6	58	40	27	19	13	9	5	4
SM077M	E. Ord.	122	13	26	19	3	15	11	8	5	4	3	2	1
SM078L		232	26	59	42	6	35	25	20	14	11	7	4	3
SM079D		129	15	48	33	10	35	23	21	14	13	8	5	4
PA032A	Middle – Late Cambrian	364	46	90	64	12	58	40	29	20	17	11	7	5
PA050A		32	3	13	8	2	11	7	7	4	4	3	3	2
SM052C		40	4	10	7	2	6	4	3	2	2	1	1	1
SM054A		165	20	44	30	6	23	15	13	8	7	5	4	2
SM054D		56	6	14	11	2	8	6	5	3	3	3	0	0
SM054P		145	18	40	29	5	25	18	15	11	8	6	4	3
SM054S		110	11	26	18	3	17	11	9	6	4	3	3	2
SM077B		365	35	97	65	8	61	41	32	22	17	11	7	5
SM077E		51	5	13	9	2	9	6	5	3	3	2	2	1

Table 2.9: Sterane concentration (ppm) for extract samples.
Parameters are explained in Appendix B.

Extract	Age	S1	S2	S3	S4	S4B	S5	S5B	S6	S7	S8	S9	S9B	S10	S10B	S11	S12	S13	S13B	S14	S14B	S15
PA009B	Middle Ordovician	19	12	4	21	18	9	14	6	13	2	5	7	7	10	2	8	17	28	15	26	9
PA049A		13	8	4	13	13	7	11	5	7	2	4	6	6	8	2	6	11	18	10	16	6
SC003A		20	13	17	20	18	9	14	30	9	5	6	9	7	11	9	19	14	19	10	17	29
SC004A		32	21	26	37	30	15	22	46	23	8	9	12	10	15	15	33	24	32	18	29	49
SC005A		27	17	21	32	25	12	17	38	15	6	7	10	8	13	12	25	19	25	14	23	39
SM056D		91	56	20	49	54	30	43	25	24	5	11	16	13	20	6	18	24	39	22	37	21
SM64A		48	31	18	51	62	33	52	23	26	8	18	28	26	37	8	25	49	77	43	75	30
SM68B		24	15	9	27	32	17	27	11	15	4	10	15	14	21	4	14	29	47	25	42	16
SM68D		8	5	7	15	19	10	16	8	7	3	7	11	10	15	4	13	21	33	18	30	14
SM078D		103	66	38	105	117	60	94	50	51	18	36	55	41	65	17	61	79	127	71	122	68
SM078H		13	10	12	12	9	4	7	16	9	4	5	4	5	5	5	27	8	11	7	11	29
SM077M	E. Ord.	11	7	8	14	15	8	13	9	8	2	5	7	6	9	3	9	11	17	10	16	12
SM078L		29	19	17	35	31	15	24	21	19	5	8	12	12	17	6	25	26	40	23	39	30
SM079D		18	11	3	15	11	6	8	5	9	2	4	6	5	7	2	7	8	13	7	12	8
PA032A	Middle – Late Cambrian	20	13	22	27	28	14	22	31	14	8	9	12	11	16	10	32	23	34	20	33	40
PA050A		24	15	5	17	13	7	10	5	11	2	4	5	5	7	1	4	10	15	8	14	6
SM052C		4	3	2	6	6	3	5	3	3	1	2	3	3	4	1	4	5	9	5	8	5
SM054A		22	14	14	23	24	12	18	18	13	5	7	10	8	13	6	17	17	25	15	24	25
SM054D		6	4	5	6	7	3	5	6	2	1	2	3	2	3	2	5	5	7	4	6	9
SM054P		12	8	9	11	12	6	10	12	6	3	5	6	5	7	5	11	8	12	7	12	16
SM054S		8	5	5	8	8	4	7	8	4	2	3	4	3	5	3	7	5	8	5	7	11
SM077B		15	11	11	22	27	14	22	15	11	5	8	13	11	16	5	20	22	35	20	34	22
SM077E		5	3	2	5	5	3	5	3	3	1	2	3	2	3	1	3	4	6	3	6	4

2.4.3. Oil Samples

2.4.3.1. Whole Oil Analysis

Table 2.10 lists basic geochemical parameters for the oil samples, including API°, total sulfur, Ni, V, $\delta^{13}C$, relative abundance of saturated, aromatic and NSO compounds, and key biomarker ratios. All samples show relatively high API° gravity values (33.93 to 45.23) and low concentrations of total sulfur (0.05 to 0.32%). They are dominated by saturated hydrocarbons over aromatic compounds and NSO's. Most samples range between 60% and 77% saturates and 14% to 32% aromatics; the remaining constituents are asphaltenes and NSO compounds. The exception is sample SM072A from Shoal Point, which contains 42.21% saturated hydrocarbons and 43.53% aromatics. All samples show low concentrations of n-alkanes greater than n-C20.

The CPI and OEP are used to characterize the origin of source material, but are also influenced by biodegradation and maturation. A slight odd-carbon number preference persists in all samples in the n-C20+ components. CPI and OEP are presented in Table 2.10.

Two groups of samples emerge in the normalized n-alkane distributions (Figure 2.10). Group 1 includes samples from the Port au Port and Cow Head areas. This cluster is characterized by n-alkane distribution ranging from n-C4 to n-C30, and a pristane/phytane ratio range of 2.01 to 2.52 (Table 2.10). A slight unresolved complex mixture (UCM) of branched and cyclic compounds underlies the peaks of these samples, and an overall concave n-alkane distribution profile is apparent.

Group 2 also includes oil from both the Port au Port (Shoal Point) and Cow Head areas. Group 2 is dominated by saturated alkanes between n-C9 and n-C17, with *n*-alkanes in the range of n-C2 to n-C6. A convex n-alkane profile is evident, and compared to Group 1, these samples have a lower pristane/phytane ratio (1.88 to 2.34) (Table 2.10) and a larger UCM .

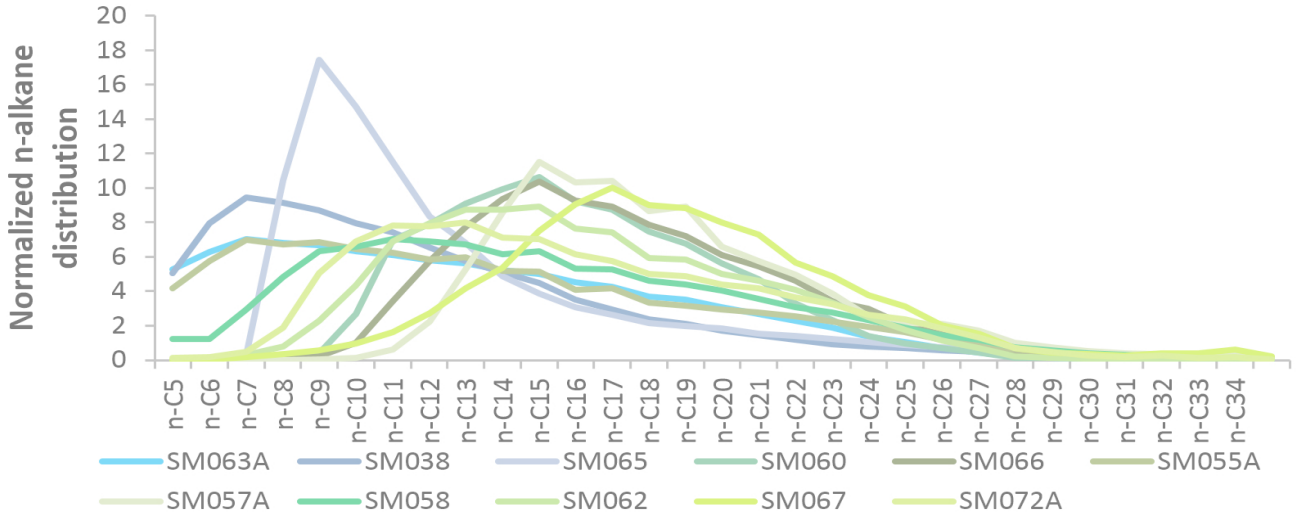

Figure 2.10: Normalized n-alkane distribution for 11 oil samples from the Port au Port Peninsula and Cow Head area. One group of oil samples (blue colors) show concave n-alkane profiles. A second group of oil samples shows convex profiles (green colors).

Table 2.10: Bulk Composition of oil samples collected from natural seeps and shallow wells.

Well Name	Sample ID	API °	<C15	% S	Ni ppm	V ppm	% Sat	% Aro	% NSO	% Asph	$^{13}C_s$	$^{13}C_a$	$^{13}C_{wc}$	Pr/Ph	Pr/nC_{17}	Ph/nC_{18}	CPI
Port au Port #1	SM038	45.23	64.9	0.16	0	5.65	76.81	15.07	8.12	0	-31.06	-29.67	-30.56	2.25	0.26	0.14	1.01
Fox Well	SM055A	35.84	37.15	0.09	2.99	2.61	60.95	31.24	7.35	0.46	-31.55	-31.01	-31.45	2.01	0.38	0.24	1.09
Sandy Point	SM057A	32.35	21.17	0.1	0	4.63	69.57	20.29	9.67	0.48	-31.05	-30.28	-30.93	2.08	0.74	0.43	0.98
Well #7	SM058	36.06	38.87	0.13	1.82	3.3	64.99	26.53	8.16	0.31	-30.7	-29.71	-30.33	2.32	0.36	0.18	1.07
Oil Point #2	SM060	33.93	39.44	0.15	0	1.85	69.22	23.81	6.8	0.17	-30.67	-29.81	-30.59	2.34	0.51	0.26	1.10
Highland Brook 1	SM062	34.25	38.26	0.12	0	1.96	68.56	22.9	8.23	0.3	-30.47	-29.47	-30.29	2.07	0.36	0.22	1.20
Highland Brook 2	SM063A	43.14	46.65	0.14	1.43	0	76.22	17.42	5.99	0.37	-30.18	-29.44	-29.89	2.52	0.36	0.16	1.13
Highland Brook W1	SM066	35.38	26	0.05	2.34	6.87	76.97	11.71	11.32	0	-29.98	-29.32	-29.94	2.31	0.6	0.3	1.07
Highland Brook W2	SM067	--	14.98	0.11	3.43	7.81	62	28.5	9	0.5	-30.83	-30.32	-30.64	2.15	0.92	0.48	1.10
Shoal Point	SM072A	--	20.34	0.32	--	--	42.21	43.53	14.03	0.24	-30.43	-29.49	-30.33	2.51	1.03	0.48	1.07

2.4.3.2. Carbon Isotopes for Oil

The $\delta^{13}C$ isotopes of the saturated and aromatic and whole oil portions of the 11 oil samples range from -29.89 to -31.45‰ VPDB ($\delta^{13}C_{wo}$) (Table 2.10, Figure 2.11). There was sufficient sample material for compound-specific carbon isotope analysis for eight of the 11 oil samples. The light-ends were preserved in four of these samples, allowing collection of the n-alkane envelope down to n-C6. The remaining four samples have lost their light ends to varying degrees, resulting in a partial n-alkane envelope being reported (Table 2.11).

The majority of samples preserved insufficient signal intensity at carbon numbers above n-C27 to provide viable data at the heavy end of the scale. The chromatography in the oils preserves a number of different patterns, as demonstrated in Figure 2.11. Within this sample set, sample SM055A (Fox Well, St. Paul's Inlet) is the most isotopically depleted (in $\delta^{13}C$) for all analyzed compounds, while samples SM066 and SM063A (Parson's Pond) show the most isotopically enriched compounds. The remaining five oil samples show isotopic values for the individual compounds lying between these endmembers. The isotopic trend of the *n*-alkanes across all the oil samples is similar, showing increasingly depleted isotopic values with increasing carbon number. These results have an error margin of +/-0.4‰.

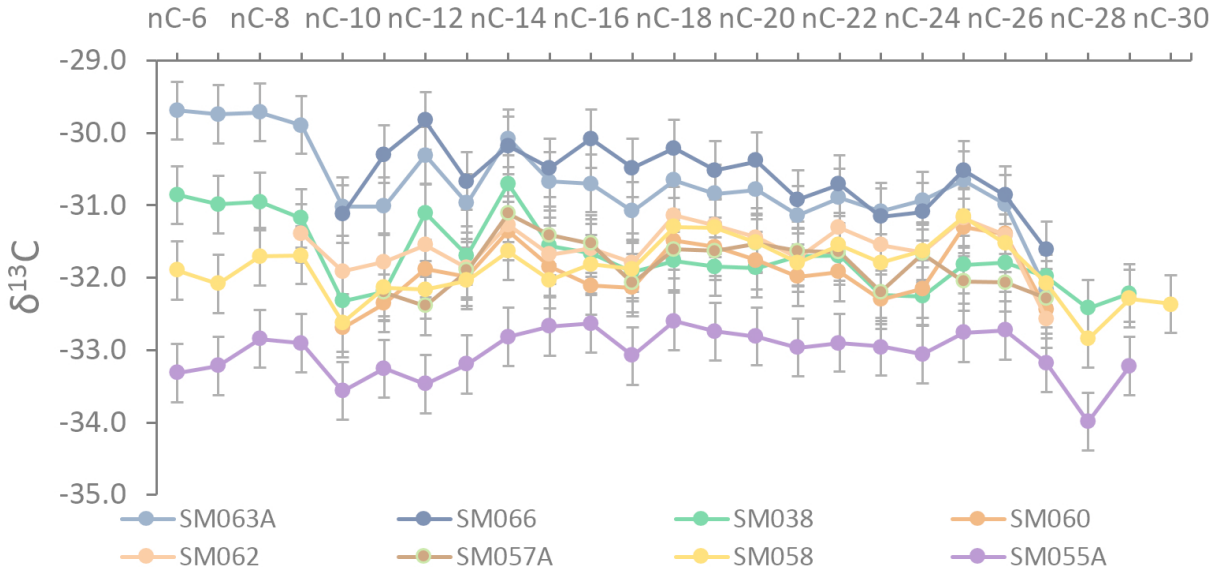

Figure 2.11: Compound specific carbon isotope profiles showing $\delta^{13}C$ (VPDB) values for the oil measured with a precision of ± 0.4‰.

Table 2.11: Compound specific isotope analysis (CSIA) for oil samples.

Compounds	SM038	SM055A	SM057A	SM058	SM060	SM062	SM066	SM063A
nC-6	-30.9	-33.3	-	-31.9	-	-	-	-29.7
nC-7	-31.0	-33.2	-	-32.1	-	-	-	-29.7
nC-8	-30.9	-32.8	-	-31.7	-	-	-	-29.7
nC-9	-31.2	-32.9	-	-31.7	-	-31.4	-	-29.9
nC-10	-32.3	-33.6	-	-32.6	-32.7	-31.9	-31.1	-31.0
nC-11	-32.2	-33.3	-32.2	-32.1	-32.4	-31.8	-30.3	-31.0
nC-12	-31.1	-33.5	-32.4	-32.2	-31.9	-31.6	-29.8	-30.3
nC-13	-31.7	-33.2	-31.9	-32.0	-32.0	-31.9	-30.7	-31.0
nC-14	-30.7	-32.8	-31.1	-31.6	-31.4	-31.3	-30.2	-30.1
nC-15	-31.6	-32.7	-31.4	-32.0	-31.8	-31.7	-30.5	-30.7
nC-16	-31.7	-32.6	-31.5	-31.8	-32.1	-31.6	-30.1	-30.7
nC-17	-31.9	-33.1	-32.1	-31.9	-32.1	-31.8	-30.5	-31.1
nC-18	-31.8	-32.6	-31.6	-31.3	-31.5	-31.1	-30.2	-30.7
nC-19	-31.8	-32.7	-31.6	-31.3	-31.6	-31.3	-30.5	-30.8
nC-20	-31.9	-32.8	-31.5	-31.5	-31.8	-31.4	-30.4	-30.8
nC-21	-31.7	-33.0	-31.6	-31.8	-32.0	-31.7	-30.9	-31.1
nC-22	-31.7	-32.9	-31.6	-31.5	-31.9	-31.3	-30.7	-30.9
nC-23	-32.2	-32.9	-32.2	-31.8	-32.3	-31.5	-31.2	-31.1
nC-24	-32.3	-33.1	-31.7	-31.6	-32.2	-31.6	-31.1	-30.9
nC-25	-31.8	-32.8	-32.1	-31.2	-31.3	-31.2	-30.5	-30.7
nC-26	-31.8	-32.7	-32.1	-31.5	-31.4	-31.4	-30.9	-31.0
nC-27	-32.0	-33.2	-32.3	-32.1	-32.4	-32.6	-31.6	-32.2
nC-28	-32.4	-34.0	-	-32.8		-	-	-
nC-29	-32.2	-33.2	-	-32.3	-	-	-	-
nC-30	-	-	-	-32.4	-	-	-	-
Pr	-32.0	-33.2	-32.7	-32.6	-32.7	-32.3	-31.4	-32.2
Ph	-33.3	-33.1	-33.1	-32.5	-32.5	-32.3	-31.6	-32.2

2.4.4. Biomarker Analysis

2.4.4.1. Steranes

All oil samples show similar sterane distributions (Table 2.12), represented as a close cluster in the ternary diagram of C27:C28:C29 (Figure 2.8). Although all are dominated by C29 over C27, C29 concentrations vary from 4 to 9% for samples SM055A, SM058, SM072A, and SM063A. I also observe a high abundance of rearranged C27 steranes (DIA) over regular 5α-cholestane (20R) in all samples. The age-related C28/C29 ratio, defined by Grantham and Wakefield (1988), yields values between 0.28 and 0.58 in this dataset (Table 2.12, Figure 2.12).

2.4.4.2. Terpanes

Important terpane ratios used for oil-to-oil and oil-to-source correlation are summarized in Table 2.13, and Table 2.14. Two endmember groups can be identified using terpane ratios.

Endmember group 1 (SM038, SM066, SM063A) is characterized by higher sterane/hopane ratios (Figure 2.13). Additionally, elevated tricyclic/hopane ratios in combination with high (C26R+S)/Ts ratios, and a relatively high concentration of pregnane and homopreganen (Figure 2.14) are observed in these samples. Homohopane epimers greater than C32 were barely observable in samples SM038, SM066, and SM063A. Sample SM057A, SM058, SM060, SM062, and SM067 show similar stepwise declining homohopane distribution patterns.

Endmember group 2 (SM055A and SM072A) has substantially lower sterane/hopane ratios (0.5 to 1.84), and shows higher absolute concentrations of extended hopanes, moretane (C30M), 18α-30-norneohopane (BNH), and 17α,21β-30-norhopane (TNH) (Table 2.13, Table 2.14). Terpane fingerprints for representative samples are illustrated in Figure 2.14.

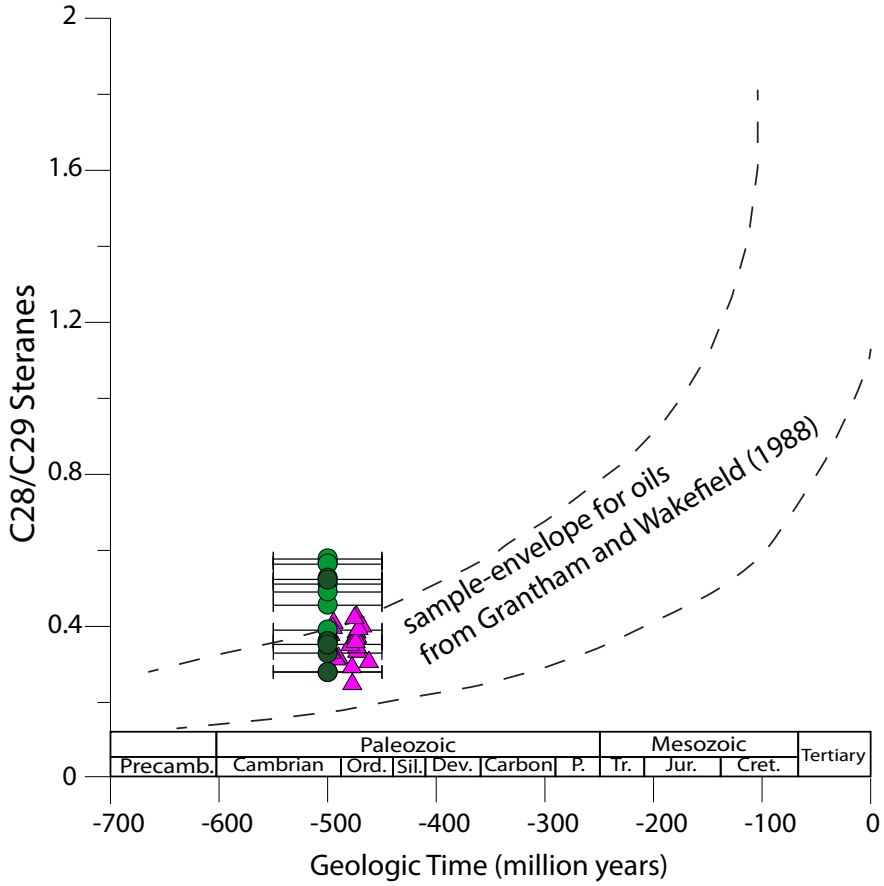

Figure 2.12: C28/C29 sterane ratios of oil samples through time.
Oil and bitumen (green), and source rock extract samples (pink) from western Newfoundland in relation to the original study by Grantham and Wakefield (1988). Differentiation into Cambrian and Ordovician oils based on C28/C29 is not possible. Oil and bitumen samples from Port au Port are indicated with dark green circles. All samples have been assigen an age of 500 Ma and an error of 50 Ma to cover the period from the middle Cambrian to the Middle- Early Ordovician. Source rock extracts show interpolated ages, based on biostratigraphic levels, which they have been collected from.

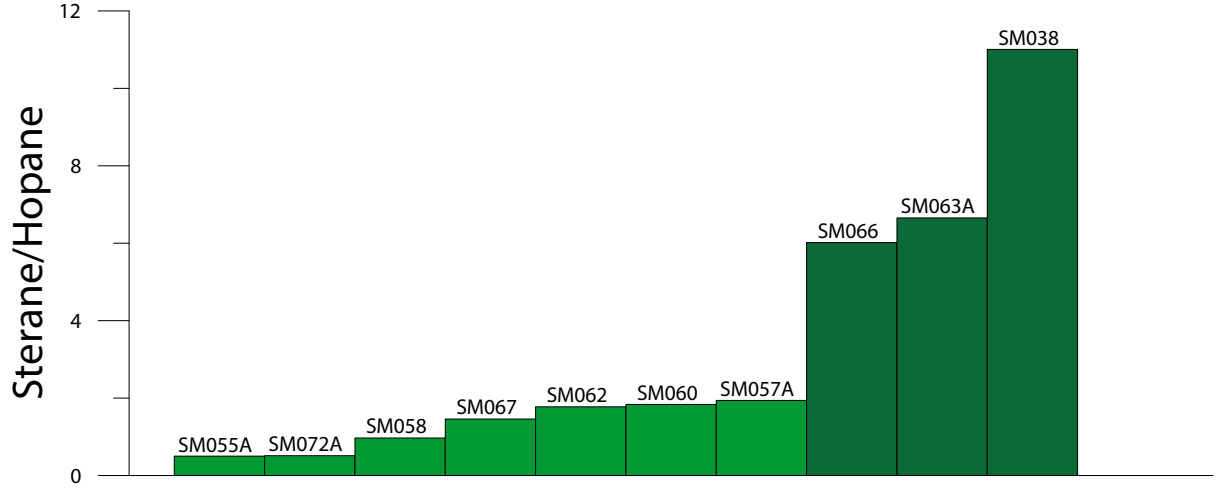

Figure 2.13: Sterane/hopane ratios for oil samples from western Newfoundland.

Table 2.12: Sterane maturity ratios of oil and bitumen samples.
Parameters are explained in Appendix B.

Sample ID		% C27	% C28	% C29	DIA/ DIA+Reg	C29 20S/R	C29 bbS/aaR	C28/ C29	S/H	C27 20S/(20S+20R)	C28 20S/(20S+20R)	C29 20S/(20S+20R)	C27 bb/(bb+aa)	C29 bb/(bb+aa)
SM038	Oil	29.23	30.51	40.26	0.59	0.68	1.30	0.51	11.01	0.57	0.78	0.41	0.75	0.97
SM055A		28.15	24.98	46.87	0.42	0.94	1.55	0.39	0.50	0.62	0.49	0.48	0.75	0.36
SM057A		27.40	31.81	40.79	0.50	0.99	1.54	0.57	1.94	0.62	0.46	0.50	0.77	0.74
SM058		28.14	27.05	44.81	0.34	0.95	1.51	0.46	0.97	0.62	0.37	0.49	0.73	0.52
SM060		28.21	31.25	40.54	0.47	0.87	1.49	0.58	1.84	0.89	0.48	0.46	0.81	0.62
SM062		26.71	29.56	43.73	0.40	0.90	1.50	0.49	1.78	0.92	0.52	0.47	0.83	0.55
SM066		27.60	30.60	41.79	0.47	0.84	1.55	0.56	6.02	0.61	0.54	0.46	0.68	0.91
SM067		27.29	31.13	41.58	0.44	0.99	1.54	0.53	1.46	0.64	0.47	0.50	0.77	0.54
SM072A		25.94	24.47	49.59	0.12	0.82	1.18	0.36	0.51	0.56	0.47	0.45	0.68	0.25
SM063A		26.76	29.18	44.06	0.33	0.83	1.60	0.52	6.65	0.63	0.54	0.45	0.71	0.81
SM034A	Bitumen	29.32	23.83	46.85	1.39	0.77	0.68	0.36	0.50	0.39	0.44	0.44	0.57	0.12
SM036A		26.92	25.09	48.00	3.49	1.59	1.26	0.33	0.32	0.61	0.56	0.61	0.74	0.28
SM050B		20.06	24.33	55.61	1.54	0.92	0.79	0.28	0.19	0.47	0.50	0.48	0.61	0.16
SM053B		4.23	84.35	11.42	2.09	1.21	0.41	0.35	0.05	0.65	0.76	0.55	0.52	0.17
SM033A		23.10	24.99	51.91	0.92	0.60	0.34	0.28	0.47	0.24	0.35	0.37	0.43	0.07

Table 2.13: Source and maturity related terpane ratios of oil and bitumen samples. Parameters are explained in Appendix B.

SampleID		Ol	Ga	Ts	C27T (TNH)	Tm	C28 DM	C28H (BNH)	C29 DM	C29H	C29D	M/ H	S/H	TriCyc	TriCyc/ H	Ts/ Tm	BNH/H (C28/H)	TNH/H (C27/H)	(BNH+TNH)/ H
SM038	Oil	0.02	0.00	0.14	0.00	0.05	0.00	0.06	0.00	0.06	0.06	0.22	11.01	3.96	9.49	3.09	1.06	1.06	1.06
SM055A		0.94	2.02	16.08	0.15	8.74	0.03	1.46	0.09	21.71	16.13	0.09	0.50	44.09	0.23	1.84	0.03	0.42	0.03
SM057A		0.07	0.21	4.64	0.11	0.70	0.06	0.43	0.04	0.84	2.86	0.10	1.94	19.79	1.46	6.60	0.26	0.52	0.33
SM058		0.40	0.50	7.27	0.12	2.72	0.08	0.58	0.04	5.74	5.60	0.08	0.97	37.36	0.76	2.67	0.05	0.46	0.06
SM060		0.12	0.31	6.27	0.00	1.11	0.07	0.65	0.05	1.67	3.92	0.07	1.84	35.73	1.56	5.64	0.15	0.38	0.15
SM062		0.18	0.43	5.70	0.05	1.59	0.06	0.75	0.07	2.45	3.83	0.08	1.78	41.63	1.66	3.58	0.16	0.52	0.17
SM066		0.01	0.00	0.48	0.03	0.08	0.06	0.13	0.04	0.55	0.22	0.14	6.02	8.05	5.14	6.06	1.31	5.71	1.65
SM067		0.28	0.49	8.52	0.08	1.92	0.15	0.81	0.31	3.35	6.02	0.07	1.46	43.65	1.14	4.43	0.10	0.42	0.11
SM072A		0.71	2.14	12.38	0.34	11.79	0.16	1.50	0.23	39.39	10.68	0.10	0.51	58.19	0.25	1.05	0.02	0.51	0.02
SM063A		0.03	0.00	1.24	0.07	0.21	0.03	0.26	0.04	0.21	0.74	0.18	6.65	14.43	4.82	6.00	0.94	0.03	1.18
SM034A	Bitumen	0.05	3.29	13.82	0.36	10.10	0.26	1.19	0.32	45.46	18.28	0.12	0.50	21.46	0.07	1.37	0.01	0.54	0.02
SM036A		0.87	3.01	30.79	0.22	11.58	0.54	1.70	0.38	38.52	26.96	0.14	0.32	48.73	0.22	2.66	0.03	0.78	0.04
SM050B		0.72	5.92	17.50	0.63	18.73	0.33	1.56	0.62	68.94	27.28	0.13	0.19	54.69	0.13	0.93	0.01	0.58	0.02
SM053B		0.85	9.26	29.09	0.67	27.88	0.73	2.68	0.89	122.37	35.71	0.23	0.05	126.40	0.28	1.04	0.03	1.20	0.03
SM033A		0.41	2.90	7.73	0.31	13.16	0.17	1.63	0.28	42.14	11.76	0.19	0.47	23.89	0.10	0.59	0.02	0.63	0.03

Table 2.14: Terpane concentration (ppm) of oil samples used in HCA and PCA. Parameters are explained in Appendix B.

	C19T	C20T	C21T	C22T	C23T	C24T	C25S	C25R	TET	C26S	C26R	Ts	Tm	C28H	C29H	C29D	C30X	OL
SM038	0	0	1	0	1	1	0	0	0	0	0	0	0	0	0	0	0	0
SM055A	2	3	6	1	10	8	3	3	6	4	3	16	9	1	22	16	10	1
SM057A	1	2	3	1	4	4	1	1	1	2	2	5	1	0	1	3	6	0
SM058	1	3	6	1	9	7	2	2	2	3	3	7	3	1	6	6	5	0
SM060	2	3	6	1	8	7	2	2	2	3	3	6	1	1	2	4	5	0
SM062	1	3	6	1	10	8	3	3	2	3	3	6	2	1	2	4	4	0
SM066	0	1	1	0	2	2	1	1	0	1	1	0	0	0	1	0	1	0
SM067	1	2	6	1	10	9	3	3	2	4	4	9	2	1	3	6	6	0
SM072A	1	4	10	2	16	11	4	4	4	5	1	12	12	1	39	11	5	1
SM063A	0	1	2	0	3	3	1	1	0	1	1	1	0	0	0	1	2	0

	C30H	C30M	C31S	C31R	GA	C32S	C32R	C33S	C33R	C34S	C34R	C35S	C35R
SM038	0	0	0	0	0	0	0	0	0	0	0	0	0
SM055A	51	5	17	11	2	12	8	8	5	5	3	2	2
SM057A	2	0	1	0	0	0	0	1	0	0	0	0	0
SM058	13	1	3	2	0	3	2	2	1	1	1	0	0
SM060	4	0	1	0	0	1	1	1	0	0	0	0	0
SM062	5	0	1	1	0	1	1	1	0	0	0	0	0
SM066	0	0	0	0	0	0	0	0	0	0	0	0	0
SM067	8	1	2	1	0	2	1	1	1	1	1	0	0
SM072A	78	8	18	12	2	14	9	8	5	4	3	2	2
SM063A	0	0	0	0	0	0	0	0	0	0	0	0	0

Table 2.15: Sterane concentration (ppm) of oil samples used in HCA and PCA. Parameters are explained in Appendix B.

	S1	S2	S3	S4	S4B	S5	S5B	S6	S7	S8	S9	S9B	S10	S10B	S11	S12	S13	S13B	S14	S14B	S15
SM038	1	1	0	1	0	0	0	0	1	0	0	0	0	0	0	0	0	0	0	0	0
SM055A	10	7	2	12	13	6	10	4	7	1	4	6	6	9	1	6	11	19	10	17	6
SM057A	4	2	0	4	3	1	2	1	3	0	1	2	2	2	0	1	2	4	2	3	1
SM058	4	3	2	6	7	3	5	2	4	1	2	3	4	5	1	3	6	10	5	8	3
SM060	6	3	2	6	5	3	4	0	4	1	2	3	4	5	1	2	4	7	3	6	2
SM062	4	3	2	6	6	3	5	0	4	1	2	3	4	5	1	3	5	9	4	8	3
SM066	1	1	0	1	1	1	1	0	1	0	0	1	1	1	0	0	1	1	1	1	0
SM067	7	4	1	8	7	4	5	2	5	1	2	4	5	6	1	3	6	9	5	8	3
SM072A	12	8	4	17	14	7	10	5	11	2	4	7	6	9	2	8	13	21	11	19	9
SM063A	3	2	1	3	2	1	2	1	2	0	1	1	2	2	0	1	2	3	2	3	1

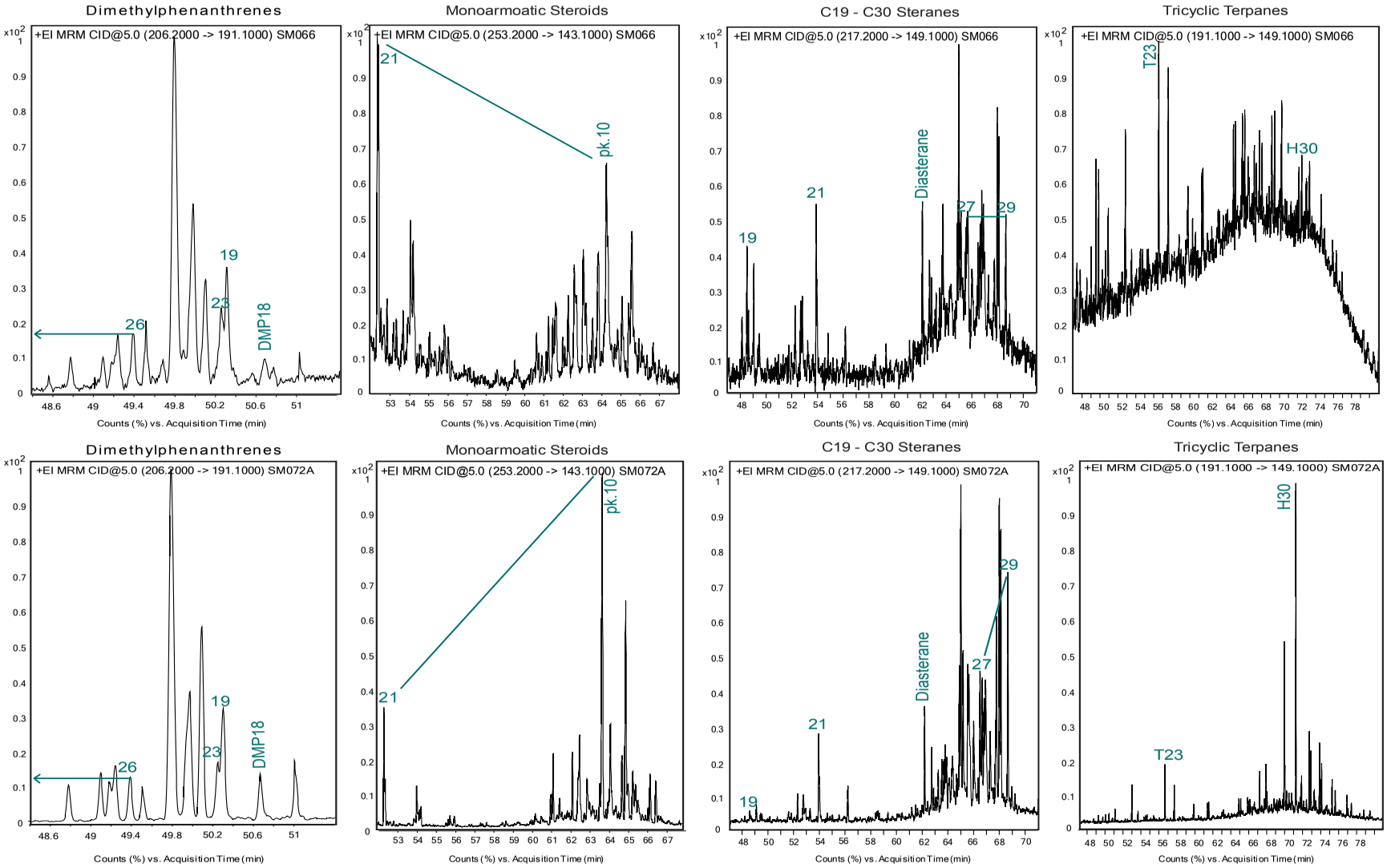

Figure 2.14: Dimethylphenanthrene, monoaromatic steroids, sterane and terpane fingerprints showing representative endmember samples (SM066 and SM072A) for the endmember oils collected in western Newfoundland.
Peak labels for Dimethylphenanthrene (26 = DMP26, 23 = DMP23, 19 = DMP19; abbreviations explained in Appendix B). Peak identification for Monoaromatic Steroids (21= C21A monoaromatic steroid; Pk 10 = C28R Type I & V, C29S Type I & V) for Steranes (19 = C19, 21 = C21, C27 = cholestane; C29 = stigmastane).

2.5. Maturity Indicators in Oil Samples

2.5.1. Sterane Isomerization Ratios

Sterane isomerization ratios are listed in Table 2.12. Ratios such as C29 20S/20R, C29 20S/(20S+20R), and isomer ratios of the αα and ββ configurations of C27 to C29 20R are thermally controlled (Peters et al., 2005). For all samples, the C27 ββ/(ββ+αα) ratios exceed the C29 ββ/(ββ+αα) ratios, exceptions being samples SM038 and SM066. Ratios for the C27 epimers range between 0.68 and 0.83, and for C29 epimers between 0.25 and 0.97 (Table 2.12). Because of the greater thermal stability of diasterane, the ratio between diasterane and regular sterane increases with thermal maturity, however, this ratio also depends on biodegradation and source input (Peters et al., 2005). Calculated ratios of diasterane to regular sterane range from 0.34 to 0.59 (Table 2.12).

2.5.2. Terpane Ratios

Thermal maturity ratios for terpane molecules are summarized in Table 2.13. The three parameters evaluated are moretane/hopane (0.07 to 0.22), tricyclic/hopane (0.25 to 9.49, with higher ratios indicating more thermally evolved samples), and 17α(H)-trisnorhopane/18α(H)-trisnorneohopane (Ts/Tm = 1.05 to 6.6, smaller ratios indicating thermally evolved samples). Using these ratios, the same previously identified two endmember groups appear. The listed ratios depend not only on the thermal maturity of the samples, but also on the organic matter input (e.g. bacterial versus algal dominated organic matter) and can therefore not be used independently for a proper maturity evaluation (Seifert and Moldowan, 1978; Peters et al., 2005). In this case, they may be more influenced by the source than the maturity of the samples; this will be discussed in section ‘2.6.4 Oil Maturity Interpretation’.

2.5.3. Methylphenanthrene Index and Naphthalene Indices

Radke et al. (1982, 1988) derived an empirical relation between phenanthrene and methylphenanthrene to estimate thermal maturity of oils. According to Radke (1988), the ratios of naphthalene, phenanthrene, and their associated methylated homologs are dependent on thermal maturity, while being negligibly influenced by biodegradation or organic facies. The original studies were conducted using oil generated from type II and type III organic matter. For a better fit, and to include oil generated from type I, II, and III organic matter, Cassani et al. (1988) modified the empirical equation developed by Radke et al. (1982), used for the present study, with results shown in Table 2.16. Sample SM055A and SM072A represent the lowest maturity oils, with calculated vitrinite reflectance values of 0.7 $\%R_c$. The highest calculated vitrinite reflectance value of 1.51 $\%R_c$ was calculated for SM038. All other samples fall between 0.73 and 0.91 $\%R_c$. Interestingly, samples SM063A and SM066 have low calculated maturities (0.73 and 0.77 $\%R_c$, respectively), despite close geochemical resemblance to SM038 (Figure 2.15).

In order to determine a more robust and independent maturity evaluation, 13 naphthalene and phenanthrene ratios have been calculated and combined to give a consensus maturity for each sample, which can be converted into a vitrinite reflectance equivalent (VREQ-5) value (Figure 2.16, Table 2.16). The VREQ-5 values for the collected oils are generally in agreement with the MPI-1 index, yet, they show a 20% higher calculated vitrinite value.

It is notable that, within our dataset, geographically related samples still demonstrate a wide range of maturities as shown by their VREQ-5 and $\%R_c$ values. For example, samples SM038 and SM072A from the Port au Port area show VREQ-5 values of 0.8 to 1.26 and calculated vitrinite reflectance values of 0.7 to 1.51 $\%R_c$. Similarly, the samples from the Parson's Pond and St. Paul's Inlet show VREQ-5 values of 0.91 to 1.11 and 0.7 to 0.91$\%R_c$.

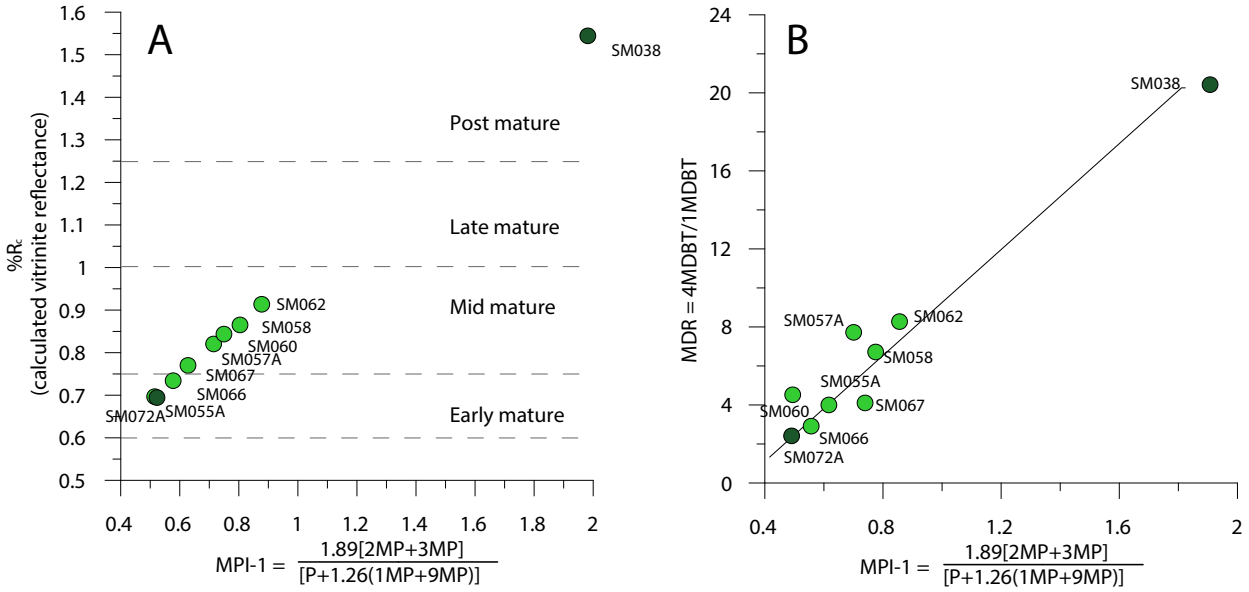

Figure 2.15: Non-biomarker maturity indicator.
A:Calculated vitrinite reflectance with a modified methylphenanthrene index (MPI-1) after Cassani et al. (1988). B: Regression between methyldibenzothiophene ratio (MDR) and MPI showing good correlation. Oil samples from Port au Port Peninsula are shown in dark green. Samples from the Cow Head area are shown in light green.

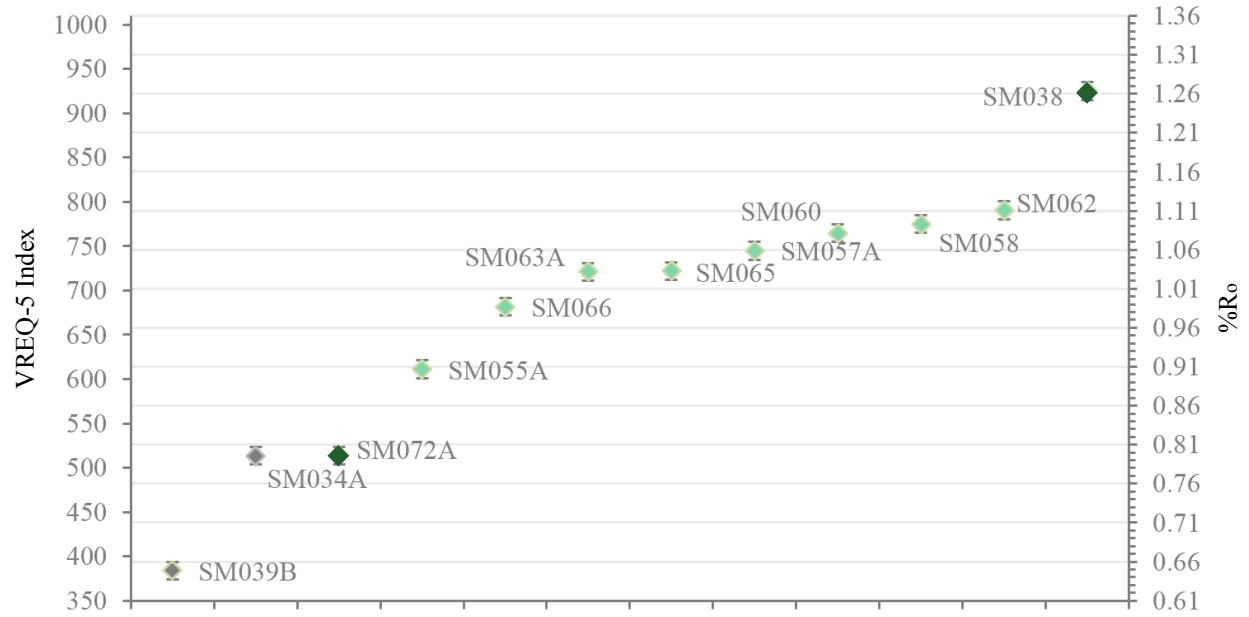

Figure 2.16: Vitrinite reflectance calculated from VREQ-5 ratios (GeoMark®).
Oil samples are shown as green diamonds with an error of ±0.1 %Ro, bitumen samples are shown in black diamonds with an accuracy of ± 0.1 %Ro. Oil samples from the Port au Port Peninsula are shown in dark green. All bitumen samples shown are from the Port au Port Peninsula.

Table 2.16: Quantitative maturity evaluation using standard biomarker ratios and aromatic ratios. Parameters are explained in Appendix B.

Maturity ratio	SM039B	SM034A	SM072A	SM055A	SM066	SM063A	SM065	SM057A	SM060	SM058	SM062	SM038
MPI-1=1.89(2+3 MP)/(P+1.26(1+9 MP)	-	-	0.49	0.49	0.56	0.61	0.62	0.7	0.74	0.78	0.86	1.91
$\%R_c$ =0.6 MPI+0.4	-	-	**0.69**	**0.7**	**0.73**	**0.77**	**0.77**	**0.82**	**0.84**	**0.87**	**0.91**	**1.51**
MN2/(MN2+1)*100	58.35	60.48	54.38	48.76	59.63	57.01	64.89	76.79	53.65	58.57	61.05	77.56
EN2/(EN2+1)*100	13.9	65.45	58.42	64.68	56.9	53.34	55.99	55.43	73.3	79.57	76.9	88.2
DMN26/(DMN26+12)*100	25.92	71.77	67.24	72.18	71.72	84.03	79.58	87.3	90.98	90.4	92.13	95.68
(DMN26+27)/(total DMNs)*100	5.78	26.09	19.52	18.56	14.9	19.87	18.46	25.28	24.72	26.85	28.22	43.69
TMN137/(TMN137+124+125)*100	47.96	58.78	49.24	70.71	80.41	88.77	88.05	89.68	89.78	88.72	89.22	93.96
TMN(137+136)/(total TMNs)*100	25.54	36.35	31.5	36.83	44.01	47.03	45.13	47.88	48.05	45.49	46.45	50.37
TeMN13/(TeMN13+14+15+16)*100	16.18	12.17	12.9	24.55	28.14	41.77	44.26	39.42	42.08	42.64	42.67	44.25
DMP(EFGK)/(Σ DMPs)*100	8.43	13.92	12.78	13.07	16.24	15.39	13.41	13.76	17.26	18.6	19.14	35.75
(MP3+2)/(MP3+2+9+1)*100	11.57	33.99	33.45	32.28	42.84	36.79	32.69	37.44	40.59	42.55	44.12	65.51
DMP26/(DMP26+18)*100	20.7	31.17	48.21	53.55	63.6	77.08	69.6	74.51	76.51	75.79	76.61	93.79
DMP23/(DMP23+19)*100	14.81	31.98	28.68	28.05	40.31	36.7	32.03	27.58	34.73	38.81	41.77	75.07
DMP18/(DMP18+12)*100	59.64	53.85	50.51	63.01	69.14	65.99	80.49	73.25	75.88	71.39	74.88	62.54
TMP_A/(TMPA+TMP128)*100	75.11	17.39	46.97	84.74	93.79	97.26	97.32	96.58	97.04	95.57	97.39	98.75
consensus II	383.89	513.4	513.79	611	681.64	721.04	721.91	744.91	764.59	774.95	790.56	925.13
VREQ-5	**0.65**	**0.8**	**0.8**	**0.91**	**0.98**	**1.03**	**1.03**	**1.06**	**1.08**	**1.1**	**1.11**	**1.26**

2.5.4. DIAMONDOIDS

Adamantane and diamantane are fused cyclohexane rings whose structure can be superimposed on a diamond lattice (Dahl et al., 1999). An increase in diamondoid concentrations starts after the thermally induced conversion of steranes and terpanes (from the αα to ββ configuration) is complete. The conversion equilibrium from αα to ββ marks the end of the oil window (Dahl et al., 1999; Peters et al., 2005). In a graph where 3, + 4-methyldiamantane is shown in combination with stigmastane (C29ααα20R), information on thermal maturity, mixing, and cracking can be obtained (Dahl et al., 1999). Using this graph (Figure 2.17) four bitumen samples show low maturities; this agrees with maturities obtained from Rock-eval analysis (0.6-0.8 $\%R_o$) for source rock samples collected adjacent to these bitumen samples.

Another subset of the oil samples (SM055A, SM058, SM062, and SM060) fall into the "mixing" field, indicating mixing of low maturity oil with high maturity (cracked) oil occurred. These samples show a decrease in stigmastane concentration from 10 ppm to 2 ppm, and an increase in 3, + 4- methyldiamantane from 9 ppm to 26 ppm. Samples along the x-axis with stigmastane concentrations below 2 ppm, but 3, + 4-methyldiamantane concentrations above 10 ppm, fall along a asymptote that shows mature oil converted to cracked oil. The cracking of mature oil to higher maturity oil is directly related to an increase in 3, + 4-methyldiamantane (Dahl et al., 1999). Due to the limited amount of samples I was not able to assign a diamantane baseline to quantify the amount of secondary cracking that took place in the cracked oils.

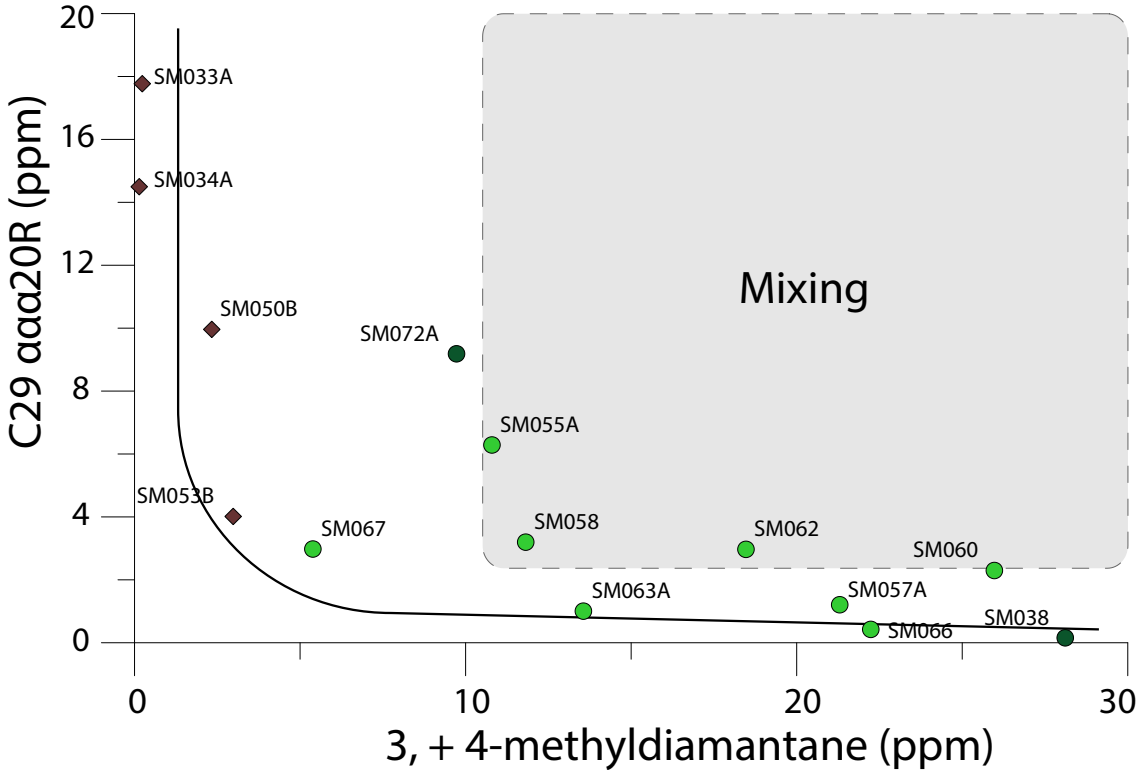

Figure 2.17: Correlation between biomarker (stigmastane) and diamondoid (3, + 4-methyldiamantane) concentrations.
Oil samples (green circles) and bitumen (brown diamonds) with different thermal maturities. Stigmastane decreases with increasing maturity. At low concentrations (stigmastane = 4ppm) diamondoid starts to increase with increasing cracking. The grey area shows potential mixing between lower maturity oil and cracked oil. Oil samples from Port au Port Peninsula are shown in dark green. Samples from the Cow Head area are shown in light green.

2.5.5. BIODEGRADATION

Oil samples collected in the 2015 field season were taken from accessible, old well sites or natural seeps expected to show high levels of biodegradation. Level of biodegradation was assessed using two scales, one which determined oil quality, and one which determined the bio-resistance of compounds (Peters and Moldowan, 1993; Wenger et al., 2002). Table 2.17 summarizes the petroleum compounds, which are quasi-sequentially removed with increasing biodegradation. There is no spatial or geographic relation between biodegraded and non-biodegraded oil samples. All oil samples retain their cyclic saturated biomarkers; therefore, biodegradation is characterized as "light" (from 1 to 3) on the scale after Peters and Moldowan (1993). Light biodegradation suggests active generation and recharge into the abandoned wells.

Three samples (SM057, SM060, and SM066) are classified as heavily biodegraded on the Wenger et al., (2002) scale, due to initiation of n-alkane removal and loss of alcylcyclohexane (Table 2.17). These samples also show the development of a UCM in the GCMS FID-graphs (Figure 2.14). This is the result of the biodegradation of *n*-alkanes and the concentration of bio-resistant compounds with highly branched hydrocarbons.

Table 2.17: Biodegradation ranking after Wenger et al. (2002) and Peters and Moldowan (1993). "+" and "-"indicate the presence or absent of molecules or UCM.

		Port au Port #1	Fox Well	Sandy Point	Well #7	Oil Point #2	Highland Brook 1	Highland Brook 2	Highland Brook W3	Highland Brook W1	Highland Brook W2	Shoal Point
	Molecules	SM038	SM055A	SM057A	SM058	SM060	SM062	SM063A	SM065	SM066	SM067	SM072A
C1-C5	propane	+	+	-	+	-	+	+	+	-	-	+
	n-butane	+	+	-	+	-	+	+	+	-	-	+
	pentanes	+	+	-	+	-	+	+	-	-	-	+
	iso-butane	+	+	-	+	-	+	+	-	-	+	+
	ethane	-	+	-	+	-	-	-	+	-	-	-
C8 to C15	n-alkanes	+	+	-	+	-	+	+	+	-	+	+
	isoalkanes	+	+	+	+	+	+	+	+	+	+	+
	isoprenoids	+	+	+	+	+	+	+	+	+	+	+
	BTEX	+	+	-	+	-	+	+	+	-	+	+
	alkylcycclohexane	+	+	-	+	-	+	+	+	-	+	+
C15-C35	n-alkane, isoalkane	+	+	+	+	+	+	+	+	+	+	+
	isoprenoids	+	+	+	+	+	+	+	+	+	+	+
	naphthalenes	+	+	+	+	+	+	+	+	+	+	+
	phenanthrenes DBT	+	+	+	+	+	+	+	+	+	+	+
	regular steranes	+	+	+	+	+	+	+	+	+	+	+
	C30-C35 hopanes	+	+	+	+	+	+	+	+	+	+	+
	C27-C29 hopanes	+	+	+	+	+	+	+	+	+	+	+
	triaromatic steranes	+	+	+	+	+	+	+	+	+	+	+
	monoaromatic steranes	+	+	+	+	+	+	+	+	+	+	+
	Gammercerane	nd	nd	nd	nd	nd	nd	nd	nd	nd	nd	nd
	Oleane	nd	nd	nd	nd	nd	nd	nd	nd	nd	nd	nd
	UCM	---	---	+++	--	+	--	---	---	++	++	+
Wenger et al.2002	Biodegradation Level	**very slight-**	**very slight-**	**heavy**	**slight**	**heavy**	**slight**	**very slight**	**slight**	**heavy**	**heavy**	**mode-rate**
Peters and Moldowan 1993	Biodegradation Level	**0-1**	**0-1**	**3-4**	**2**	**3**	**1-2**	**0-1**	**2**	**3-4**	**3**	**3**

2.6. Discussion

The data reported enable us to assess the quality of Lower Paleozoic source rocks, characterize oils and extracts, and relate oils to specific source rock intervals and extracts from the study area. Thermal maturity is a major factor controlling the interpretation of oil families; thus the maturity data are interpreted before the oil-to-source correlation.

2.6.1. Source Rock Quality and Distribution

The source rock data permit a systematic analysis from the middle Cambrian to the Middle Ordovician strata that include continental slope and rise deposits, and from the organic-rich platform. (James and Stevens, 1986; Botsford, 1987; Weaver 1988).

The concentration in TOC averages 1.8% in Lower to Middle Ordovician Green Point and Shallow Bay Formations, with maximum values close to 3% TOC (Table 2.3). Rocks associated with the Lower to Middle Ordovician Middle Arm Point Formation, the most distal portion of the continental slope (Botsford, 1987), show excellent source potential with concentrations of TOC up to 9.45% in the richest intervals, and true petroleum potential (Table 2.3). The maturity for those outcrops are marginally mature to mature. The source quality for the Green Point and Shallow Bay Formations, expressed in HI and OI, shows values characteristic of type II/III organic matter (Figure 2.4B). The high values in HI and low values of OI for the Middle Arm Point Formation fall in the range for type I/II organic matter (Figure 2.4B, Table 2.3), similar to the organic matter described by Fowler et al. (1995). Samples collected from platform rocks (e.g. Table Cove) did not show any significant potential (Table 2.3). The study area includes 170 km of coastal outcrop with significant potential for heterogeneities. Thus, I am unable to correlate individual beds across measured sections, or establish convincing proof for a systematic change in TOC content or organic matter type from proximal to distal continental slope.

Due to methodical sampling and well constrained biostratigraphy, however, I am able to identify a previously unrecognized potential source rock in middle to late Cambrian Green Point Formation and Cooks Brook Formation characterized by TOC values over 2 wt% and type II/III organic matter (Figure 2.6). A large sample set collected in the Bay of Islands (Cooks Brook

Formation) shows poor petroleum potential at present-day (Figure 2.4B). I propose that the tectonic emplacement of ophiolites over deep marine deposits in the Bay of Islands area, during the Taconian orogeny, caused deep burial and over-maturation of the potential source rocks. Alternatively, it is possible that the over-maturation is related to a post-Taconian to Silurian event, that developed a poor cleavage in the Bay of Island (Waldron et al., 2003). This is supported by pyrolysis data that shows especially low petroleum potential where ophiolites are juxtaposed against, or overlay, the source rocks. Further, the petroleum potential increases with increasing distance from the ophiolite complex. I argue that the Cooks Brook Formation and Middle Arm Point Formation in the Bay of Islands area had the same petroleum potential as the equivalent rocks on Port au Port Peninsula and Cow Head area. To demonstrate that the samples collected in the Bay of Islands are over-mature, and not just low in original potential, I back-calculated the original TOC, S1 extractable, and the conversion factor for the range of HI values measured for the immature Middle Arm Point Formation on Port au Port Peninsula. I assumed an original Production Index (PI_o) of 0.02. The mass balance equations used were based on the work of Cooles et al. (1986), shown in Appendix A.

The results of those calculations are summarized in Table 2.18. For varying original HI, the original TOC is substantially larger and compares well with the measured date for Middle Arm Point Formation on the Port au Port Peninsula. This substantiates the interpretation I made from S2, PI, and T_{max} data. I can conclude that the properties of the overmature rocks in the Bay of Islands show close resemblance, after correction, with the immature samples from the Middle Arm Point samples collected on the Port au Port Peninsula.

Table 2.18: Recalculated generative potential.
Recalculated generative potential for varying HI indexes after Cooles et al. (1986) and Espitalé et al. (1987) (see APPENDIX A). PI_o = assumed original production Index (0.02); f = expulsion factor; TOC_o = original total organic carbon; TOC = measured total organic carbon; S1 = free hydrocarbon; S1 Ex= expelled free hydrocarbon; PaP = Port au Port.

	HI_o (mg HC/g TOC)	PI_o	f (%)	TOC_o (wt%)	S1 Ex (mg HC/g TOC)
Lobster Cove	800	0.02	1	5.73	46.41
	600	0.02	0.99	3.83	23.09
	400	0.02	0.98	2.88	11.39
Cooks Brook	800	0.02	1	5.02	40.71
	600	0.02	1	3.35	20.2
	400	0.02	0.99	2.51	9.95
Allochthon PaP	800	0.02	0.89	6.19	36.42
	600	0.02	0.79	4.14	10.93
Cow Head	800	0.02	0.77	4.26	24.79
	600	0.02	0.53	2.83	7.17

2.6.2. Characteristics of Cambrian and Ordovician Extracts

Cluster Analysis and Principle Component Analysis were performed on the basis of bulk composition, isotope data, sterane and terpane ratios, and absolute concentrations (Table 2.4, Table 2.7, Table 2.8, Table 2.9). Because maturity influences the source interpretation, we excluded maturity-sensitive biomarker ratios from the cluster analysis. Parameters that are influenced by both source and maturity appear to be more influenced by source composition, as demonstrated by samples from the Cambrian and Ordovician with the same maturity differing compositionally in the same way as samples with different maturities.

Using different agglomeration methods, I am able to consistently identify two clusters, one Ordovician and one Cambrian (Figure 2.18). Centroid, median, and complete linkage methods give slightly different results, clustering three Ordovician samples (SM064A, SC004A, and SM078D) in individual clusters, respectively. Generating distinct clusters with different agglomeration methods proves that the clusters are distinct and not random. Incremental linkage method is often used for samples differing only slightly in composition. Therefore, data in this thesis is represented in dendrograms using the incremental linking method. One outlier sample (SM078D) can be detected with all employed linkage methods and is shown in Figure 2.18. The clusters do not take into consideration the geographic distribution of the samples, i.e. samples from a measured section may appear in both clusters, depending on their stratigraphic level. Moreover, parameters that are associated with a change in thermal maturity change in the same measured section significantly from the Cambrian to Ordovician strata, suggesting that a particular biomarker response is more influenced by source composition than thermal maturity.

Higher concentrations of aromatic hydrocarbons, NSO, and asphaltenes in all extracts compared to the oil samples are related to their lower mobility and adsorption behavior (Figure 2.8) (Tissot and Welte, 1984). Variations in the aromatic and saturate concentration within the Cambrian and Ordovician extract clusters are potentially related to minor lithological changes in the source rock. The collected Cambrian to Ordovician source rocks predate the proliferation of

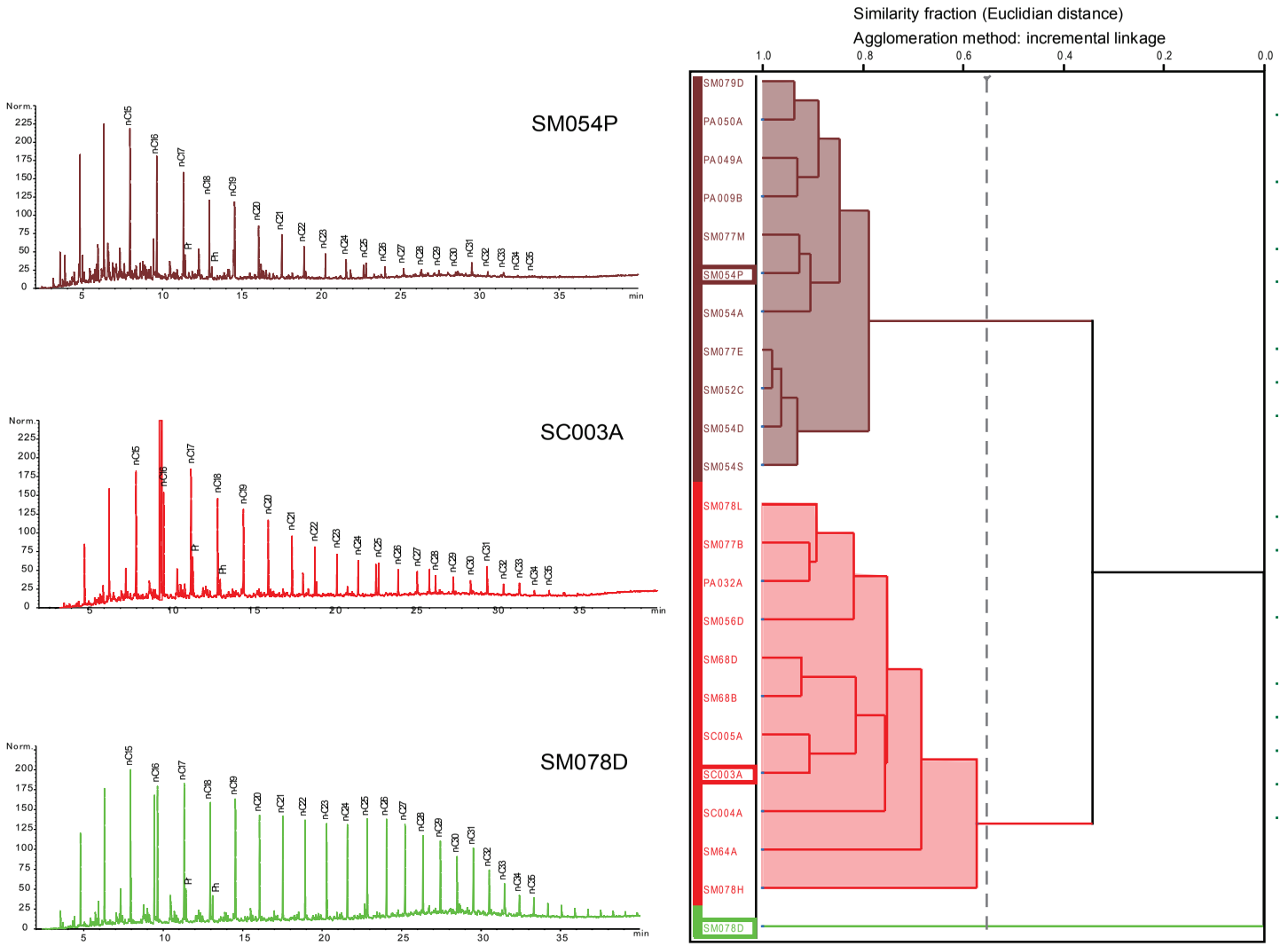

Figure 2.18: Hierarchical cluster analysis (HCA) using sterane and terpane concentrations and ratios of extracts.
HCA was performed with Pirourette®; parameters (Table 2.7,Table 2.8, Table 2.9) are auto-scaled; calculation of Euclidean distances and an incremental linkage method results in a similarity (dashed line) of 0.56, distinguishing two cluster. The cluster identified include Ordovician samples (red) with one outlier sample (green) and Cambrian samples (brown). Representative GCMS graphs show the visual differences of the FID fingerprints.

higher land plants. Therefore, stigmastane present in the extract data cannot be assigned to higher plant-derived C29-sterols (Table 2.6), but instead is better explained by C29-sterols related to algal lipid-membranes (Figure 2.8) (Grantham and Wakefield, 1988).

The biomarker signature for the Cambrian source extracts from western Newfoundland is influenced by primitive, bacterially-derived organic matter, with low concentrations of phenanthrene, methylphenanthrenes and associated isomers (3-MP, 2-MP, 9-MP, 1MP), and thiophenes (Figure 2.7) (Radke, 1982, 1984; McKirdy et al., 1983). Following parameters have been identified by multiple researchers in the past and are related to a change in source composition (Hughes, 1984; Palacas et al., 1984; Tissot and Welte, 1984; Moldowan et al., 1985; Connan et al., 1986, Riolo et al., 1986). Specifically, Ordovician extract samples show, on average, a higher concentration of steranes (C29), phenanthrenes, and thiophenes, higher sterane/hopane and C26(R+S)/Ts ratios, and lower TET/C23, with only minor changes in trisnorhopane (Ts) and tricyclic concentrations.

Significantly lower concentrations of aryl-isoprenoids (C18, C19, C20), tricyclic diterpanes (C19T, C20T), and tetracyclic terpanes in the Cambrian samples than in Ordovician samples suggests a shift in composition of the western Newfoundland source rocks (Figure 2.7). According to the observations of contrasting biomarker composition for these Cambrian and Ordovician source extracts I proposing the interpretation of a shift in source composition from a bacterial to an algal-derived organic matter assemblage.

2.6.3. Oil Maturity Interpretation

Maturity of the oil samples is summarized in Table 2.16, and ranges from a vitrinite reflectance value of 0.69 to 1.51 $\%R_c$. According to the Peters and Moldowan (1993) and Wenger et al. (2002) biodegradation scales, at this level of maturity, biomarkers have not yet been affected by biodegradation (Figure 2.14, Table 2.17), and can therefore be used for maturity and source evaluations.

Various biomarker isomerization and non-biomarker ratios reach their equilibrium at different thermal stresses; thus, they are used to delineate maturity ranges. To cover the full maturi-

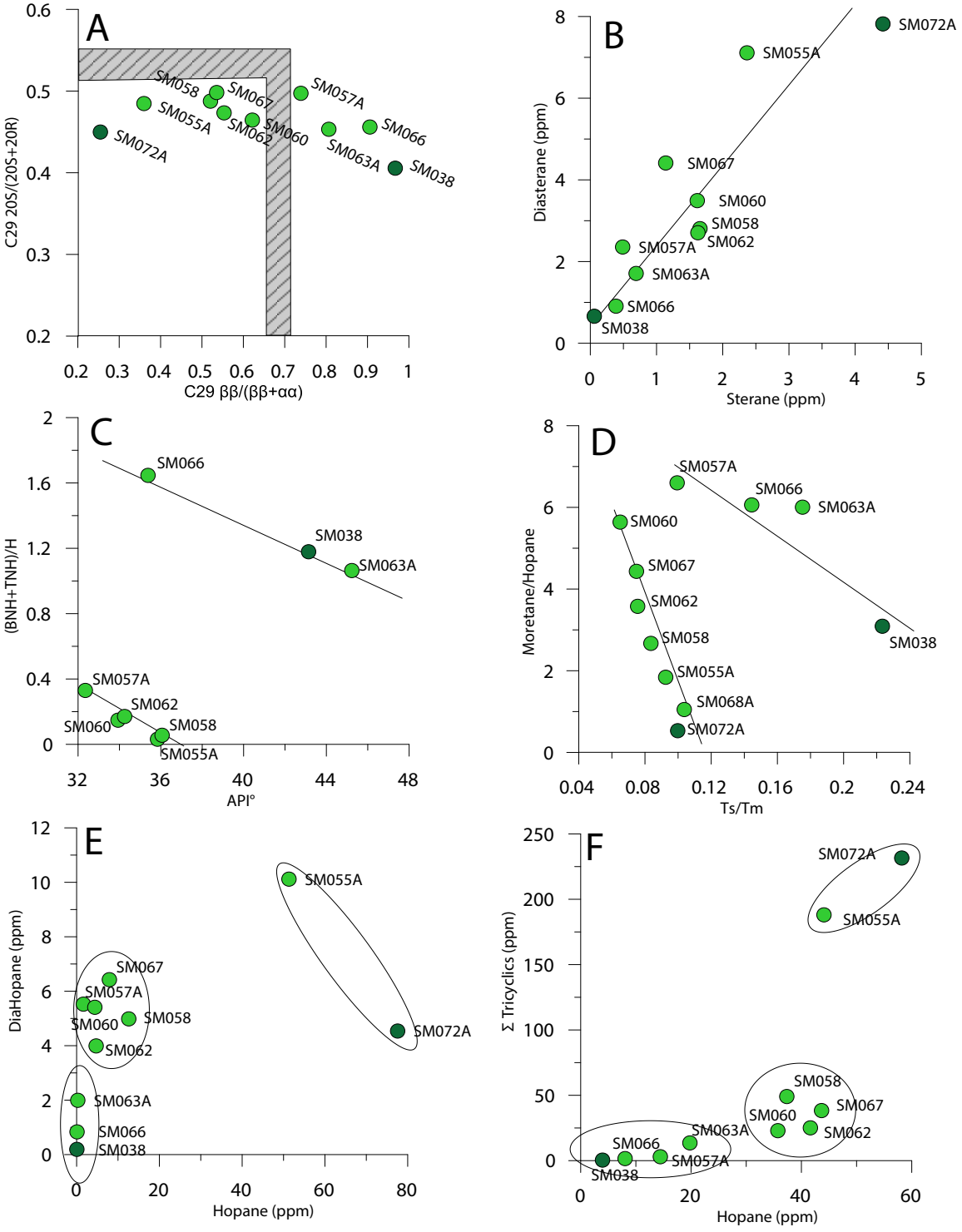

Figure 2.19: Different maturity indicators using sterane isomerization ratios and terpane isomerization ratios. A: shows sterane isomerization ratios for C29 (20R) and (20S) as well as αα and ββ, B shows diasterane versus sterane. C: indicates two different regression lines potentially associated with two different sources. D: shows source and maturity dependent terpane ratios indicating two individual sources. E,F: showing diahopane (DiaHopane) versus hopane and tricyclics versus hopane, indicating two endmember oils and potential mixing. Oil samples from Port au Port Peninsula are shown in dark green. Samples from the Cow Head area are shown in light green.

ty spectrum, from marginally mature to over-mature, a number of isomerization ratios were used to evaluate the oil samples. These data are converted to calculated vitrinite reflectance, using the empirical relationship between phenanthrene and methylphenanthrene proposed by Radke et al. (1982, 1988) and later modified by Cassani et al. (1988), as well as an appraisal of various phenanthrene and naphthalene ratios combined in the VREQ-5 vitrinite values.

Regarding biomarker maturity indicators, I primarily rely on the sterane and terpane isomerization ratios (Figure 2.19A). Terpane and sterane isomerization ratios are consistent strengthening our interpretation (Table 2.12, Table 2.13). Maturity ratios that are also influenced by the source input supplement this interpretation, and add to a better understanding of potentially active source rocks in the study area.

Most terpane ratios are not only influenced by thermal maturity, but also by source composition. Rullkötter and Marzi (1988) in a study of Toarcian shales from north Germany, assign a high moretane/hopane ratio to rocks deposited in a hypersaline environment, whereas Isaksen and Bohacs (1995) observed an increase in the moretane/hopane ratio in transgressive highstand system tracts in sediments of the Triassic Barent Sea. As moretane is less thermally stable than hopane, its abundance decreases with thermal maturity (Seifert and Moldowan, 1980).

In the oil samples collected in western Newfoundland the ratio of tricyclic-terpanes/hopane is both maturity and source dependent, placing source-unrelated samples on different maturity trajectories (Figure 2.19F). With increasing maturity, more tricyclic hydrocarbons than hopanes are generated. Additionally, tricyclics migrate faster than 17α–hopanes, and have a greater affinity for the rock matrix (Peters et al., 1990).

The conversion from Tm/Ts starts at relatively high maturities, and can generally be used to evaluate higher maturity oils (above 0.75 $\%R_o$). This contrasts with sterane and terpane ratios, which can only be used reliably below 0.75 $\%R_o$ (Seifert and Moldowan, 1978). The concentration of Tm is also dependent on the input of organic matter and the depositional environment. Ratios of Ts/Tm in our dataset are uniformly greater than 1, consistent with moderately mature samples (Connan et al., 1986). Because the ratios of moretane/hopane and Tm/Ts are both ma-

turity and source dependent, samples from different source rocks can fall on different regression lines. In this case it allows us to argue for two different sources in the study area, as two regression lines are evident in Figure 16D. Similarly, graphs illustrating tricyclic hopanes/hopane and rearranged hopane/hopane show two endmember clusters (and one potentially mixed cluster), again suggestive of two source rocks (Figure 2.19E-F).

A cross plot between C29 (20S/20S+20R) and C29 ββ/(ββ+αα) is most commonly used to characterize immature to mature samples. Equilibrium for 20S/(20S+20R) is reached at 0.52 to 0.55 (equivalent to a maturity of 0.8 ± 0.1 R_o%) and for ββ/(ββ+αα) at 0.67 to 0.71 (equivalent to a maturity of 0.9 ± 0.1 R_o%); both are indicated as a light grey area on Figure 2.19A. Values for 20S/(20S+20R) display typical behavior, whereas the ratio for ββ/(ββ+αα) shows values above 0.71 for SM038 (Port au Port No. 1 well, Port au Port Peninsula), SM063A (Highland Brook 2, Parson's Pond), and SM066 (Highland Brook W1, Parson's Pond) (Table 2.12). These higher values could be related to different heating rates in the subsurface (Mackenzie and McKenzie, 1983) or different level of clay catalysis (Huang Difan et al., 1990) Samples with the lowest ββ/(ββ+αα) ratio are SM072A (Shoal Point, Port au Port Peninsula), and SM055A (Fox Well, St. Paul's Inlet).

The distribution of ββ/(ββ+αα) ratios suggests that either one source rock generated oils over a range of thermal maturities in both the Port au Port and St. Paul's Inlet areas, or two distinct sources generated oil from different stratigraphic or structural levels.

In order to compare the qualitative maturity measurements to more quantifiable thermal stresses, calculated vitrinite reflectances from MPI-1 and VREQ-5 are used (Table 2.16). Sample SM038 from the Port au Port No. 1 well exhibits the highest maturity in all maturity dependent sterane and terpane ratios. The equivalent vitrinite reflectance, based on the MPI-1 ratio, is 1.5%R_c. This indicates that SM038 was generated in the condensate to dry gas window. This sample also has an API° of 45.23, and the vitrinite reflectance calculated based on VREQ-5 (1.26%R_c) associates it with the light oil field. I interpret the higher calculated vitrinite reflectance to represent secondary cracking of the produced from Port au Port No.1. The originally

lower maturity oil had experienced some degree of secondary cracking, resulting in the erasure of the parameters indicating low maturity. Thus, analysis of SM038 shows the maturity parameters of the deeply buried reservoir, rather than the maturity parameters of the generating source rock. This is substantiated by a crossplot of stigmastane versus 3, + 4-methyldiamantane (Figure 2.17), which shows the sample on the "cracking" asymptote.

Additional geologic evidence for this interpretation of SM038 is the absence of source rocks below or adjacent to the reservoir (sitting in the footwall of the Round Head Thrust) for the Port au Port No.1 well. The established source rocks in the area dip towards the northwest, away from the reservoir, and are carried in the hanging wall of the Round Head Thrust (Figure 2.20). During the thick-skinned Acadian thrusting, a geometry was created in which the Humber Arm Allochthon (containing source rocks) was absent in the footwall to the south, and was only carried in the hanging wall to the north (Figure 2.20) (Stockmal and Waldron, 1998; Waldron et al., 1998). Additionally, none of the potential source rocks in the hanging wall sit deep enough to generate hydrocarbons with the identified maturities.

Maturity values calculated for SM072A (Shoal Point, Port au Port Peninsula) consistently produce the lowest calculated vitrinite reflectance values (0.7 to 0.8 $\%R_c$), which correlate well with isomer maturity indicators and diamondoid parameters. This suggests that the missing source rocks from the footwall of the Round Head Thrust to the south of the Port au Port Peninsula were generating oil (from the Ordovician source) within the early oil window in the hanging wall to the north.

Both samples (SM038 and SM72A) come from the Port au Port Peninsula, but show significantly different source-related biomarker composition and different maturities (possibly linked to different periods of oil generation). Lacombe (2017) proposes a pre-Acadian emplacement of a sheet of Humber Arm Allochthon, which was thinned and rapidly emplaced due to hydrocarbon generation and related overpressure. I propose that the oil produced from Port au Port No.1 well (SM038) was generated from this Cambrian sliver. The oil generated and trapped in the carbonate platform experienced deep burial and some degree of secondary cracking during

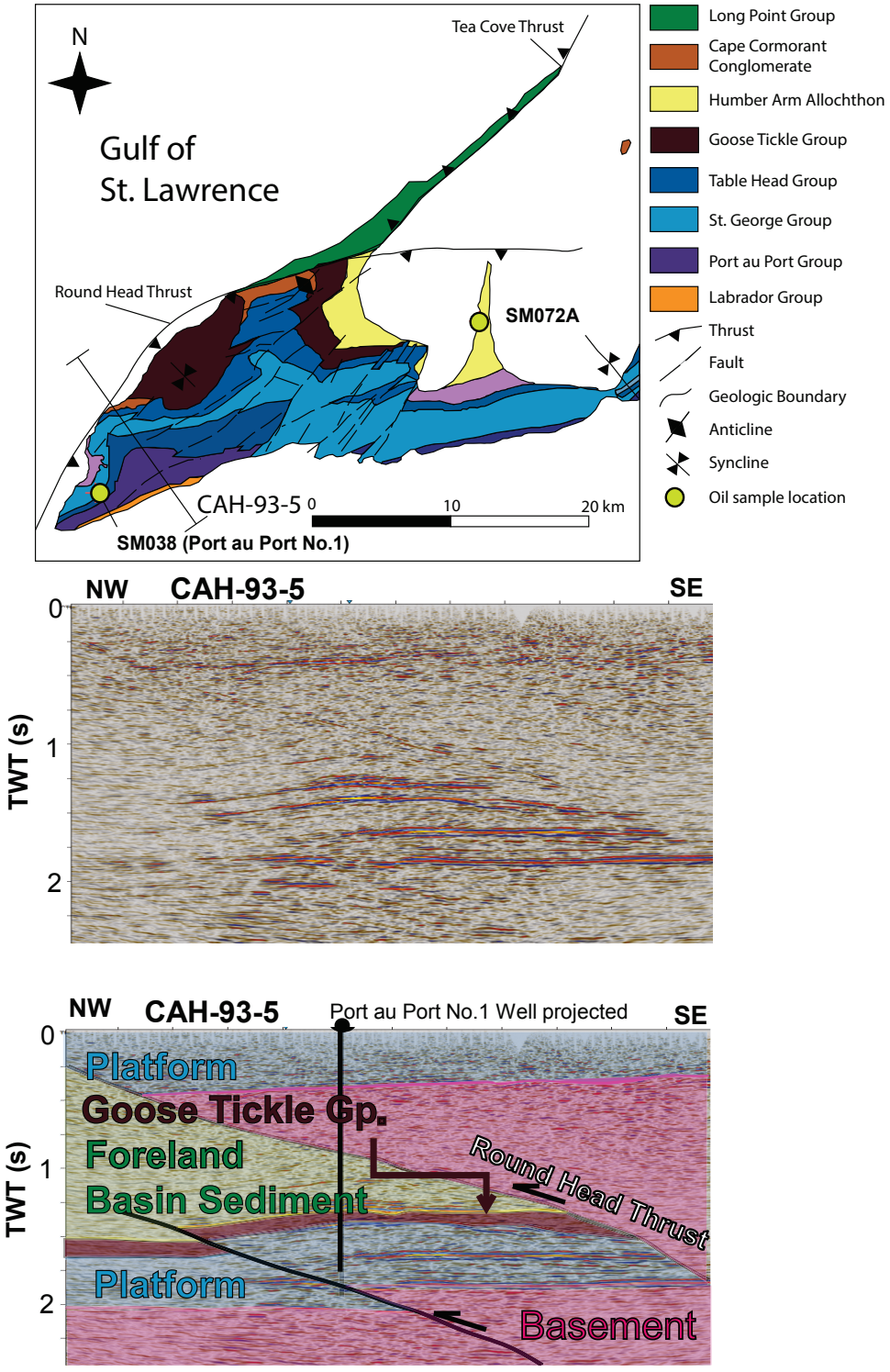

Figure 2.20: Geologic map and seismic profile CAH-93-5 showing the subsurface geometry on the south tip of Port au Port Peninsula.

Geologic map of Port au Port Peninsula illustrating the structural relations created by the Round Head Thrust. Seismic line CAH-93-5 showing the structure tested by Port au Port No.1 well. Line location indicated on geologic map (modified from Cooper et al., 2001). Pink = Laurentian basement; blue = platform succession (top= Table Point Formation); yellow = Goose Tickle Formation (top = base of Lourdes Formation).

the Acadian Inversion resulting in the high observed maturity at present day. The oil collected from Shoal Point (SM072A) was generated after the Acadian Inversion from the Ordovician source rock carried in the hanging wall of the Round Head Thrust (Figure 2.20). In contrast to this, the broad maturity range of the oil samples (0.7 to 1.1 $\%R_o$) collected in the Cow Head area is linked to the dipping character of the source rocks. This generates oils with different thermal maturities at various burial depths from both Cambrian and Ordovician source rocks.

2.6.4. Interpretation of Age, Composition and Depositional Environment from Oil Data

2.6.4.1. Depositional Environment

Hughes et al. (1984, 1995) use biodegradation-resistant dibenzothiophene/phenanthrene (DBT/P) versus pristine/phytane to characterize the depositional environment of various source rocks. For our source rock extracts and oil samples, DBT/P versus pristine/phytane, illustrated in Figure 2.9B, shows the majority fall in a "marine shale" field. This is consistent with previous work completed in western Newfoundland (Macauley, 1987, 1990; Weaver, 1988; Weaver and Macko, 1988; Sinclair,1990; Fowler et al., 1995). Using relations postulated in Chung et al. (1992), I can conclude most samples falling into a Paleozoic-Mesozoic marine shale field (Figure 2.9C). A few exceptions from the Green Point Formation show a greater influence from carbonate rocks, these are extracts SM054P, SM052C, and PA032A.

Further supporting the interpretation of a clastic, shale-dominated source rock is the ratio of rearranged C27-steranes (DIA) to regular C27-steranes (Reg). This ratio relates to the presence of acid sites in clay minerals (which catalyzes the conversion of sterenes to diasterenes, the precursor for diasteranes) (Rubinstein et al., 1975; Sieskind et al., 1979). Slightly lower DIA/Reg values in oil samples SM055A, SM072A, and SM058 may be related to a source richer in carbonate.

The tight cluster of oil samples seen in the C27:C28:C29 (cholestane;ergostane;stigmastane) ternary diagram (Figure 2.8) indicates a similar depositional environment and organic matter type for the two proposed source rocks. A predominance of C29- over C27-steranes has been recognized in pre-Devonian oils by many authors, and is related to high cyanobacteria input producing C29-sterane precursor molecules (McKirdy and Hahn, 1982; Fowler and Douglas, 1984; Rullkötter et al., 1986). Despite the cluster seen in the sterane distribution, samples vary significantly enough in stigmastane concentration to indicate two distinct sources. The extract samples enriched in stigmastane indicate organic matter dominated by bacteria, while the extract samples with less stigmastane may contain more algal-derived organic matter (Figure 2.8A).

A high ratio of rearranged steranes to normal C27-steranes is recognized by Moldowan et al. (1985) as characteristic for Ordovician and early Paleozoic oils. Fowler et al. (1995) described a similar phenomenon and ascribed it to a clastic source rock. Those high ratios of C27-sterane in clastic rocks can be even more pronounced when active acid catalysis promotes the conversion (Sieskind et al., 1979). I see similar patterns in our data (Table 2.6), again supporting an interpretation of an early Paleozoic clastic source rock.

Redox conditions can be derived from the Ph/n-C18 to Pr/n-C17 graph (Figure 2.9A). Despite the oil and extract samples falling in the oxidizing depositional field, the ratios are likely influenced by thermal maturity and biodegradation. This leads to lower ratios and data points closer to the origin, making it difficult to draw any definitive conclusions about the redox conditions in the basin.

2.6.4.2. Age of Expelled Oil

The paraffinic composition of the oil samples, as well as low sulfur values and low $\delta^{13}C$ isotope values, are typical for Ordovician oils (e.g. Martin et al., 1963; Fowler and Douglas, 1984; Reed et al., 1986; Longman and Palmer, 1987; Hoffmann et al., 1987; Jacobson et al., 1988, 1995; Douglas et al., 1991; Blokker et al., 2001). Measured carbon isotope values fall within the normal range for marine Paleozoic crude oils (Sofer, 1984; Hatch et al., 1987; Andrusevich et al., 2000). Biodegradation and water washing have minimal influence on the isotope composition of oil (Schoell, 1984).

High pristane/phytane ratios (2.01 to 2.51) indicate a marine shale as source rock. Depleted carbon isotope composition (-31.45 to -29.94‰ VPDB) support the interpretation of a Paleozoic origin of the source material (Andrusevich et al., 1998). Pristane/phytane in combination with carbon isotope values supports the interpretation of a Paleozoic marine source rock (Figure 2.9C) (Chung et al., 1992). The low carbon isotope values observed in western Newfoundland samples suggests that the source rocks generating those oils were deposited before the Middle Ordovician Carbon Isotope Excursion (Hatch et al., 1987). While the carbon isotope values are very low, they do not unambiguously distinguish the Cambrian from the Ordovician source rock

interval. Compound-specific isotope analysis, however, supports the interpretation of two distinct sources in the same area (Figure 2.11). Specifically, samples SM063A, SM066, and SM055A from the Cow Head area show large enough differences in their compound-specific carbon isotopes (n-C6 to n-C30) to differentiate two endmembers. The two endmembers (SM063A, SM066 vs. SM055A) have carbon isotope values differing by more than 2‰ for each compound when directly compared. This is generally accepted to be a sufficient difference to argue for separate sources (Chung et al., 1981; Sofer, 1984; Peters et al., 2005).

The sterane C28/C29 ratio is age-dependent in marine sources (Moldowan et al., 1985; Grantham and Wakefield, 1988). Ratios in excess of 0.5 are generally too high for a Cambrian to Ordovician source, and are more characteristic for late Paleozoic to lower Mesozoic source rocks (Grantham and Wakefield, 1988). An increase in the C28/C29 ratio is related to a rise in ergostane (C28) concentration through geologic time, which in turn is related to proliferation of algal diversity (Granthham and Wakefield, 1988). However, this ratio cannot be used for definitive age determination of an oil source. The high observed ratios in western Newfoundland (0.48 to 0.61), for both extracts and oil (Figure 2.12), are interpreted to be the product of an unusually high concentration of algae in western Newfoundland source rocks, and are unlikely to be the result of contamination by younger crude oils.

2.6.4.3. Compositional Difference between Cambrian and Ordovician Samples

A number of parameters from the oil samples support the interpretation of a Cambrian source rock with predominantly bacterially-derived (prokaryotic) organic matter and an Ordovician source rock with algal-derived (eukaryotic) organic matter. The selected parameters independently and consistently identify two endmember groups. Both identified endmember groups contain samples from various sample locations throughout the study area.

Variations in stigmastane first led us to consider the possibility of two distinct sources, an interpretation further supported by normalized n-alkane profiles (Figure 2.10). Jacobson et al. (1988) describe two endmember compositions for Ordovician source rocks. Type A is dominated

by a distinct odd carbon number preference typically derived from *G. prisca*, resulting in type I/II organic matter. Type B is characterized by *n*-alkanes with a reduced odd carbon number preference and the presence of isoprenoids, mainly derived from type II/III organic matter originating from degraded and oxidized microplankton (Douglas et al., 1991; Peters et al., 2005). Because of the occurrence of pristine, phytane, and a full n-alkane profile with no OEP in our oil-dataset (Figure 2.10, Table 2.10), I suggest the underlying bulk compisiton of all oil samples consists of type B organic matter, as defined by Jacobson et al. (1988). Differences observed in the OEP and n-alkane profile can be ascribed to slight changes in source composition. Specifically, one group of samples display concave profiles usually associated with non-waxy marine oils, whereas the other group form a convex profiles normally associated with waxy, terrigenous oil (Sofer, 1984). Because the source rocks are too old to be sourced by terrigenous organic material, the waxy character and convex shape of the n-alkane profiles could be attributed to a slightly higher input of *G. prisca* into type B organic matter (Figure 2.10). This contrasts the second group, displaying concave n-alkane profiles, which likely contains little or no *G. prisca* in its type B organic matter; thus, resulting in a non-waxy, marine oil (Figure 2.10). Alternatively, the non-waxy character could be a result of higher maturity and loss of the heavier *n*-alkanes due to thermal cracking and relative enrichment of lighter chain *n*-alkanes during migration. However, the first interpretation, that *G. prisca* is responsible for the observed patterns in the data, is supported by previous work (Fowler et al., 1995).

The marginal odd preference observed in the samples from western Newfoundland is unusual for Ordovician samples; however, the low DBT/P ratios (Figure 2.9) are consistent with an interpretation of a marine shale with type B organic matter (i.e. a low input of *G. prisca*). Low ratios of DBT/P as a result of degradation is unlikely due to its breakdown requiring an energy intensive pathway (Kirimura et al., 2001).

Further support for the presence of two sources is provided by bisnorhopane (BNH) and trisnorhopane (TNH) values. BNH and TNH are directly derived from free bitumen in source rocks, and indicate the presence of organic matter derived from chemo-autotrophic bacteria

(Peters et al., 2005). BNH/H and TNH/H ratios are common parameters used to correlate oil and source rock. A relative increase in one or both of these ratios for related samples is generally interpreted to indicate increasing maturity (Grantham et al., 1980; Hughes et al., 1985). BNH/H ratios are significantly higher in samples SM038, SM066, and SM063A (endmember group 1) than the other samples. On a (BNH+TNH)/H versus API gravity plot, I observe oils on two distinct regression lines (Figure 2.19C). This can be used as an argument for two active source rocks (Peters et al., 2005). Samples falling on the lower regression line show lower ratios of BNH/H (Table 2.13), and are therefore less influenced by the potentially prokaryotic organism responsible for the unique signature observed for endmember group 1 in the western Newfoundland oils.

Because tricyclics and hopanes have different precursor molecules, significant variation in tricyclics and hopanes can be explained by changes in source composition (Figure 2.19F). High ratios of tricyclic terpanes and diterpanes relative to pentacyclic terpanes (e.g. TriCyc/H) in samples SM038, SM066, and SM063A (Table 2.13) compare well to Cambrian oils from Oman (Grantham, 1986), the Bikaner-Nagaur Basin (Dutta et al., 2013), and parts of the Tarim Basin, China (Yang, 1991). This contrasts the lower tricyclic/hopane (TriCyc/H) ratios but higher concentration of tetracyclic terpanes (TET) and C23 tricyclic molecules (C23T) found in the other endmember group containing sample SM072A and SM055A.

Yang (1991) also discusses a high GCMS-response in pregnane and homopregnane for Cambrian-Ordovician source rocks; this correlates well with our findings (Figure 2.14). The interpretation of two acting sources is further strengthened by the homohopane distribution pattern for the oil samples (Picha and Peters, 1998), in which we can see the same identified endmembers in samples SM063A and SM066 (group 1), and SM055A and SM072A (group 2) (Figure 2.21). The remaining samples (SM057A, SM058, SM060, SM062, SM067) fall between those endmembers (suggestive of mixing).

All discussed biomarker parameters support a Cambrian source rock with bacterially-derived organic matter generating oil family 1, and represented by samples SM038, SM066, and SM063A with endmember group 1, and an Ordovician source rock with algal-derived organic

matter generating oil family 2, represented by samples SM072A and SM055A with endmember group 2.

Only the high sterane/hopane ratios found in samples SM038, SM066, and SM063A contradict the interpretation of a bacterially-derived organic matter. Typically, bacteriohopanepolyols in the bacterial membrane are considered primary precursor molecules for hopane, leading to the high hopane usually observed in oils sourced by bacteria-rich organic matter. However, for samples SM038, SM066, and SM063A, the overall concentrations of hopane and sterane are lower than in samples SM072A and SM055A. Additionally, they show similar sterane/hopane ratios to each other, despite significantly different calculated thermal maturities. This suggests the sterane/hopane ratio is mostly controlled by source, and is relatively independent of maturity. Additionally, work by Ourisson et al. (1982), suggests it is possible that early Paleozoic bacteria used steranes and tricyclic terpanes, instead of hopanes, in their membrane molecules due to their similar function in lipid membranes. Supporting this, high concentrations of steranes over hopanes have been detected in gram-negative myxobacteria and certain methanogenic bacteria with significant amounts of steroids incorporated into their cellular membrane (Bird et al., 1971; Kohl et al., 1983). Both these factors offer possible explanations for the unusually high concentration of sterane in a bacterially-derived organic matter.

Statistical analysis (HCA), using different agglomeration-linkage methods (i.e. single-, complete-, median-, centroid-, incremental-, and flexible-linkage) with parameters listed in Table 2.14 and Table 2.15 show the same clusters illustrated in Figure 2.22. Only the single-linkage agglomeration method clusters samples SM072A and SM055A in individual clusters, yet, showing them as closely related. To keep the data presentation consistent I am using the same (incremental) linking method as for the source rock extracts.

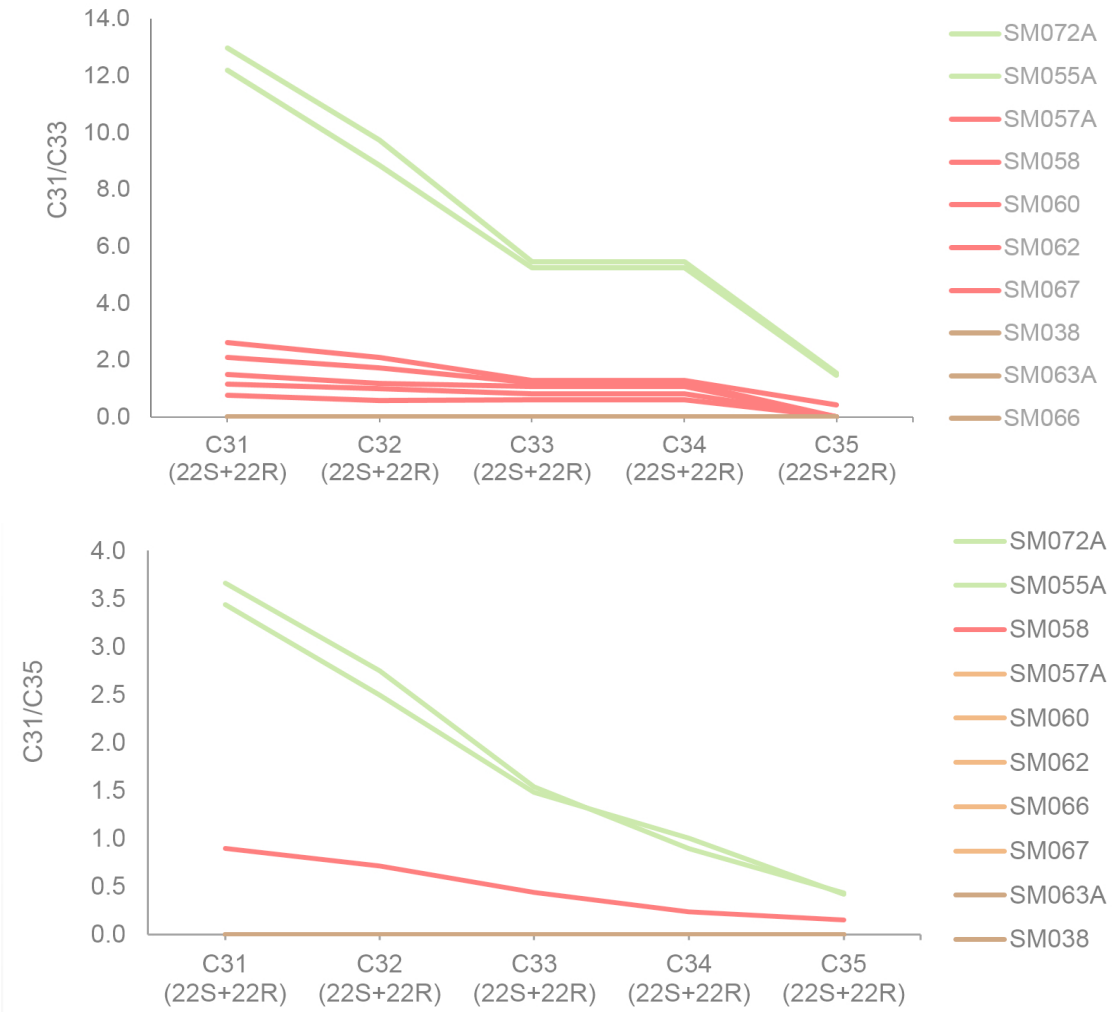

Figure 2.21: Homohopane distribution pattern indicate two endmember oils and potential mixing. Samples shown in orange (SM057A, SM058, SM069, SM062, SM067) represent potentially mixed samples.

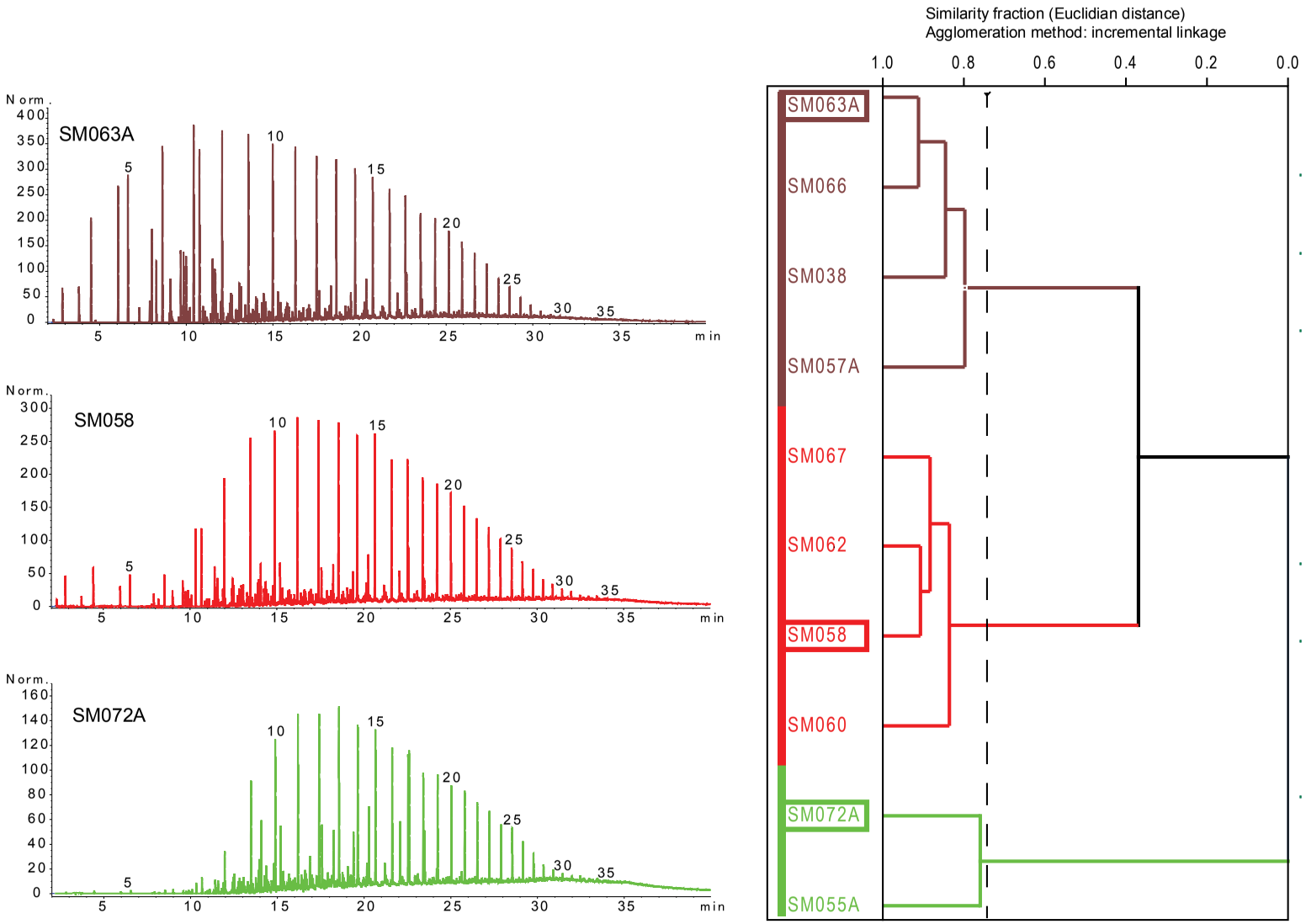

Figure 2.22: FID diagrams are showing examples for the two endmember oil families (brown and green) and a potentially mixed group (red). Statistical analysis (HCA) using sterane and terpane concentrations (Table 2.14, Table 2.15) as well as sterane, terpane ratios and other source related parameters summarized in Table 2.5, Table 2.6, Table 2.10, as well as carbon isotope data Table 2.11 resulted in the shown dendrogram. Excluded from the statistical analysis are maturity dependent parameters.

2.7. Oil to Source Correlation

Oil-to-source correlation includes the following steps:

- Using pyrolysis data to identify potential source intervals.
- Identifying biomarkers in the extract data that exhibit statistically significant changes from the Cambrian to Ordovician source intervals.
- Interpreting whole oil geochemistry and carbon isotope data in combination with detailed biomarker analysis to gain an understanding of age, organic matter composition, depositional environment, and potential oil families.
- Cross-correlating oil families with extract families and bitumen, linking them to specific source rock intervals.

The systematic sampling along measured sections with well-constrained biostratigraphic ages, in addition to the previously discussed parameters, also allows us to identify two potential sources. One, within the Middle Ordovician Green Point Formation and more distal Middle Arm Point Formation, was previously identified by Macauley, (1987, 1990), Weaver (1988), Weaver and Macko (1988), Sinclair (1990), and Fowler et al. (1995). The organic matter for this interval is interpreted as type I/II organic matter with high TOC (max. 9.45%, based on Rock-eval pyrolysis data) (Figure 2.6). Samples with those characteristics show excellent source potential. A second source in the middle to upper Cambrian Green Point Formation and Cooks Brook Formation was previously unrecognized, and is interpreted as type II/III organic matter based on Rock-eval pyrolysis data. TOC content in this middle to upper Cambrian source reaches a maximum of 2.21 wt% (Cooks Brook Formation, Seal Cove) indicating good source potential in its organic-rich layers.

The stratigraphic thickness of the Lower to Middle Ordovician source rock is approximated to 150 to 250 m, based on outcrop measured sections (Botsford, 1987; James and Stevens,1987). It is difficult to assign a cumulative thickness for the organic rich shale beds, because there is no visual differentiation possible between organically lean and organically rich intervals. The sampling interval is too coarse to resolve the potential high frequency changes in organic

matter content. The middle to upper Cambrian source rock is between 50 to 200 m thick, consisting of interbedded lean and organically rich sections (Botsford, 1987; James and Stevens,1987). A significant number of samples represent lean intervals, with TOC values around 0.07 to 0.5 wt%. Similarly, it is difficult to assign a cumulative thickness for the organically rich layers to the Cambrian source rocks, because the sampling interval is too coarse. Thermal maturity, calculated from T_{max} pyrolysis data, falls into the low to mid mature window (0.65 to 0.89 $\%R_o$) for most source rock samples, however, samples collected in close proximity to the ophiolites in the Bay of Islands area are characterized as post-mature. Yet, calculations of paleo-generative potential for the post-mature rocks indicate that their quality and quantity compare well with immature samples from the most distal region of the continental rise deposits.

The geochemistry of the 23 selected extract samples from the Cambrian and Ordovician intervals provides data consistent with our understanding of the depositional environment and age of the rocks, specifically a pre-Devonian clastic source rock with type I/II and type II/III organic matter for all extracts. Bulk composition shows an organic matter similar to the type B organic matter defined by Jacobson et al. (1988). Biomarkers listed in Table 2.5 and Table 2.6 characterize the organic matter further as bacterially-derived with minor algal influence in the Cambrian source rock, and algal domination in the Ordovician.

The analyzed oil and bitumen samples show similar biomarker and carbon isotope distributions to the extracts; both record the change in biomarker composition from a bacterial to a more algal-derived organic matter type. Therefore, I am able to correlate oil samples to the two established extract groups and to distinct source intervals from the Cambrian and Ordovician (Figure 2.22).

An additional argument for a Cambrian source is the high maturity of the oil found in the Port au Port No.1 well (SM038). This oil contains the same biomarkers found in Cambrian source rocks and extracts from western Newfoundland, and additionally, reveals a “cracked” character based on diamondoid analysis. The Cambrian and Ordovician source rocks are missing in the footwall of the Round Head Thrust. However, mapping relations have shown that at least

two separate sheets of the Humber Arm Allochthon were emplaced during the Taconian Orogeny, placing potentially mature Cambrian source rocks adjacent to the Round Head Thrust scarp (Lacombe, 2017). Therefore, charge into the reservoir is feasible before or during the tectonic inversion in the Acadian. After the inversion, the source rocks are now absent in the footwall of the Round Head Thrust.

Oils found in the Parson's Pond area (SM066, SM063A) show the same biomarker signature as the oil from Port au Port No.1 well, but have characteristics of much lower thermal maturities. This indicates that the source rock responsible for SM038 oil in Port au Port Peninsula also exists in the Cow Head area. The different thermal maturities of the Parson's Pond oils are, however, related to structural imbrication of said Cambrian source rock. Depending on how deeply buried the source rock was, it generated oil with different thermal maturities, but with the same source-related biomarker. The low maturity oil found on Shoal Point (Port au Port Peninsula) perfectly correlates with bitumen from an active seep and source rocks collected from Tea Cove interpreted as the most distal portion of the continental rise deposits (Middle Arm Point Formation). Graptolites from this formation yield Middle Ordovician ages (Lacombe, 2017). The thermal maturity of these rock samples is 0.65 $\%R_o$ and arguably insufficient for oil generation; however, they should have experienced sufficient thermal stress in the subsurface farther north to generate low maturity oil found on Shoal Point.

The biomarker signature found in the Shoal Point oil correlates well with the Middle Ordovician source rock. Oil most similar to the Shoal Point oil (SM072A) was found in Fox Well #2 (SM055A) in St. Paul's Inlet, just south of Parson's Pond. SM055A also shows low maturities and has the same characteristic biomarker signature as SM072A. Other oil samples collected from the Parson's Pond area show stronger resemblance to the Shoal Point and Fox Well oil in their biomarker signature, but have varying maturities, explained by the dipping character of the imbricated source rocks.

Biomarker ratios and isomer ratios indicate that mixing between the proposed Cambrian and Ordovician source is likely. The extent of the mixing, however, cannot be determined with

the current dataset. Low biodegradation of the oil found in the Parson's Pond area suggest that both proposed sources are presently active.

2.8. Conclusion

Our data demonstrate that two hydrocarbon source rocks are active on the western Newfoundland margin, one in the middle to upper Cambrian Green Point and Cooks Brook formations, and another in the Middle Ordovician Green Point and Middle Arm Point formations. The two intervals show characteristic biomarker distributions in source extracts, bitumen, and oil, which demonstrate a change from a primitive bacterial organic matter associated with the middle to upper Cambrian source, to more algal-dominated organic matter associated with the Middle Ordovician source. Both sources are active in the Parson's Pond area, generating oil with varying thermal maturities depending on the structural position of the source within the imbricated Humber Arm Allochthon. In the Port au Port Peninsula, only the Ordovician source could be shown as active with the natural seep on Shoal Point.

Chapter 3: Conclusion

In this research project I was able to identify and characterize two source rock units in western Newfoundland and successfully correlate them to oil found in the study area. This contributes to an advance in current knowledge of the organic geochemistry in the area.

The deep marine deposits of the Humber Arm Allochthon contain two source rock intervals (Figure 3.1): a Cambrian source rock deposited during the Cambrian Series 3 to the Furongian, composed of type II/III organic matter; and a Middle Ordovician source rock, characterized by high TOC values (max. 9.45 wt%) and type I/II organic matter. Due to the imbricated character of the deep marine gravity flow deposits, and their lateral heterogeneity, a clear trend in source richness from shelf proximal to shelf distal could not be established. However, the Middle Arm Point Formation, representing the most distal portion of the continental slope and rise deposits, contains the organically richest intervals. The thermal maturity of outcrop samples in the Port au Port Peninsula and Cow Head areas range from 0.65 to 0.89 $\%R_o$ (calculated from T_{max}). Samples collected from the Bay of Islands are characterized as over-mature. However, recalculated original generative potential yields comparable results to the immature Middle Arm Point Formation on Port au Port Peninsula.

Biomarker analysis further characterizes the organic matter of both source intervals as type B after Jacobson et al. (1988). Marker molecules in the Cambrian source indicate a strong influence from bacterially-derived organic matter. Based on statistical analysis a distinct shift in biomarker composition from the Cambrian source to the more viable Ordovician source is evident (Figure 3.2). The organic matter composing the Ordovician source has a stronger algal influence, with some input from the Ordovician organism *G. prisca* likely.

The collected oil samples can be subdivided into two endmember groups based on compound-specific carbon isotope and biomarker data, with a third group of samples indicating potential mixing. These three groups can also be identified using statistical algorithms, such as hierachical cluster analysis (HCA) and principle component analysis (PCA) (Figure 3.3). Biomarker ratios identifying oil originating from a bacterially-derived source (i.e. Cambrian source),

and molecular markers pointing to a more algal dominated source rock (i.e. Ordovician source), can be found in our oil samples. This leads to the interpretation of two oil families, which can be linked to distinct source intervals.

Maturity evaluation based on isomer ratios, aromatic molecules, and diamondoid analysis reveals information regarding the complex charge history of the Port au Port No.1 well. Pre-Acadian charge, from a low maturity Cambrian source rock, into carbonate reservoirs across the Round Head Thrust was followed by deep burial and secondary cracking in the reservoir. This led to high maturities in the oil produced from the well. The wide range of maturities from oil samples collected in the Cow Head area (0.7 to 1.11 $\%R_c$) is related to the dipping character of the imbricated source rocks. This, in combination with mixing of the two endmember oils, produces an intricate history for the oil seeps found in the Cow Head area.

An important future step will be to integrate these data into a regional petroleum basin model. This will allow us to assess the thermal development of this basin, and will improve our understanding of oil generation and migration in complex tectonic fold and thrust belts in general.

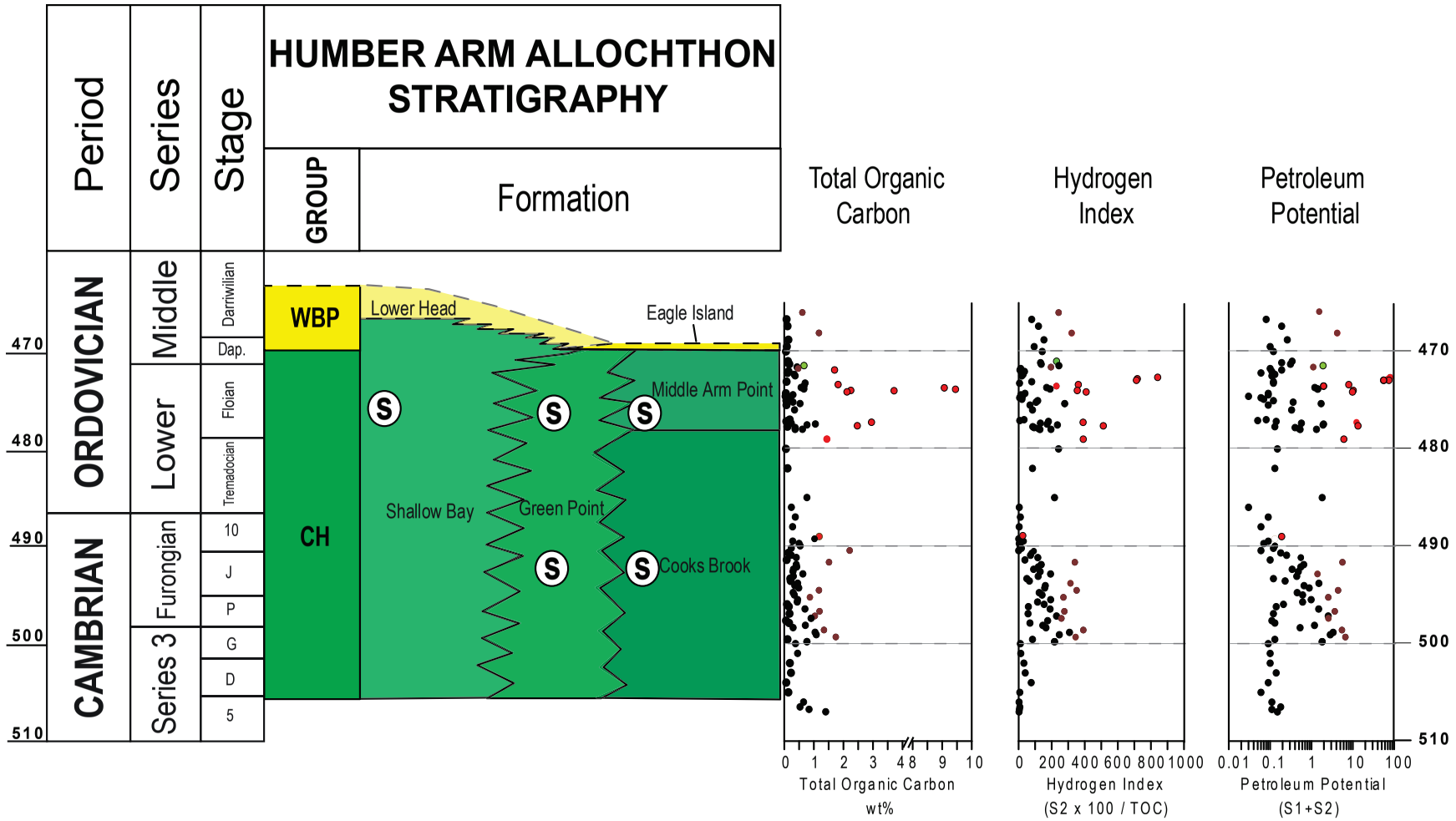

Figure 3.1: Pyrolysis analysis identifying two potential source intervals.
A middle to upper Cambrian and a Middle Ordovician interval characterized by high TOC wt.%, Hydrogen Index (S2x100)/TOC and Petroleum Potential (S1+S2). S= Source rock; R = Reservoir; WBP = Western Brook Pond Group; CH = Cow Head Group. Samples selected for extract analysis are highlighted in red and green (Ordovician cluster) and brown (Cambrian cluster) (Figure 3.2).

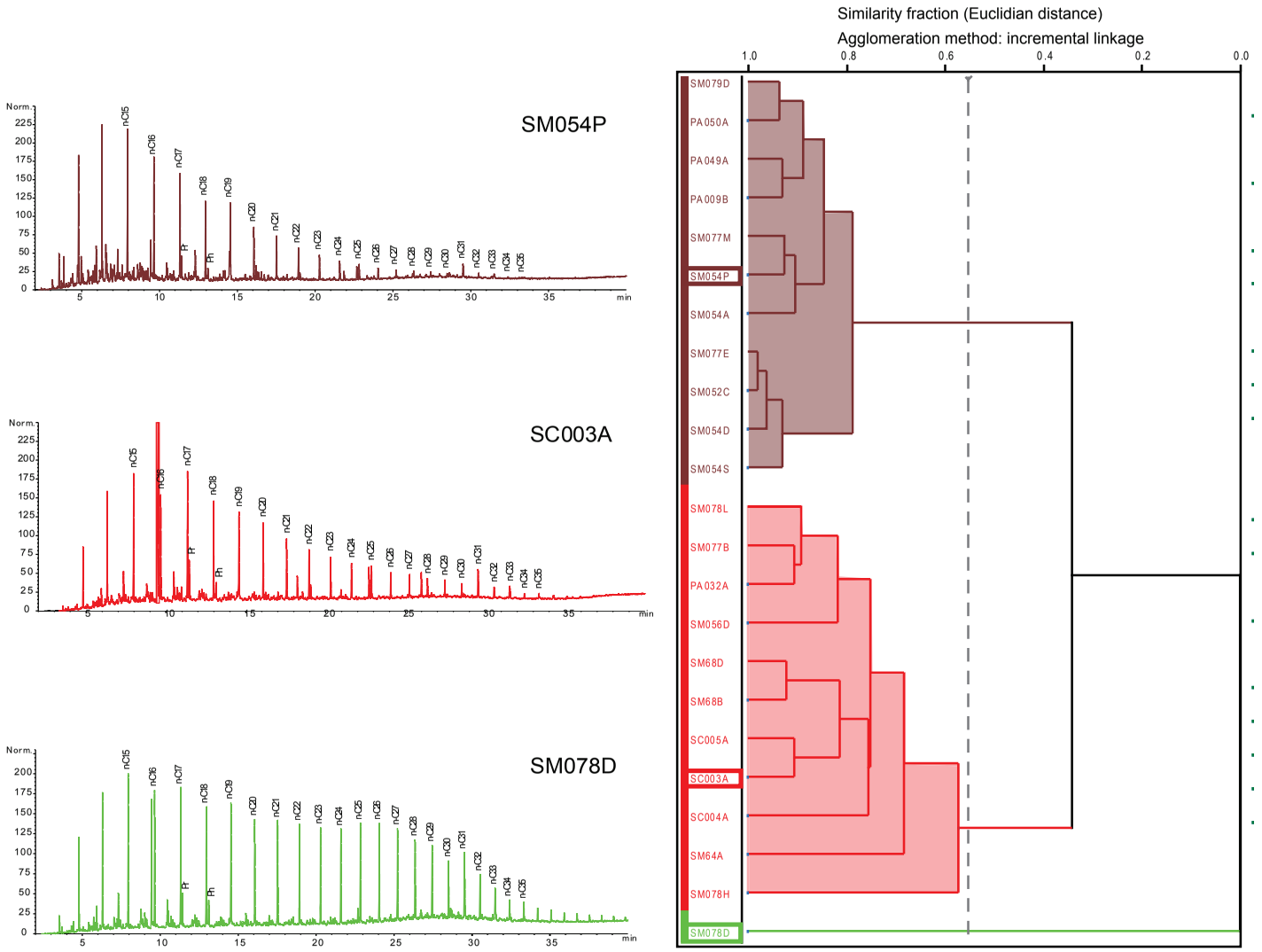

Figure 3.2: Hierarchical cluster analysis (HCA) using sterane and terpane concentrations of extracts.
HCA was performed with Pirourette®; parameters (Table 2.7,Table 2.8, Table 2.9) are auto-scaled; calculation of Euclidean distances and an incremental linkage method results in a similarity (dashed line) of 0.56, distinguishing two cluster. The cluster identified include Ordovician samples (red) with one outlier sample (green) and Cambrian samples (brown). Representative GCMS graphs show the visual differences of the FID fingerprints.

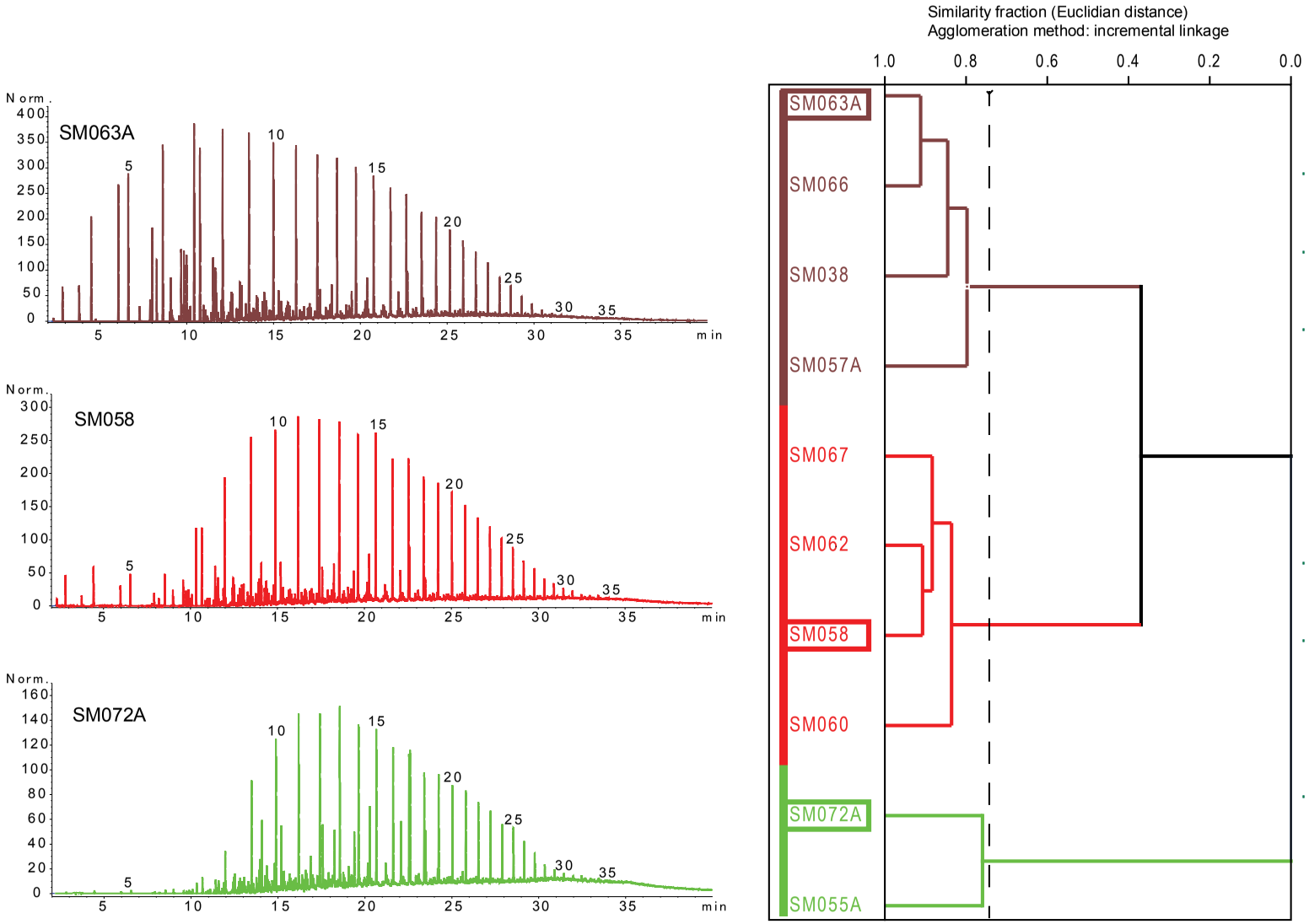

Figure 3.3: FID diagrams are showing examples for the two endmember oil families (brown and green) and a potentially mixed group (red). Statistical analysis (HCA) using sterane and terpane concentrations (Table 2.14, Table 2.15) as well as sterane, terpane ratios and other source related parameters summarized in Table 2.5, Table 2.6, Table 2.10, as well as carbon isotope data Table 2.11 resulted in the shown dendrogram. Excluded from the statistical analysis are maturity dependent parameters.

References

Andrusevich, V. E., M. H. Engel, and J. E. Zumberge, 2000, Effects of paleolatitude on the stable carbon isotope composition of crude oils: Geology, v. 28, no. 9, p. 847–850, doi:10.1130/0091-7613(2000)028<0847:EOPOTS>2.3.CO;2.

Baker, H. A., 1928, General report of the government geologist for 1928: Geological Survey of Newfoundland.

Batten Hender, K.L., and Dix, G.R., 2008, Facies development of a Late Ordovician mixed carbonate-siliciclastic ramp proximal to the developing Taconic orogen: Lourdes Formation, Newfoundland, Canada: Facies, v. 54, p. 121–149.

Bergström, S.M., Riva, J., and Kay, M., 1974, Significance of conodonts, graptolites, and shelly faunas from the Ordovician of western and north-central Newfoundland: Canadian Journal of Earth Sciences, v. 11, p. 1625–1660.

Berkowitz, N., 1997, Fossil hydrocarbons: chemistry and technology: San Diego, Academic Press, 351 p.

Bird, C. W., J. M. Lynch, F. J. Pirt, and W. W. Reid, 1971, Steroids and squalene in Methylococcus capsulatus grown on methane.: Nature, v. 230, no. 5294, p. 473–474.

Blokker, P., P. van Bergen, R. Pancost, M. E. Collinson, J. W. de Leeuw, and J. S. S. Damste, 2001, The chemical structure of Gloeocapsomorpha prisca microfossils: implications for their origin: Geochimica et Cosmochimica Acta, v. 65, no. 6, p. 885–900.

Botsford, J. W., 1987, Depositional history of Middle Cambrian to Lower Ordovician deep water sediments, Bay of Islands, western Newfoundland, PhD: Memorial University of Newfoundland, 508 p.

Boyce, W. D., J. W. Botsford, and J. . Ash, 1992, Preliminary trilobite biostratigraphy of the Cooks Brook Formation (Northern Head Group), Humber Arm Allochthon, Bay of Islands, western Newfoundland: Current Research, Newfoundland Department of Mines and Energy, Geological Survey Branch, v. 92–1, p. 55–68.

Bray, E. E., and E. D. Evans, 1961, Distribution of n-paraffins as a clue to recognition of source beds: Geochimica et Cosmochimica Acta, v. 22, no. 1, p. 2–15.

Brown, C. B., 1938, Anglo-Ecuadorian report on oil in Newfoundland: Private report to Anglo Ecuadorian Oilfields Ltd.

Burden, E.T., Calon, T., Normore, L., and Strowbridge, S., 2001, Stratigraphy and structure of sedimentary rocks in the Humber Arm Allochthon, southwestern Bay of Islands, Newfoundland: Current Research (2001) Newfoundland Department of Mines and Energy, Geological Survey, Report 2001-1, p. 15–22.

Burden, E.T., Quinn, L., Nowlan, G.S., and Nill, L.A.B., 2002, Palynology and micropaleontology of the Clam Bank Formation (Lower Devonian) of western Newfoundland, Canada: Palynology, v. 26:1, p. 37–41.

Cahn, R. S., C. Ingold, and V. Prelog, 1966, Specification of Molecular Chirality: Angewandte Chemie International Edition in English, v. 5, no. 4, p. 385–415, doi:10.1002/anie.196603851.

Cassani, F., O. Gallango, S. Taluskdar, C. Vallejos, and U. Ehrmann, 1988, Methylphenanthrene maturity index of marine source rock extracts and crude oils from the Maracaibo Basin: Advances in Organic Geochemistry, v. 13, no. 1–3, p. 73–80.

Cawood, P. A., J. A. van Gool, and G. R. Dunning, 1996, Geological development of eastern Humber and western Dunnage zones: Corner Brook–Glover Island region, Newfoundland: Canadian Journal of Earth Sciences, v. 33, no. 2, p. 182–198.

Cawood, P. A., P. J. McCausland, and G. R. Dunning, 2001, Opening Iapetus: constraints from the Laurentian margin in Newfoundland: Geological Society of America Bulletin, v. 113, no. 4, p. 443–453.

Cawood, P.A., and Nemchin, A.A., 2001, Paleogeographic development of the east Laurentia margin: Constraints from U-Pb dating of detrital zircons in the Newfoundland Appalachians: Geological Society of America Bulletin, v. 113, p. 1234–1246.

Chow, N., and N. P. James, 1987, Cambrian Grand Cycles: A northern Appalachian perspective: Geological Society of America Bulletin, v. 98, no. 4, p. 418, doi:10.1130/0016-7606(1987)98<418:CGCANA>2.0.CO;2.

Chung, H. ., M. A. Rooney, M. B. Toon, and G. E. Claypool, 1992, Carbon isotope composition of marine crude oils: The American Association of Petroleum Geologists Bulletin, v. 76, no. 7, p. 100–1007.

Connan, J., J. Bouroullec, D. Dessort, and P. Albrecht, 1986, The microbial input in carbonate-anhydrite facies of a sabkha palaeoenvironment from Guatemala: a molecular approach: Organic Geochemistry, v. 10, no. 1–3, p. 29–50.

Cooles, G. P., As. Mackenzie, and T. M. Quigley, 1986, Calculation of petroleum masses generated and expelled from source rocks: Organic geochemistry, v. 10, no. 1–3, p. 235–245.

Cooper, M., J. Weissenberger, I. Knight, D. Hostad, D. Gillespie, H. Williams, E. Burden, J. Porter-Chaudhry, D. Rae, and E. Clark, 2001, Basin evolution in western Newfoundland: new insights from hydrocarbon exploration: AAPG bulletin, v. 85, no. 3, p. 393–418.

Dahl, J. E., J. M. Moldowan, K. E. Peters, G. E. Claypool, M. A. Rooney, G. E. Michael, M. R. Mello, and M. L. Kohnen, 1999, Diamondoid hydrocarbons as indicators of natural oil cracking: Nature, v. 399, no. 6731, p. 54–57.

Dallmeyer, R. D., and H. Williams, 1975, 40Ar/39Ar release spectra of hornblende from the Bay of Islands metamorphic aureole, western Newfoundland: their bearing on the timing of ophiolite obduction at the Ordovician continental margin of eastern North America: Canadian Journal of Earth Sciences, v. 12, p. 1685–1690.

Dewey, J. F., and J. F. Casey, 2013, The sole of an ophiolite: the Ordovician Bay of Islands Complex, Newfoundland: Journal of the Geological Society, v. 170, no. 5, p. 715–722, doi:10.1144/jgs2013-017.

Douglas, A. ., J. S. S. Damsté, M. . Fowler, T. . Eglinton, and J. . de Leeuw, 1991, Unique distributions of hydrocarbons and sulphur compounds released by flash pyrolysis from the fossilised alga Gloeocapsomorpha prisca, a major constituent in one of four Ordovician kerogens: Geochimica et Cosmochimica Acta, v. 55, no. 1, p. 275–291, doi:10.1016/0016-7037(91)90417-4.

Dubé, B., G. R. Dunning, K. Lauziere, and J. C. Roddick, 1996, New insights into the Appalachian Orogen from geology and geochronology along the Cape Ray fault zone, southwest Newfoundland: Geological Society of America Bulletin, v. 108, no. 1, p. 101–116.

Dutta, S., S. Bhattacharya, and S. V. Raju, 2013, Biomarker signatures from Neoproterozoic–Early Cambrian oil, western India: Organic Geochemistry, v. 56, p. 68–80, doi:10.1016/j.orggeochem.2012.12.007.

Enachescu, M., E., 2011, Petroleum Petroleum Exploration Opportunities in Exploration Opportunities in Anticosti Basin Anticosti Basin, Offshore OffshoreWestern Western Newfoundland and Labrador Newfoundland and Labrador - Call for Bids NL11 Call for Bids NL11-01.

Espitalé, J., F. Marquis, and L. Sage, 1987, Petroleum geology of North West Europe: London,

Graham and Trotman, London, 71-86 p.

Fleming, J. M., 1970, Petroleum exploration in Newfoundland and Labrador, geologic map: Department of Mines, Agriculture and Resources, Mineral Resources Division : St. John's, NL, Canada, Mineral Resources Report. Newfoundland and Labrador, Mineral Resources Division, 1970.

Fowler, M. G., and A. G. Douglas, 1984, Distribution and structure of hydrocarbons in four organic-rich Ordovician rocks: Organic Geochemistry, v. 6, p. 105–114.

Fowler, M. G., A. P. Hamblin, D. Hawkins, L. D. Stasiuk, and I. Knight, 1995, Petroleum geochemistry and hydrocarbon potential of Cambrian and Ordovician rocks of western Newfoundland: Bulletin of Canadian Petroleum Geology, v. 43, no. 2, p. 187–213.

Grantham, P. J., 1986, The occurence of unusual C27 and C29 sterane predominances in two types of Oman crude oil: Organic geochemistry, v. 9, no. 1, p. 1–10.

Grantham, P. J., J. Posthuma, and K. de Groot, 1980, Variation and significance of the C27 and C28 triterpane content of a North Sea core and various North Sea crude oils: Physics and Chemistry of the Earth, v. 12, p. 29–38, doi:10.1016/0079-1946(79)90086-7.

Grantham, P. J., and L. L. Wakefield, 1988, Variation in the sterane carbon number distribution of marine source rock derived crude oils through geologic time: v. Organic Geochemistry, no. 12, p. 61–73.

Hatch, J. R., S. R. Jacobson, B. J. Witzke, B. J. Risatti, D. E. Anders, L. W. Watney, D. K. Newell, and A. K. Vuletich, 1987, Possible Late Middle Ordovician Organic Carbon Isotope Excursion: Evidence from Ordovician Oil and Hydrocarbon Source Rocks, Mid-Continent and East-Central United States: The American Association of Petroleum Geologists Bulletin, v. 71, no. 11, p. 1342–1354.

Hibbard, J. P., C. R. Van Staal, and D. W. Rankin, 2007, A comparative analysis of pre-Silurian crustal building blocks of the northern and the southern Appalachian orogen: American Journal of Science, v. 307, no. 1, p. 23–45.

Hoffmann, C. F., C. B. Foster, T. G. Powell, and R. E. Summons, 1987, Hydrocarbon biomarkers from Ordovician sediments and the fossil alga Gloeocapsomorpha prisca Zalessky 1917: Geochimica et Cosmochimica Acta, v. 51, no. 10, p. 2681–2697, doi:10.1016/0016-7037(87)90149-9.

Howley, J. P., 1875, Report of geological exploration in Port au Port and St. George's Bay, Report of Progress for the year 1874: Geological Survey of Newfoundland.

Huang Difan, L. Jinchao, and Z. Dajiang, 1990, Maturation sequence of continental crude oils in hydrocarbon basins in China and its significance: Organic Geochemistry, v. 16, no. 1–3, p. 521–529.

Huang, H., S. R. Larter, and G. D. Love, 2003, Analysis of wax hydrocarbons in petroleum source rocks from the Damintun depression, eastern China, using high temperature gas chromatography. Organic Geochemistry, v. 34, no. 12, p. 1673–1687, doi:10.1016/S0146-6380(03)00172-4

Hughes, W. B., 1984, Use of thiophenic organosulfur compounds in characterizing crude oils derived from carbonate versus siliciclastic sources: AAPG Studies in Geology, v. 18, p. 181–196.

Hughes, W. B., A. G. Holba, and L. I. Dzou, 1995, The ratios of dibenzothiophene to phenanthrene and pristane to phytane as indicators of depositional environment and lithology of petroleum source rocks: Geochimica et Cosmochimica Acta, v. 59, no. 17, p. 3581–3598.

Isaksen, G. H. and Bohacs, K. M. 1995, Geological controls of source rock geochemistry

through relative sea level; Triassic Barents Sea. Petroleum Source Rocks, 25-50.

Jacobi, R. D., 1981, Peripheral bulge – a causal mechanism for the Lower/Middle Ordovician unconformity along the western margin of the Northern Appalachans: Earth and Planetary Science Letters, v. 56, p. 245–251.

Jacobson, S. R., S. C. Finney, J. R. Hatch, and G. A. Ludvigson, 1995, Gloeocapsomorpha prisca-driven organic carbon isotope excursion, late Middle Ordovician (Rocklandian), North American mid-continent: new data from Nevada and Iowa.

Jacobson, S. R., J. R. Hatch, S. C. Teerman, and R. Askin, 1988, Middle Ordovician Organic Matter Assamblages and Their Effect on Ordovician-Derived Oils: The American Association of Petroleum Geologists Bulletin, v. 72, no. 9, p. 1090–1100.

James, N. P., C. R. Barnes, R. K. Stevens, and I. Knight, 1987, Evolution of a lower Paleozoic continental margin carbonate platform, northern Canadian Appalachians: AAPG Bulletin: Annual convention with divisions Sepm/emd/dpa., v. 71, no. 5, p. 572.

James, N. P., J. W. Botsford, and S. H. Williams, 1987, Allochthonous slope sequence at Lobster Cove Head: evidence for a complex Middle Ordovician platform margin in western Newfoundland: Canadian Journal of Earth Sciences, v. 24, no. 6, p. 1199–1211, doi:10.1139/e87-115.

James, N. P., and R. K. Stevens, 1986, Stratigraphy and correlation of the Cambro-Ordovician Cow Head Group, western Newfoundland: Geological Survey of Canada Bulletin, 143 p.

Kamo, S. L., C. F. Gower, and T. E. Krogh, 1989, Birthdate for the lapetus Ocean? A precise U-Pb zircon and baddeleyite age for the Long Range dikes, southeast Labrador: Geology, v. 17, no. 7, p. 602–605.

Kirimura, K., T. Furuya, Y. Nishii, Y. Ishii, K. Kino, and S. Usami, 2001, Biodesulfurization of Dibenzothiophene and Its Derivatives through the Selective Cleavage of Carbon-Sulfur Bonds by a Moderately Thermophilic Bacterium Bacillus subtilis WU-S2B: Journal of Bioscience and Bioengeneering, v. 91, no. 3, p. 262–266.

Klappa, C. F., P. R. Opalinski, and N. P. James, 1980, Ordovician Table Head Group of western Newfoundland: a revised stratigraphy: Canadian Journal of Earth Sciences, v. 17, p. 1007–1019.

Knight, I., and Boyce, W.D., 1987, Lower to middle Cambrian terrigenous-carbonate rocks of Chimney Arm, Canada Bay: Lithostratigraphy, preliminary biostratigraphy and regional significance: Current Research (1987) Newfoundland Department of Mines and Energy, Mineral Development Division, v. Report 87-, p. 359–365.

Knight, I., and N. P. James, 1987, The stratigraphy of the Lower Ordovician St. George Group, western Newfoundland: the interaction between eustasy and tectonics: Canadian Journal of Earth Sciences, v. 24, no. 10, p. 1927–1951.

Knight, I., N. P. James, and T. E. Lane, 1991, The Ordovician St. George Unconformity, northern Appalachians: the relationship of plate convergence at the St. Lawrence Promontory to the Sauk/Tippecanoe sequence boundary: Geological Society of America Bulletin, v. 103, no. 9, p. 1200–1225.

Knight, I., and Boyce, W.D., 1991, Deformed Lower Paleozoic platform carbonates, Goose Arm–Old Man's Pond: Newfoundland Department of Mines and Energy, Geological Survey Branch, v. Report 91-, p. 141–153.

Kohl, W., A. Gloe, and H. Reichenbach, 1983, Steroids from the Myxobacterium Nunnocystis exedens: Journal of General Microbiology, v. 129, p. 1629–1635.

Lacombe, R., 2017, Stratigraphic and Structural Relationships in the Foreland Basin and Hum-

ber Arm Allochthon on Port au Port Peninsula, western Newfoundland: University of Alberta, 162 p.

Leslie, A. G., M. Smith, and N. J. Soper, 2008, Laurentian margin evolution and the Caledonian orogeny— A template for Scotland and East Greenland, in A. K. Higgins, J. A. Gilotti, and M. P. Smith, eds., The Greenland Caledonides: Evolution of the Northeast Margin of Laurentia: Geological Society of America Memoir, p. 307–343.

Lindholm, R.M., and Casey, J.F., 1989, Regional significance of the Blow Me Down Brook Formation , western Newfoundland : New fossil evidence for an Early Cambrian age: Geological Society of America Bulletin, v. 101, p. 1–13.

Longman, M. W., and S. E. Palmer, 1987, Organic geochemistry of mid-continent Middle and Late Ordovician oils: The American Association of Petroleum Geologists Bulletin, v. 71, no. 8, p. 938–950.

Macauley, G. (ed.), 1990, Ordovician oil shale-source rock sediments in the central and eastern Canada mainland and eastern Arctic areas, and their significance for frontier exploration: Ottawa, Canada, Energy, Mines, and Resources Canada, Paper / Geological Survey of Canada 90–14, 51 p.

Macauley, G., 1987, Organic Geochemistry of some Cambro-Ordovician Outcrop Samples Western Newfoundland: Geologic Survey of Canada 1503.

Mackenzie, A. S., and D. McKenzie, 1983, Isomerization and aromatization of hydrocarbons in sedimentary basins formed by extension: Geological Magazine, v. 120, no. 5, p. 417, doi:10.1017/S0016756800027461.

Maletz, J., Egenhoff, S., Böhme, M., Asch, R., Borowski, K., Höntzsch, S., Kirsch, M., and Werner, M., 2011, A tale of both sides of Iapetus – upper Darriwilian (Ordovician) graptolite faunal dynamics on the edges of two continents: Canadian Journal of Earth

Sciences, v. 48, p. 841–859.

Martin, R. L., J. C. Winters, and J. A. Williams, 1963, Distribution of n-Paraffins in Crude oils and their Implication to Origin of Petroleum: Nature, v. 199.

McKirdy, D. M., A. K. Aldridge, and P. J. M. Ypma, 1981, A geochemical comparison of some crude oils from Pre-Ordovician carbonate rocks: United Kingdom, John Wiley and Sons : Chichester, United Kingdom, p. 99–107.

McKirdy, D. M., and J. H. Hahn, 1982, The composition of kerogen and hydrocarbons in Precambrian rocks Physical and chemical sciences research reports: Germany, Springer-Verlag : Berlin, Federal Republic of Germany, p. 123–154.

Moldowan, J. M., W. K. Seifert, and E. J. Gallegos, 1985, Relationship between petroleum composition and depositional environment of petroleum source rocks: AAPG bulletin, v. 69, no. 8, p. 1255–1268.

Nes, W. R., and M. L. McKean, 1977, Biochemistry of steroids and other isopentenoids: Baltimore, University Park Press, 690 p.

Ourisson, G., P. A. Rohmer, and M. Rohmer, 1984, The Microbial Origin of Fossil Fuels: Scientific American, v. 251, no. 2, p. 44–51.

Palacas, J. G., D. E. Anders, and J. D. King, 1984, South Florida Basin; prime example of carbonate source rocks of petroleum: AAPG Studies in Geology, v. 18, p. 71–96.

Peng, S., L. E. Babcock, and R. A. Cooper, 2012, The Cambrian Period, in F. M. Gradstein, J. G. Ogg, M. Schmitz, and G. Ogg, eds., A Geologic Time Scale 2012: Amsterdam, Elsevier, p. 437–488.

Peters, K. E., and J. M. Moldowan, 1991, Effects of source, thermal maturity, and biodegradation on the distribution and isomerization of homohopanes in petroleum: Organic geo-

chemistry, v. 17, no. 1, p. 47–61.

Peters, K. E., and J. M. Moldowan, 1993, The biomarker guide: interpreting molecular fossils in petroleum and ancient sediments: Englewood Cliffs, N.J, Prentice Hall, 363 p.

Peters, K. E., J. M. Moldowan, and P. Sundararaman, 1990, Effects of hydrous pyrolysis on biomarker thermal maturity parameters: Monterey Phosphatic and Siliceous members: Organic Geochemistry, v. 15, no. 3, p. 249–265, doi:10.1016/0146-6380(90)90003-I.

Peters, K. E., C. C. Walters, and J. M. Moldowan, 2005, The biomarker guide: Cambridge, UK ; New York, Cambridge University Press, 2nd edition.

Picha, F. J., and K. E. Peters, 1998, Biomarker oil-to-source rock correlation in the Western Carpathians and their foreland, Czech Republic: Petroleum Geoscience, v. 4, no. 4, p. 289–302.

Quinn, L. A., 1992a, Foreland and trench slope basin sandstones of the Goose Tickle group and Lower Head Formation, western Newfoundland: Ottawa, National Library of Canada = Bibliothèque nationale du Canada.

Quinn, L.A., 1992b, Diagenesis of the Goose Tickle Group, western Newfoundland, EL # 92-103-01-EG: Report for Mobil Oil, 26 p.

Quinn, L., 1995, Middle Ordovician foredeep fill in western Newfoundland, in Hibbard, J.P., van Staal, C. R., and Cawood, P. A., eds., Current perspectives in the Appalachian-Caledonian oroge: Geologic Association of Canada, v. 41, p. 43–64.

Quinn, L., Bashforth, a R., Burden, E.T., Gillespie, H., Springer, R.K., and Williams, S.H., 2004, The Red Island Road Formation: Early Devonian terrestrial fill in the Anticosti Foreland Basin, western Newfoundland: Canadian Journal of Earth Sciences, v. 41, p. 587–602.

Quinn, L., S. . Williams, D. A. . Harper, and E. N. . Clarkson, 1999, Late Ordovician foreland basin fill: Long Point Group of onshore western Newfoundland: Bulletin of Canadian Petroleum Geology, v. 47, p. 63–80.

Radke, M., 1988, Application of aromatic compounds as maturity indicators in source rocks and crude oils: Marine and Petroleum Geology, v. 5, no. 3, p. 224–236.

Radke, M., D. Leythaeuser, and M. Teichmüller, 1984, Relationship between rank and composition of aromatic hydrocarbons for coals of different origins: Organic Geochemistry, v. 6, p. 423–430.

Radke, M., D. H. Welte, and H. Willsch, 1982, Geochemical study on a well in the Western Canada Basin: relation of the aromatic distribution pattern to maturity of organic matter: Geochimica et Cosmochimica Acta, v. 46, no. 1, p. 1–10.

Reed, J. ., H. A. Illich, and B. Horsfield, 1986, Biochemical evolution significance of ORdovician oils and their sources: Advances in Organic Geochemistry, v. 10, p. 347–358.

Riolo, J., G. Hussler, P. Albrecht, and J. Connan, 1986, Distribution of aromatic steroids in geological samples: their evaluation as geochemical parameters: Organic Geochemistry, v. 10, no. 4–6, p. 981–990.

Rubinstein, I., O. Sieskind, and P. Albrecht, 1975, Rearranged sterenes in a shale: occurrence and simulated formation: Journal of the Chemical Society, Perkin Transactions 1, no. 19, p. 1833, doi:10.1039/p19750001833.

Rullkötter, J., and R. W. Marzi, 1988, Natural and artificial maturation of biological markers in a Toarcian shale from northern Germany: Organic Geochemistry, v. 13, no. 4–6, p. 639–645.

Rullkötter, J., P. A. Meyers, R. G. Schaefer, and K. W. Dunham, 1986, Oil generation in the

Michigan Basin; a biological marker and carbon isotope approach: Organic Geochemistry, v. 10, no. 1–3, p. 359–375.

Schoell, M., 1984, Recent advances in petroleum isotope geochemistry: Organic Geochemistry, v. 6, p. 645–663.

Seifert, W. K., and J. M. Moldowan, 1978, Applications of steranes, terpanes and monoaromatics to the maturation, migration and sopurce of crude oils: Geochemica et Cosmochemica Acta, v. 42, p. 77–95.

Seifert, W. K., and J. M. Moldowan, 1980, The effect of thermal stress on source-rock quality as measured by hopane stereochemistry: Physics and Chemistry of the Earth, v. 12, p. 229–237.

Sieskind, O., G. Joly, and P. Albrecht, 1979, Simulation of the geochemical transformations of sterols; superacid effect of clay minerals: Geochimica et Cosmochimica Acta, v. 43, no. 10, p. 1675–1680.

Sinclair, I. K., 1990, A Review of the Upper Precambrian and Lower Paleozoic Geology of western Newfoundland and the Hydrocarbon Potential of the Adjacent Offshore Area in the Gulf of St. Lawrence: Canada-Newfoundland Offshore Petroleum Board, v. GL-CNOPB, no. 90–1, p. 79.

Sofer, Z., 1984, Stable Carbon Isotope Compositions of Crude Oils: Application to Source Depositional Environments and Petroleum Alteration: The American Association of Petroleum Geologists Bulletin, v. 68, no. 1, p. 31–49.

van Staal, C. R., S. M. Barr, and J. B. Murphy, 2012, Provenance and tectonic evolution of Ganderia: Constraints on the evolution of the Iapetus and Rheic oceans: Geology, v. 40, no. 11, p. 987–990, doi:10.1130/g33302.1.

van Staal, C.R., Zagorevski, A., McNicoll, V. J., 2014, Time-Transgressive Salinic and Acadian Orogenesis, Magmatism and Old Red Sandstone Sedimentation in Newfoundland: Geoscience Canada, v. 41, no. 2, p. 138, doi:10.12789/geocanj.2014.41.031.

Stenzel, S. R., I. Knight, and N. P. James, 1990, Carbonate platform to foreland basin: revised stratigraphy of the Table Head Group (Middle Ordovician), western Newfoundland: Canadian Journal of Earth Sciences, v. 27, p. 14–26.

Stevens, R. K., 1970, Cambro-Ordovician flysch sedimentation and tectonics in west Newfoundland and their possible bearing on a proto-Atlantic Ocean, in P. Lajoie, ed., Flysch Sedimentology in North America: Geolocical Association of Canada Special Paper 7, p. 165–177.

Stockmal, G. S., A. Slingsby, and J. W. F. Waldron, 1998, Deformation styles at the Appalachian structural front, western Newfoundland: implications of new industry seismic reflection data: Canadian Journal of Earth Sciences, v. 35, p. 1299–1306.

Stockmal, G. S., and J. W. F. Waldron, 1993, Structural and tectonic evolution of the Humber Zone, western Newfoundland, 1: Implications of balanced cross sections through the Appalachian structural front, Port au Port Peninsula: Tectonics, v. 12, p. 1056–1075.

Stockmal, G. S., and J. W. F. Waldron, 1990, Structure of the Appalachian deformation front in western Newfoundland: implications of multichannel seismic reflection data: Geology, v. 18, p. 765–768.

Stukas, V., and P. H. Reynolds, 1974, 40Ar/39Ar dating of the Long Range dykes, Newfoundland: Earth and Planetary Science Letters, v. 22, p. 256–266.

Tissot, B. P., and D. H. Welte, 1984, Petroleum formation and occurrence: Berlin ; New York, Springer-Verlag, 699 p.

Waldron, J. W., S. D. Anderson, P. A. Cawood, L. B. Goodwin, J. Hall, R. A. Jamieson, S. E. Palmer, G. S. Stockmal, and P. F. Williams, 1998, Evolution of the Appalachian Laurentian margin: Lithoprobe results in western Newfoundland: Canadian Journal of Earth Sciences, v. 35, no. 11, p. 1271–1287.

Waldron, J. W. F., R. Corney, and G. S. Stockmal, 1991, Acadian Inversion of a Taconian basin, Appalachian deformation front, western Newfoundland: Tectonic Studies Group Annual Meeting, Edinburgh, Scotland, Abstracts.

Waldron, J. W., and C. R. van Staal, 2001, Taconian orogeny and the accretion of the Dashwoods block: A peri-Laurentian microcontinent in the Iapetus Ocean: Geology, v. 29, no. 9, p. 811–814.

Waldron, J. W., and G. S. Stockmal, 1991, Mid-Paleozoic thrusting at the Appalachian deformation front: Port au Port Peninsula, western Newfoundland: Canadian Journal of Earth Sciences, v. 28, no. 12, p. 1992–2002.

Waldron, J. W., G. S. Stockmal, R. E. Corney, and S. R. Stenzel, 1993, Basin development and inversion at the Appalachian structural front, Port au Port Peninsula, western Newfoundland Appalachians: Canadian Journal of Earth Sciences, v. 30, no. 9, p. 1759–1772.

Waldron, J. W. F., G. S. Stockmal, R. C. Courtney, and J. DeWolfe, 2003, The Appalachian foreland basin beneath the Gulf of St. Lawrence: Abstracts, Geological Society of America, Northeastern section, Annual Meeting, Halifax, NS.

Weatherhead, W. R. A., 1922, Report on the oil prospects of Newfoundland, Private company report: Report on the oil prospects of Newfoundland.

Weaver, F. J., 1988, Source Rock Studies of Natural Seep Oils near Parsons Pond on the West Coast of Newfoundland, Master Thesis: Memorial University of Newfoundland, 178

p.

Weaver, F. J., and S. A. Macko, 1988, Source rocks of western Newfoundland: Organic geochemistry, v. 13, no. 1–3, p. 411–421.

Wenger, L. M., C. L. Davis, G. H. Isaksen, and others, 2002, Multiple controls on petroleum biodegradation and impact on oil quality: SPE Reservoir Evaluation & Engineering, v. 5, no. 5, p. 375–383.

West, N., R. Alexander, and R. I. Kagi, 1990, The use of silicalite for rapid isolation of branched and cyclic alkane fractions of petroleum: Organic Geochemistry, v. 15, no. 5, p. 499–501.

Westrop, S. R., 1992, Upper Cambrian (Marjuman–Steptoean) trilobites from the Port Au Port Group, western Newfoundland: Journal of Paleontology, v. 66, no. 2, p. 228–255, doi:10.1017/S0022336000033758.

White, C. E., T. Palacios, S. Jensen, and S. M. Barr, 2012, Cambrian–Ordovician acritarchs in the Meguma terrane, Nova Scotia, Canada: Resolution of early Paleozoic stratigraphy and implications for paleogeography: Geological Society of America Bulletin, v. 124, no. 11–12, p. 1773–1792.

Williams, H., 1979, Appalachian Orogen in Canada: Canadian Journal of Earth Sciences, v. 16, p. 792–807.

Williams, H., 1975, Structural succession, nomenclature, and interpretation of transported rocks in western Newfoundland: Canadian Journal of Earth Sciences, v. 12, no. 11, p. 1874–1894.

Williams, H., and R. N. Hiscott, 1987, Definition of the lapetus rift-drift transition in western Newfoundland: Geology, v. 15, no. 11, p. 1044–1047.

Yang, B., 1991, Geochemical characteristics of oil from well Shaca 2 in the Tarim Basin: Journal of Southeast Asia Earth Sciences, v. 5, no. 1–4, p. 401–406.

Zhang, S., and Barnes, C.R., 2004, Arenigian (Early Ordovician) sea-level history and the response of conodont communities, western Newfoundland: Canadian Journal of Earth-Sciences, v. 41, p. 843–865.

Appendix A: Calculation of Original Generative Potential

One key parameter in the calculation is the fractional conversion factor (f), which is a measure for the original petroleum potential to petroleum generated. The ratio is expressed in equation 1 of Cooles et al. (1986), where $S2_o$ is the original S2 and $S2_x$(CF) represents the measured S2 after generation and explosion (corrected for weight-loss). The correction factor (CF) for weight loss can be expressed with the measured TOC from pyrolysis using a basic assumption from Espitalé et al., (1987), who estimated that the generated petroleum contains 83.3 wt% of organic carbon. Therefore, CF can be expressed with equation 2, where TOC_o is the original TOC and TOC_x is the measured TOC content from pyrolysis. After rearranging and substituting equation 1 we can express the conversion factor f with HI (=S2/TOC) and PI (=S1/(S1+S2)) formulated in equation 3. The same equation can be solved for original TOC (equation 4). To perform the calculations I used pyrolysis data S1, S2, measured TOC, HI and PI.

$$f = \frac{S2_O - S2_X(CF)}{S2_O} \tag{1}$$

$$CF = \frac{TOC_O - 83.33 \times (S1_O + S2_O)}{TOC_X - 83.33 \times (S1_X + S2_X)} \tag{2}$$

$$f = 1 - \frac{\frac{HI_X}{100 - 0.0833 \times [\frac{HI_X}{(1 - PI_X)}]}}{\frac{HI_O}{100 - 0.0833 \times [\frac{HI_O}{(1 - PI_O)}]}} \tag{3}$$

$$TOC_O = \frac{HI_X \times TOC_X \times 83.33}{HI_O \times (1 - f) \times (83.33 - TOC_X) - HI_X \times TOC_X} \tag{4}$$

APPENDIX B: BIOMARKER IDENTIFICATION TABLE

Code	Biomarker ID	m/z
C19T	C19H34 tricyclic diterpane	191
C20T	C20H36 tricyclic diterpane	191
C21T	C21H38 tricyclic diterpane	191
C22T	C22H40 tricyclic terpane	191
C23T	C23H42 tricyclic terpane	191
C24T	C24H44 tricyclic terpane	191
C25S	C25H46 tricyclic terpane	191
C25R	C25H46 tricyclic terpane	191
TET	C24H42 teteracyclic terpane	191
C26S	C26H48 tricyclic terpane	191
C26R	C26H48 tricyclic terpane	191
Ts	18a, 21b-22,29,30-trisnorhopane	191
C27T	17a,18a,21b-25,28,30-trisnorhopane	177
Tm	17a, 21b-22,29,30-trisnorhopane	191
C28DM	C28 demethylated hopane	177
C28H	17a, 18a, 21b-28,30-bisnorhopane	191
C29DM	C29 demethylated hopane	177
C29H	17a, 21b-30-norhopane	191
C29D	18a-30-norneohopane	191
C30X	17a, 15a-methyl-27-norhopane (diahopane)	191
OL	oleanane	191
C30H	17a, 21b-hopane	191
C30M	17b, 21a-moretane	191
C31S	17a, 21b-30-homohopane (22S)	191
C31R	17a, 21b-30-homohopane (22S)	191
GA	gammacerane	191
C32S	17a, 21b-bishomohopane (22S)	191
C32R	17a, 21b-bishomohopane (22R)	191
C33S	17a, 21b-trishomohopane (22S)	191
C33R	17a, 21b-trishomohopane (22R)	191
C34S	17a, 21b-extended hopane (22S)	191
C34R	17a, 21b-extended hopane (22R)	191
C35S	17a, 21b-extended hopane (22S)	191
C35R	17a, 21b-extended hopane (22R)	191

Code	Biomarker ID	m/z
S1	13b, 17a-diacholestane (20S)	217
S2	13b, 17a-diacholestane (20R)	217
S3	5a-cholestane (20S) + 5b-cholestane (20R)	217
S4	5a, 14b, 17b-cholestane (20R) +13b, 17a-diastigmastane (20S)	217
S4B	same as S4 (m/z=218)	218
S5	5a, 14b, 17b-cholestane (20S)	217
S5B	same as S5 (m/z=218)	218
S6	5a-cholestane (20R)	217
S7	diastigmastane	217
S8	5a-ergostane (20S)	217
S9	5a, 14b, 17b-ergostane (20R) + 5b-ergostane (20R)	217
S9B	same as S9 (m/z=218)	218
S10	5a, 14b, 17b-ergostane (20S)	217
S10B	same as S10 (m/z=218)	218
S11	5a-ergostane (20R)	217
S12	5a-stigmastane (20S)	217
S13	5a, 14b, 17b-stigmastane (20R)	217
S13B	same as S13 (m/z=218)	218
S14	5a, 14b, 17b-stigmastane (20S) + 5b-stigmastane (20R)	217
S14B	same as S14 (m/z=218)	218
S15	5a-stigmastane (20R)	217

Code	Compound	MRM Transition
MN2	2-methylnaphthalene	142.1→141.1
EN2	2-ethylnaphthalene	141.1→141.1
DMNs	Σ-dimethylnaphthalene	156.1→141.1
DMN12	1,2-dimethylnaphthalene	156.1→141.2
DMN26	2,6-dimethylnaphthalene	156.1→141.3
DMN27	2,7-dimethylnaphthalene	156.1→141.4
TMNs	Σ-trimethylnaphthalene	170.1→155.1
TMN136	1,3,6-trimethylnaphthalene	170.1→155.2
TMN137	1,3,7-trimethylnaphthalene	170.1→155.3
TeMN13	2,3,6,7-tetramethylnaphthalene	184.1→169.1
TeMN14	1,2,6,7-tetramethylnaphthalene	184.1→169.2
TeNM15	1,2,3,7-tetramethylnaphthalene	184.1→169.3
TeNM16	1,2,3,6-tetramethylnaphthalene	184.1→169.4
DMPs	Σ-dimethylphenanthrene	206.2→191.1
DMP_E	3-ethylphenanthrene	206.2→191.2
DMP26	2,6-dimethylphenanthrene	206.2→191.3
DMP27	2,7-dimethylphenanthrene	206.2→191.4
DMP23	2,3-dimethylphenanthrene	206.2→191.5
DMP12	1,2-dimethylphenanthrene	206.2→191.6
DMP18	1,8-dimethylphenanthrene	206.2→191.7
DMP19	1,9-dimethylphenanthrene	206.2→191.8
MP1	1-methylphenanthrene	192.1→191.1
MP2	2-methylphenanthrene	192.1→191.2
MP3	3-methylphenanthrene	192.1→191.3
MP9	9-methylphenanthrene	192.1→191.4
TMP_A	trimethylphenanthrene peak A	220.2→205.2
TMP128	1,2,8-trimethylphenanthrene	220.2→205.3

Appendix C: Measured Sections

Appendix C accompanies Chapter 2.

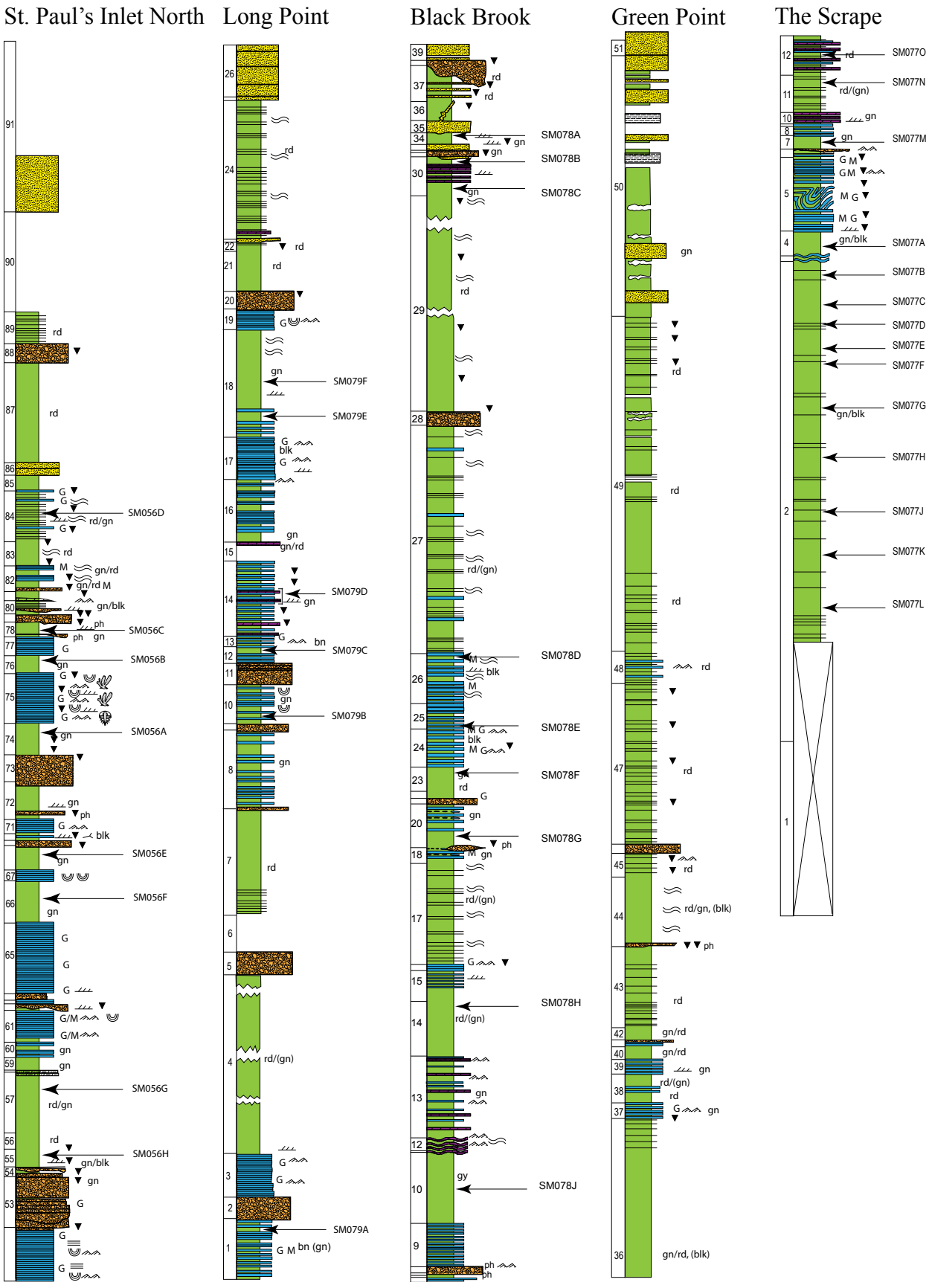
St. Paul's Inlet North
Long Point
Black Brook
Green Point
The Scrape
SM056D
SM056C
SM056B
SM056A
SM056E
SM056F
SM056G
SM056H
SM079F
SM079E
SM079D
SM079C
SM079B
SM079A
SM078A
SM078B
SM078C
SM078D
SM078E
SM078F
SM078G
SM078H
SM078J
SM077O
SM077N
SM077M
SM077A
SM077B
SM077C
SM077D
SM077E
SM077F
SM077G
SM077H
SM077J
SM077K
SM077L

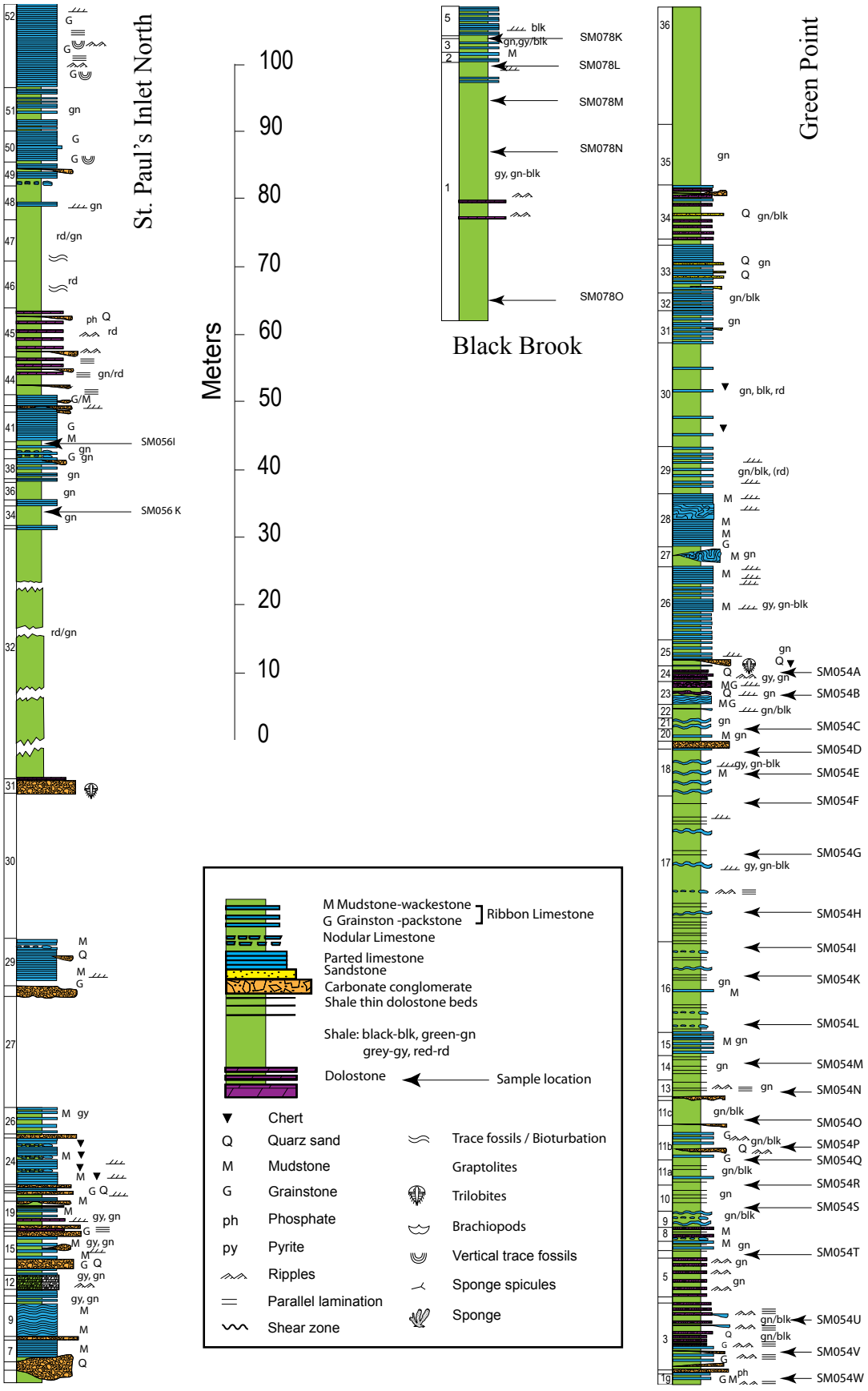
St. Paul's Inlet North
Meters
100
90
80
70
60
50
40
30
20
10
0
SM056I
SM056 K
Black Brook
blk
gn,gy/blk
M
SM078K
SM078L
SM078M
SM078N
gy, gn-blk
SM078O
Green Point
gn
Q gn/blk
Q gn
Q
gn/blk
gn
gn, blk, rd
gn/blk, (rd)
M
M
M
G
M gn
M
M gy, gn-blk
gn
Q
Q gy, gn
MG
Q gn
MG
gn/blk
gn
M gn
SM054A
SM054B
SM054C
SM054D
gy, gn-blk
M
SM054E
SM054F
SM054G
gy, gn-blk
SM054H
SM054I
SM054K
gn
M
SM054L
M gn
gn
SM054M
gn
SM054N
gn/blk
SM054O
G
gn/blk
SM054P
Q
G
SM054Q
gn/blk
SM054R
gn
SM054S
gn/blk
M
M gn
SM054T
gn
gn
gn/blk
SM054U
Q
gn/blk
G
SM054V
G
G M ph
SM054W
rd/gn
rd
ph Q
rd
gn/rd
G/M
G
M
gn
G gn
gn
gn
gn
rd/gn
M
Q
M
G
M gy
M
M
G Q
M
M
gy, gn
G
M gy, gn
M
G Q
gy, gn
gy, gn
M
M
M
Q
M Mudstone-wackestone
G Grainston -packstone
Ribbon Limestone
Nodular Limestone
Parted limestone
Sandstone
Carbonate conglomerate
Shale thin dolostone beds
Shale: black-blk, green-gn
grey-gy, red-rd
Dolostone
Sample location
Chert
Q Quarz sand
M Mudstone
G Grainstone
ph Phosphate
py Pyrite
Ripples
Parallel lamination
Shear zone
Trace fossils / Bioturbation
Graptolites
Trilobites
Brachiopods
Vertical trace fossils
Sponge spicules
Sponge

St. Paul's Inlet North

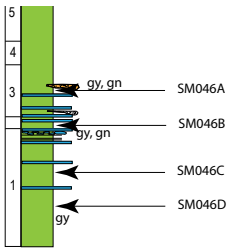

Green Point

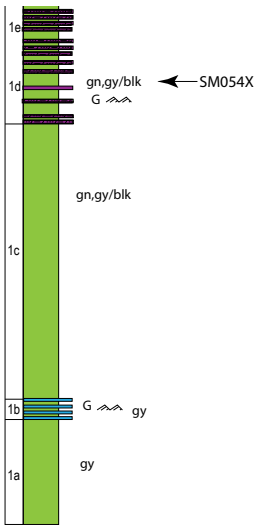

Measured sections modified after James and Stevens (1987). Numbers on the left of the stratigraphic column refer to the bed numbers described in James and Stevens (1987).

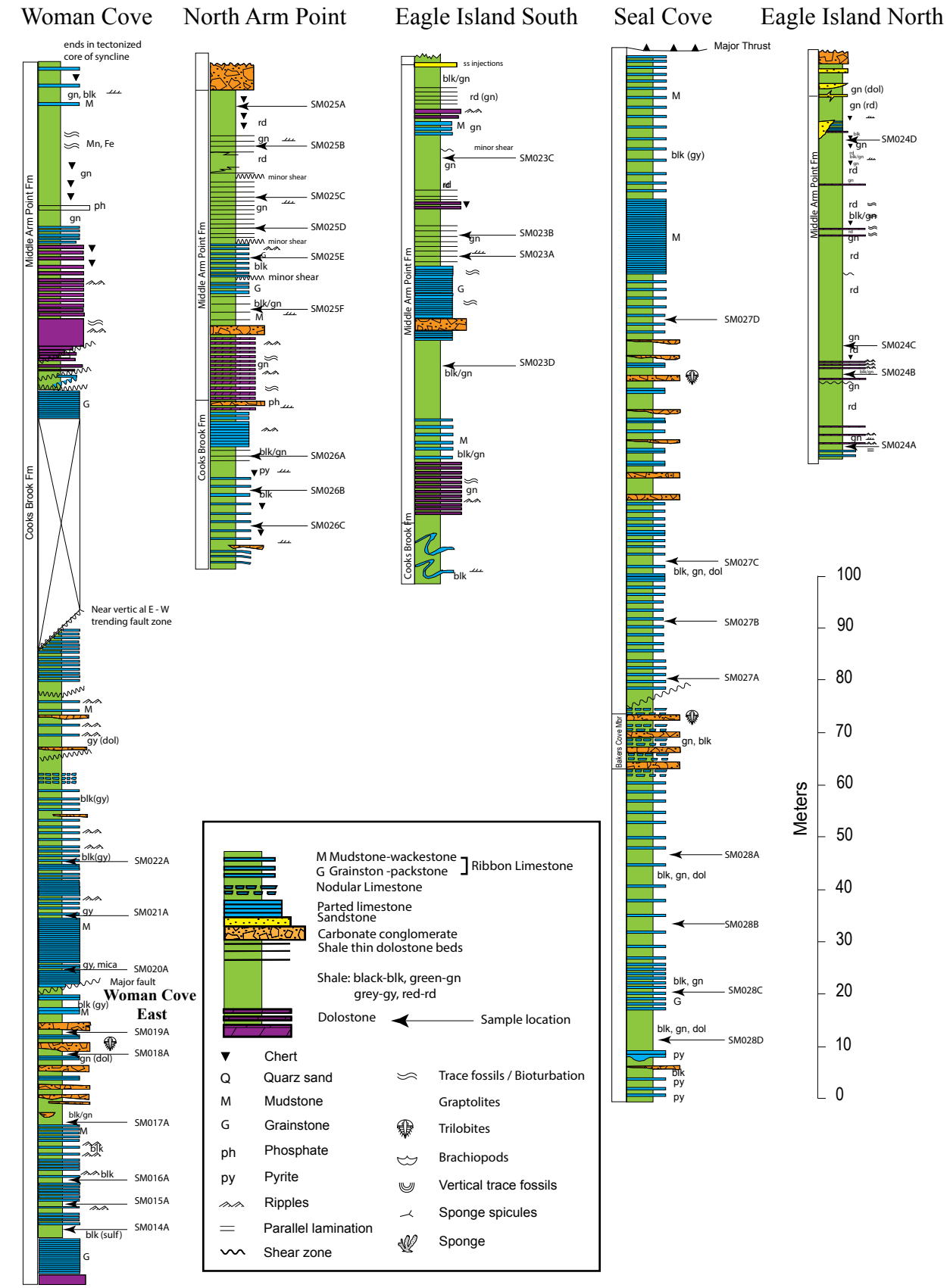

Measured sections modified after Botsford (1987).